THE 2ND INTERNATIONAL WORKSHOP ON SIMULATION FOR ENERGY, SUSTAINABLE DEVELOPMENT & ENVIRONMENT

SEPTEMBER 10-12 2014

BORDEAUX, FRANCE

EDITED BY

AGOSTINO BRUZZONE
FRANÇOIS CELLIER
JANOS SEBESTYEN JANOSY
FRANCESCO LONGO
GREGORY ZACHAREWICZ

PRINTED IN RENDE (CS), ITALY, SEPTEMBER 2014

ISBN 978-88-97999-36-2 (paperback)
ISBN 978-88-97999-42-3 (PDF)

ISBN 978-88-97999-36-2 (PAPERBACK)
ISBN 978-88-97999-42-3 (PDF)

THE 2ND INTERNATIONAL WORKSHOP ON SIMULATION FOR ENERGY, SUSTAINABLE DEVELOPMENT & ENVIRONMENT, SESDE 2014

SEPTEMBER 10-12 2014 - Bordeaux, France

ORGANIZED BY

DIME – UNIVERSITY OF GENOA

LIOPHANT SIMULATION

SIMULATION TEAM

IMCS – INTERNATIONAL MEDITERRANEAN & LATIN AMERICAN COUNCIL OF SIMULATION

DIMEG, UNIVERSITY OF CALABRIA

MSC-LES, MODELING & SIMULATION CENTER, LABORATORY OF ENTERPRISE SOLUTIONS

MODELING AND SIMULATION CENTER OF EXCELLENCE (MSCOE)

LATVIAN SIMULATION CENTER – RIGA TECHNICAL UNIVERSITY

LOGISIM

LSIS – LABORATOIRE DES SCIENCES DE L'INFORMATION ET DES SYSTEMES

MIMOS – MOVIMENTO ITALIANO MODELLAZIONE E SIMULAZIONE

MITIM PERUGIA CENTER – UNIVERSITY OF PERUGIA

BRASILIAN SIMULATION CENTER, LAMCE-COPPE-UFRJ

MITIM - MCLEOD INSTITUTE OF TECHNOLOGY AND INTEROPERABLE MODELING AND SIMULATION – GENOA CENTER

M&SNET - MCLEOD MODELING AND SIMULATION NETWORK

LATVIAN SIMULATION SOCIETY

ECOLE SUPERIEURE D'INGENIERIE EN SCIENCES APPLIQUEES

FACULTAD DE CIENCIAS EXACTAS. INGEGNERIA Y AGRIMENSURA

UNIVERSITY OF LA LAGUNA

CIFASIS: CONICET-UNR-UPCAM

INSTICC - INSTITUTE FOR SYSTEMS AND TECHNOLOGIES OF INFORMATION, CONTROL AND COMMUNICATION

NATIONAL RUSSIAN SIMULATION SOCIETY

CEA - IFAC

LOCAL SPONSORS

UNIVERSITY OF BORDEAUX

IMS LAB

AQUITAINE REGION

I3M 2014 INDUSTRIAL SPONSORS

CAL-TEK SRL

LIOTECH LTD

MAST SRL

SIM-4-FUTURE

I3M 2014 MEDIA PARTNERS

INDERSCIENCE PUBLISHERS – INTERNATIONAL JOURNAL OF SIMULATION AND PROCESS MODELING

INDERSCIENCE PUBLISHERS – INTERNATIONAL JOURNAL OF CRITICAL INFRASTRUCTURES

INDERSCIENCE PUBLISHERS – INTERNATIONAL JOURNAL OF ENGINEERING SYSTEMS MODELLING AND SIMULATION

INDERSCIENCE PUBLISHERS – INTERNATIONAL JOURNAL OF SERVICE AND COMPUTING ORIENTED MANUFACTURING

IGI GLOBAL – INTERNATIONAL JOURNAL OF PRIVACY AND HEALTH INFORMATION MANAGEMENT

HALLDALE MEDIA GROUP: MILITARY SIMULATION AND TRAINING MAGAZINE

HALLDALE MEDIA GROUP: THE JOURNAL FOR HEALTHCARE EDUCATION, SIMULATION AND TRAINING

EUROMERCI

EDITORS

AGOSTINO BRUZZONE
MITIM-DIME, UNIVERSITY OF GENOA, ITALY
agostino@itim.unige.it

FRANÇOIS CELLIER
DEPARTEMENT INFORMATIK, ETH ZÜRICH, SWITZERLAND
FCellier@Inf.ETHZ.CH

JANOS SEBESTYEN JANOSY
MTA EK CENTRE FOR ENERGY RESEARCH HUNGARIAN ACADEMY OF SCIENCES, HUNGARY
jjs@sunserv.kfki.hu

FRANCESCO LONGO
DIMEG, UNIVERSITY OF CALABRIA, ITALY
f.longo@unical.it

GREGORY ZACHAREWICZ
IMS UNIVERSITÉ BORDEAUX 1, FRANCE
Gregory.zacharewicz@ims-bordeaux.fr

INTERNATIONAL MULTIDISCIPLINARY MODELING & SIMULATION MULTICONFERENCE, I3M 2014

GENERAL CO-CHAIRS

AGOSTINO BRUZZONE, *MITIM-DIME, UNIVERSITY OF GENOA, ITALY*
YURI MERKURYEV, *RIGA TECHNICAL UNIVERSITY, LATVIA*

PROGRAM CO-CHAIRS

FRANCESCO LONGO, *DIMEG, UNIVERSITY OF CALABRIA, ITALY*
EMILIO JIMÉNEZ, *UNIVERSITY OF LA RIOJA, SPAIN*

THE 2ND INTERNATIONAL WORKSHOP ON SIMULATION FOR ENERGY, SUSTAINABLE DEVELOPMENT & ENVIRONMENT, SESDE 2014

GENERAL CO-CHAIRS

JANOS SEBESTYEN JANOSY, *MTA EK CENTRE FOR ENERGY RESEARCH HUNGARIAN ACADEMY OF SCIENCES,HUNGARY*
FRANÇOIS E. CELLIER, *DEPARTEMENT INFORMATIK, ETH ZÜRICH, SWITZERLAND*

PROGRAM CHAIR

GREGORY ZACHAREWICZ, *IMS UNIVERSITÉ BORDEAUX 1, FRANCE*

SESDE 2014 INTERNATIONAL PROGRAM COMMITTEE

MICHAEL AFFENZELLER, *UPPER AUSTRIA UNIVERSITY OF APPLIED SCIENCES, AUSTRIA*
ANGELO ALGIERI, *UNIVERSITY OF CALABRIA, ITALY*
THÈCLE ALIX, *IMS UNIVERSITÉ BORDEAUX 1, FRANCE*
TERRY BOSSOMAIER, *CHARLES STURT UNIVERSITY, AUSTRALIA*
ELEONORA BOTTANI, *UNIVERSITY OF PARMA, ITALY*
PHILIPPE BRUNET, *UNIVERSITY OF BOURGNOGNE, FRANCE*
AGOSTINO BRUZZONE, *UNIVERSITY OF GENOA, ITALY*
DANIEL BUCHBINDER, *ALTERNA, GUATEMALA*
RODRIGO CASTRO, *UNIVERSIDAD DE BUENOS AIRES, ARGENTINA*
FRANÇOIS E. CELLIER, *ETH ZÜRICH, SWITZERLAND*
NI-BIN CHANG, *UNIVERSITY OF CENTRAL FLORIDA, USA*
DANIELA CHRENKO, *UNIVERSITY OF BOURGOGNE, FRANCE*
GERSON CUNHA, *LAMCE/COPPE/UFRJ, BRASIL*
TIANZHEN HONG, *BERKELEY LAB, USA*
STEPHAN HUTTERER, *UPPER AUSTRIA UNIVERSITY OF APPLIED SCIENCES, AUSTRIA*
JANOS SEBESTYEN JANOSY, *MTA EK CENTRE FOR ENERGY RESEARCH HUNGARIAN ACADEMY OF SCIENCES, HUNGARY*
LUIS LE MOYNE, *UNIVERSITY OF BOURGOGNE, FRANCE*
ARNIS LEKTAUERS, *RIGA TECHNICAL UNIVERSITY, LATVIA*
FRANCESCO LONGO, *UNIVERSITY OF CALABRIA, ITALY*
MARINA MASSEI, *UNIVERSITY OF GENOA, ITALY*
ROBERTO MONTANARI, *UNIVERSITY OF PARMA, ITALY*
YOUNG MOON, *SYRACUSE UNIVERSITY, USA*
CELINE MORIN, *UNIVERSITY OF VALENCIENNES, FRANCE*
LETIZIA NICOLETTI, *CAL-TEK, ITALY*
MARIA CELIA SANTOS LOPES, *LAMCE/COPPE/UFRJ, BRASIL*
SIDI MOHAMMED SENOUCI, *UNIVERSITY OF BOURGOGNE, FRANCE*
TONINO SOPHY, *UNIVERSITY OF BOURGOGNE, FRANCE*
ALBERTO TREMORI, *SIMULATION TEAM, ITALY*
DA YAN, *TSINGHUA UNIVERSITY, CHINA*
GREGORY ZACHAREWICZ, *IMS UNIVERSITÉ BORDEAUX 1, FRANCE*

TRACKS AND WORKSHOP CHAIRS

SIMULATION PRO ENERGY, ENVIRONMENT AND DEVELOPMENT - SPEED
CHAIR: ANGELO ALGIERI, UNIVERSITY OF CALABRIA, ITALY

TRANSPORTATIONS
CO-CHAIRS: ARNIS LEKTAUERS, RIGA TECHNICAL UNIVERSITY, LATVIA; LUIS LE MOYNE, UNIVERSITY OF BOURGOGNE, FRANCE

SMART GRID PLANNING, OPTIMIZATION AND CONTROL - SPOC
CHAIRS: MICHAEL AFFENZELLER, UPPER UNIVERSITY OF APPLIED SCIENCES, AUSTRIA; STEPHAN HUTTERER, UPPER UNIVERSITY OF APPLIED SCIENCES, AUSTRIA

SUSTAINABLE LAND USE AND TRANSPORT ADOPTING M&S
CHAIR: DANIEL BUCHBINDER, ALTERNA, GUATEMALA

CONSUMERSISM AND SUSTAINABILITY
CHAIR: DANIEL BUCHBINDER, ALTERNA, GUATEMALA

CHAIRS' MESSAGE

Welcome to the 2nd International Workshop on "Simulation for Energy, Sustainable Development and Environment" (SESDE)!

The SESDE Workshop aims at charting an innovative course in application areas such as energy, environment and sustainable development adopting Modelling and Simulation as primary approach. "Sustainable development is development that meets the needs of the present without compromising the ability of future generations to meet their own needs": this is the classic definition of sustainable development popularized in *Our Common Future*, a report published by the World Commission on Environment and Development in 1987, also known as the Brundtland report. Needless to say, Sustainable Development is strongly related to Energy and Environment.

Renewable Energy, Energy Efficiency and Optimisation, Emissions Reduction, Energy Management, Integrated Energy Systems and Smart Grid Planning Optimisation and Control (SPOC) and Simulation Pro Energy, Environment and Development Transportations are just some of the topics raised by the SESDE Workshop that are becoming, as the time goes by, more and more crucial.

SESDE papers examine these themes that really concern us in the light of leaving a better world for future generations. More pathways are needed to be followed both by developed and developing countries taking great care of our world, so innovative projects and researches in this area would be the means to reach our ambitious goals.

We would also like to take this opportunity to inform authors that the SESDE 2014 proceedings will be indexed by SCOPUS (as already happened for the previous year proceedings); we are sure that this is a value-added for our authors.

It is therefore a pleasure to welcome you in Bordeaux, where SESDE is co-located with the "International Multidisciplinary Modelling & Simulation Multiconference" (I3M), with the purpose to share a very fruitful experience and to enjoy the meeting in the best possible way.

Janos Sebestyen Janosy
MTA EK Centre for Energy Research
Hungarian Academy of Sciences, Hungary

FRANÇOIS Cellier
Departement Informatik, Eth Zürich
Switzerland

Gregory Zacharewicz,
Ims Université Bordeaux 1
France

ACKNOWLEDGEMENTS

The SESDE 2014 International Program Committee (IPC) has selected the papers for the Conference among many submissions; therefore, based on this effort, a very successful event is expected. The SESDE 2014 IPC would like to thank all the authors as well as the reviewers for their invaluable work.
A special thank goes to all the organizations, institutions and societies that have supported and technically sponsored the event.

I3M 2014 INTERNAL STAFF

AGOSTINO G. BRUZZONE, *MISS-DIPTEM, UNIVERSITY OF GENOA, ITALY*
MATTEO AGRESTA, *SIMULATION TEAM, ITALY*
CHRISTIAN BARTOLUCCI, *SIMULATION TEAM, ITALY*
ALESSANDRO CHIURCO, *DIMEG, UNIVERSITY OF CALABRIA, ITALY*
FRANCESCO LONGO, *DIMEG, UNIVERSITY OF CALABRIA, ITALY*
MARINA MASSEI, *LIOPHANT SIMULATION, ITALY*
MARZIA MATTIA, *DIMEG, UNIVERSITY OF CALABRIA, ITALY*
LETIZIA NICOLETTI, *CAL-TEK SRL*
ANTONIO PADOVANO, *DIMEG, UNIVERSITY OF CALABRIA, ITALY*
EDOARDO PICCO, *SIMULATION TEAM, ITALY*
GUGLIELMO POGGIO, *SIMULATION TEAM, ITALY*
ALBERTO TREMORI, *SIMULATION TEAM, ITALY*

I3M 2014 LOCAL ORGANIZATION COMMITTEE

GREGORY ZACHAREWICZ, *UNIVERSITY OF BORDEAUX, FRANCE*
THECLE ALIX, *UNIVERSITY OF BORDEAUX, FRANCE*
JEAN CHRISTOPHE DESCHAMPS, *UNIVERSITY OF BORDEAUX, FRANCE*
JULIEN FRANÇOIS, *UNIVERSITY OF BORDEAUX, FRANCE*
BRUNO VALLESPIR, *UNIVERSITY OF BORDEAUX, FRANCE*

This International Workshop is part of the I3M Multiconference: the Congress leading **Simulation around the World and Along the Years**

Index

A PRELIMINARY EXPLORATION ON THE GLOBAL BUILDING ENERGY EFFICIENCY

Chenxia Jia,

Affiliation Equipment Engineering Deparment, Sichuan College of Architectural Technology, Deyang 618000, China.

Chenxiajia@163.com,

ABSTRACT
Building energy efficiency in china has made remarkable achievements, summarized a large number of valuable experience for many years. Energy-saving external wall and the window is the main way of energy-saving design and energy-saving renovation. Through proper use of energy-saving design principles is a good way to achieve energy saving purpose. And heating and air conditioning system operation and management of architectural energy saving plays a key role.

Keywords: building energy efficiency, building energy consumption, energy saving design, operation and energy saving

1. INTRODUCTION

Since the 90s, the theory of sustainable development was put forward. And for the urgency of the environment and resources protection, the theme of building energy efficiency has become the hot spot in the world. According to the statistics, building energy consumption has accounted for nearly 30% of terminal energy consumption in whole society in china. With the rapid development of the economy and the continuous improvement of people's living standard, the building energy consumption is also growing in our country, which is anticipated to reach as 40-50% in 2020 (Li Bingren 2010; Building energy conservation research center 2010). Such big building energy consumption causes the pressure of energy and environmental, which will be unable to bear the social and economic development in china. Therefore, China has put the focus of the building energy saving on energy conservation and emissions reduction crucial areas, is through policy, legal and economic means in the national building energy efficiency work. And building energy efficiency in china has made remarkable achievements, summarized a large number of valuable experience for many years.

2. THE MAIN WAY OF BUILDING ENERGY EFFICIENCY

It found that building energy consumption is mainly given priority to the building heating and air conditioning, which account for about 50 to 70% of total energy consumption (Jiang Yi 2006; Jiang Yi 2005). Heating and air conditioning energy consumption is mainly composed by the heat transfer and heat consumption of envelop configuration of buildings. And by the two ways it account for about 73% to 77% on the energy consumption of heating and air conditioning. In heat transfer and heat consumption, the share of external wall accounted for about 25-34%. And the followed is the air infiltration heat through the gap of doors and Windows, which accounts for about 23% to 27%. Therefore, building energy conservation is one of the main research objects of energy saving problem of buildings envelop configuration. That is to say, the external walls and windows are key parts of energy saving. Main way of energy saving is to reduce the surface area and strengthen the heat preservation of the building palisade structure, and increase the tightness of doors and windows.

2.1. External wall

For external wall insulation, mainly through two ways, one is with the brick of more heat preservation effect than the traditional wall materials such as solid clay brick. The correlational research is in full swing, Such as Di Yuhui (Di Yuhui 2000) did the technical and economic analysis on the annual heating energy consumption of a residential building with different wall. And he pointed out the aerated concrete is a kind of suitable substitutes; Promote the use of aerated concrete not only could protect arable land, but also could save energy. Another way is to the wall heat preservation processing, mainly has exterior insulation and external wall insulation. The external thermal insulation is convenient for construction. And it has no affect on the use of building during construction. In addition the heat preservation effect of the external thermal insulation is excellent. And external thermal insulation is convenient for the envelop retrofit of existing buildings. For the reasons above the external thermal insulation is be used more commonly.

In the other head, there are four main thermal insulation system of external wall, such as EPS board and thin plaster external thermal insulation system, mechanical fixed way external thermal insulation system, hanging board exterior insulation system, thermal insulation block external thermal insulation

system. The EPS insulating plate has many good characters, such as light quality, excellent sound insulation performance, strong resistance in low temperature, low water absorption, big surface friction coefficient, certain elasticity, uniformity of thickness,cheap price and small heat thermal conductivity (just 0.003 W/m). In addition, the EPS insulating plate is easy for cutting and polishing, of which the size can be cut in various shapes and need thickness. The heat preservation effect of the EPS insulating plate is easy to guarantee. In the reconstruction of existing residential building energy efficiency, the EPS board performance excellent as the thermal insulation material in the exterior insulation system. It has significant technical and economic effect, which can meet the technical requirements of energy conservation transformation of the construction. EPS board has successful application in foreign countries nearly 50 years and it has more than 20 years in domestic. The heat preservation effect and use effect of the EPS board is verified successful (Zhang Hao, Wei Jianji, and Zhou Xueling 2004).

2.2. External wall

Energy saving of external doors and Windows is mainly achieved by improving gas tightness of doors and Windows. The mainly measures for improving gas tightness of doors and Windows are using of layers or single box double glass window, using energy-saving glass, improvement of outer door window frame materials, heat preservation of external doors, etc. In addition, sun-shading of buildings in summer has great potential in energy-saving, which can significantly improve the indoor thermal environment, adjust indoor light distribution, prevent glare, and reduce UV damage. Because of it is convenient to install, use and maintain, the inner curtain is widely applied. The most common are inner curtain are Venetian blinds, roller blinds, vertical blinds, accordion curtain and so on. In the other head, the thermal barrier of inner curtain is better than the external solar shading. That is because when inner curtain used, sun shines on the glass and then sunlight come through the glass to the shading device, the room is warmed up. But building external solar shading could make most of the sunshine only reach to the shading device and radiant heat of the sun can't directly reach to interior space of the room. Therefore, the temperature of room with external shading is 10-20% lower than with inner curtain. So external shading is preferred in the design of energy-saving in summer, such as blinds, awnings, sunshade veil curtain, coated glass, awnings, or visor, or climbing plants in the balcony window. Sunshade design is not a independent of the architecture design of energy saving, it even through the whole process of architectural design, from site selection, layout, the design of the building facade, plant configuration of the environment and the structure, to the HVAC design of the building, etc. Therefore, in addition to the technical requirements of energy saving, it also has to match up with the building overall design. The so-called best shade should also take care of environment, base on visual perception, including two-sided effects by window overlooking the outdoor scene or outside watching architecture (Zhang Wen 2003).

3. ENERGY-SAVING DESIGN PRINCIPLES

Orientation and spacing, sunshine and ventilation are the most important factors that affect indoor environmental quality.

The glass of the window occupies about 80% area of the external window. Heat gain/loss from the glass of the window is the main causes of the indoor overheat or cooling load of air conditioning, in burning hot summer or cold winter. Under the condition of satisfying day lighting, the area ratio of window to wall should be limited in a reasonable range. The solar radiation energy through the window is not the same in the different toward, so the reasonable area ratio of window to wall is also different. The reasonable ratio of window in south is maximum (< 0.35), the east-west is second largest (< 0.30), and the north is minimum (< 0.25).

Heat transfer and heat consumption of housing construction decreased with the increasement of the total building area, but of which the relationship is not in linear. when building area is 1000 - 2000 square meters, the reduction of heat transfer and heat consumption of unit building area is 57-58%; When building area is 2000 - 4000 square meters, he reduction of heat transfer and heat consumption of unit building area is 85-86%; When building area is 4000 - 8000 square meters, heat transfer and heat consumption will decrease by 14-15%.

In general, the shape coefficient of the residence should maintain in the scope of not more than 0.3.

4. BUILDING ENERGY CONSUMPTION IN OPERATION AND MANAGEMENT

As mentioned above, building energy consumption is mainly composed of building heating and air conditioning energy consumption. When the system put into use, the way of operation and management of the system plays a key role to energy saving.

4.1. Building heating energy consumption

Areas of suitable for heating in our country is occupied about 70% of China's land area, mainly including the northeast, north China, and northwest. The energy saving of heating system has a great potential in china. The existing successful saving energy promotion strategy mainly has the following kinds (Chen Yiliang 1994).

Reform the heating charge system. In the past, the heating fee has been charged according to the size of the area for a long time in our country. This Charging mode leads to serious waste of energy. The technology level of heating is low and the quality of heating can not be effective supervised and guarantied. And charging users according to user's practical heat can raise the consciousness of energy conservation.

Improve the system design to meet the requirements for controlling the heat medium. The user can't adjust the quantity of heat according to their needs in the single pipe system and constant flow mode. The heating quality and energy saving can be improved when the dynamic adjusting VWV system is been used.

Use the advanced heating system control, adjustment and measurement instruments or equipments.

Practice has proved that the central heating can improve energy utilization efficiency. When heating area is more than 100-150 thousands square meters, the boiler room should be built. Otherwise it will do more harm than good.

Utilize of water treatment technology in heating. A very important problem in the heating system is to prevent the fouling and corrosion inhibition, which can ensure the normal operation of heating boiler, systems and equipment.

4.2. Energy consumption of central air conditioning

There are some ways to realize the purpose of energy saving of central air conditioning system (Lian Xiaohu, Li Ze, and Xie Junlong 1999).

1. Choose the appropriate cooling and heat sources.

Most of the energy consumption in central air-conditioning system is used up in cold source. So it is great significance for the rational allocation of cooling and heat sources of the central air conditioning system. The Common configurations of cold/heat source are as follow.

Water chiller unit + Boiler. Energy efficiency ratio (EER) is high in design conditions, generally about 3.7-5. When centrifugal compressor unit used as the host, the EER is the highest, about 5, but the unit capacity of this type is larger. Generally the air conditioning refrigerating capacity in more than 300 RT (cold tons), centrifugal compressor is choose. Air conditioning refrigerating capacity during 150-300 RT, screw compressor is used. Air conditioning refrigerating capacity is less than 150 RT, piston compressor is more appropriate.

Heat pump unit. In summer cooling and winter heating, under the design conditions, EER of water chilling unit is lower, usually around 3.The energy saving and environmental protection have good effect.

LiBr absorption unit. The characters of this unit is low EER, economize on electricity and no energy conservation. It is suitable for where have waste heat and waste heat.

2. Use cool storage air conditioning and variable power load.
3. Run air conditioning system in saving energy way.

- Reduce indoor given value standard.
- New air volume should be reduced in cold winter or hot summer, while in transition season it should be increased according to the outdoor climate change.
- Prevent the extreme cold and heat.
- Room temperature is overheating in summer or undercooling in winter, more energy is consumed. And it is not suitable for human comfort and health.
- Use heat recovery and heat exchange device.
- Change the air conditioning equipment start and stop time.
- Frequency conversion control.
- Automation system of Equipment.

Automation systems of construction equipment centralize management and optimal control of air conditioning, electrical, health, fire alarm and so on.

5. CONCLUSIONS

In the practice of building energy conservation, the work of construction energy conservation has made remarkable achievements and a lot of valuable experiences have summed up in our country. The envelop configuration of buildings is the focus of work of building energy efficiency. The energy saving design principles has been summarized in this paper, and effectively using of them can easily attain the goal of building energy efficiency. The Energy consuming of heating and air conditioning system accounts for larger proportion of construction energy. Operation management of energy heating and air conditioning system plays a key role in saving building energy consumption. Building energy conservation work, of course, are far way to go for. The actual energy consumption of building is not only related to meteorological conditions and envelop configuration of buildings but also to the human factors such as habits and ways. It is clear that the influencing factors of building energy saving effect is quite complicated, and those factors do the contribution to the building energy conservation is not a linear addition, but a very complicated nonlinear relationship.

REFERENCES

Li B.R., 2010. Ministry of Housing and Urban-Rurl Development coping with climate change to concentrate on building energy efficiency. *City Residence*, 10, 23–25.

Li B.R., 2011. *Building energy consumption accounts for about a third of the social total energy consumption in China*. Available from: http://www.chinagb.net/[accessed 1 April 2011]

Building energy conservation research center of in Tsinghua University, 2010. *China building energy efficiency annual development report.* Beijing, China building industry press. Available from:http://www.chinairn.com/doc /70300/769419.html/[accessed 1march 2010]

Jiang Y., 2006. The key to building energy consumption trend and energy saving in China. *Green building*, special issue, 9–15.

Jiang Y., 2006. Building energy consumption situation in our country and the effective energy saving way. *Journal of HV&AC*, 35(5), 30-41.

Di, Y.H., 2000. The wall of energy saving in heating of the building. *Energy saving and environmental protection*, 6, 29–30.

Zhang, H., Wei J.J. and Zhou X.L., 2004. The application of the external thermal insulation technology in building energy-saving renovation. *Journal of Pingyuan University*, 21, 30–31.

Zhang, W., 2003. The application of shading in the residential. Housing science, 1, 38–40.

Chen, Y.L., 1994. Building heating energy saving and environmental improvemen. The population of China • Resources and environment, 4, 54–57.

Lian, X.H., Li, Z. and Xie J.L.,1999. Air conditioning building energy efficiency and its main ways. Journal of Ezhou University, 3, 16–19.

AUTHORS BIOGRAPHY

Chenxia Jia, Director of the teaching and research office of HV&AC and industrial equipment installation in Affiliation Equipment Engineering department, Sichuan College of Architectural Technology. The main research scope are building energy saving, HV&AC and so on.

MODELLING AND SIMULATION TO DESIGN MULTI-STOREY TIMBER BUILDING USING MULTI-OBJECTIVE PARTICLE SWARM OPTIMISATION

Stéphanie Armand Decker[a,c], Amadou Ndiaye[b], Alain Sempey[a], Philippe Galimard[a], Marie Pauly[c] , Philipe Lagière[a,c], Frédéric Bos[a]

[a] Univ. Bordeaux, I2M, UMR 5295, F-33400 Talence, France.
[b] INRA, I2M, USC 1368, F-33400 Talence, France
[c] Nobatek-INEF4, F-64600 Anglet, France,

sdecker@nobatek.com

ABSTRACT

In order to promote multi-storey timber building projects, a preliminary design methodology with optimisation step and decision-making support is proposed. The objective is to optimise building envelope composition taking into account trade-off between heating needs, summer thermal comfort, floor vibration comfort, global warming potential and embodied energy objectives. These objectives, that are conflicting and can implement in the same time continuous and discrete variables, will be then modelled as objective functions to be optimised in multi-objective manner. To obtain thermal objectives, a time consuming option is to couple an optimiser with a detailed simulation models. Another alternative is to generate meta-models and implement them directly to the optimiser as objective-functions. The multi-objective optimisation will be achieved using the metaheuristic Particle Swarm Optimisation (PSO) to determine the Pareto front of optimised solutions. A case-study is explored using two thermal meta-models. A Pareto front is obtained and analysed.

Keywords: Multi-objective optimisation, Energy simulation, Meta-model, Particle Swarm Optimisation

1. INTRODUCTION

Wood is a low environmental impacts material with a dry and rapid implementation in the building process, facilitated by a potential high prefabrication level. However in France, timber building is still underdeveloped with a building incorporation rate of 10% against 15% in Germany and 35% in Scandinavia and North America (Gabenisch et al. 2012). Furthermore, a lack of knowledge in timber building, especially for multi-storey slows its development (FCBA and CSTB 2009). To expand multi-storey timber building there is a need to develop design methods and tools with regulatory constraints consideration.

Building is a complex system, subject of multidisciplinary design studies generally considered by technological fields. In order to design preliminarily optimised building envelope and structure composition considering thermal, structural and environmental objectives, it is necessary to increase design understanding trade-offs involved. This makes it a challenging multi-objective optimisation problem.

To promote multi-story timber buildings with multidisciplinary design, a multi-objective optimisation method is under development. The objectives are to optimise the envelope and the structure composition of a building. Architectural geometry, location and use are fixed parameters. The minimising of energy needs, thermal discomfort, CO2-eq emission and embodied energy of the building and the maximizing of floor vibration comfort are considered objectives. Regulatory structural constraints are considered by preliminary design calculations to ensure the safety of the structure. In longer-term the objective functions will be completed by adding acoustic insulation, lighting autonomous and structural cost to the multi-objective optimisation process.

The preliminary design methodology couples multi-objective optimisation to multi-criteria decision. First, the overall approach is to perform a search process through the multi-objective optimization for the calculation of the Pareto front of optimal compromises between the different objectives to be optimised. Then, a decision process is implemented through a multi-criteria analysis to help decision in choosing the optimal compromise, from the Pareto front, to be implemented. Objectives and significant variables are initially selected. Relationships between them are then established and represented as influence graph. Next, explanation of links between variables and objectives which consists in assembling knowledge and implementing necessary research to explain the relationships between variables and objectives is done. Objective functions are then designed as explicit qualitative function or algorithm. Optimisation and multicriteria analysis process are then implemented consecutively.

To explicit thermal objectives use of dynamic simulation model is required. However such detailed model easily requires more than ten minutes estimating thermal performance. Total simulation time may

quickly become important especially when several iterations are necessary to find a set of optimal solutions. Efficient methods of searching the design space became necessary. One promising method is the use of stochastic algorithms to optimise discontinuous and multi-objective building design problems (Attia et al. 2013). However, many hundreds or even thousands of design samples can still be necessary to converge to an optimum design or Pareto front. Optimisation processes still lead to a large computational burden, especially when detailed simulation models are used.

On this work, to save valuable time during the optimisation process and its implementation, detailed simulation models are replaced by surrogate models. Surrogate models or meta-models express the outputs in terms of decision variables as an analytic function. Such functions represent the explanation of links between variables and objectives for thermal objectives. First, they are easy to implement into the optimisation process and may facilitate sensitivity analysis on decision variables. Finally, they may be used to perform many objective function evaluations without running full simulations each time. Such approach has already been used by (Eisenhower et al. 2012) that developed a methodology for the use of meta-models in building optimisation problem with over 1000 parameters. They optimised thermal comfort and energy use with a gradient based optimiser that used the derivatives available from the meta-model. (Tresidder et al. 2012) fitted a Kriging meta-model to simulation results, which was then optimised using a Genetic Algorithm.

This article presents the calculation methodology employed to optimise the building envelope composition taking into account trade-off between heating needs, summer thermal comfort, floor vibration comfort, global warming potential and embodied energy objectives. Firstly, the thermal, mechanical and environmental objectives are presented. Secondly, explanation of links between variables and thermal objectives by using a surrogate model would be explained. Third, the optimisation process and implementation would be detailed and the compliance to the problem clarified. Finally a case study is presented and first results are discussed.

2. OBJECTIVES OF THE DESIGN OF MULTI-STOREY TIMBER BUILDING

The objective is to optimise building envelope composition taking into account trade-off between heating needs, summer thermal comfort, floor vibration comfort, global warming potential and embodied energy objectives.

2.1. Thermal objectives

Two thermal objectives to optimise have been selected: Heating needs and summer comfort.

2.1.1. Heating needs:

It is the energy demand to keep the building at a setpoint temperature T_{set} during the winter. The objective F_1 is to minimize the gap between the desired H_d and obtained heating needs H_n as (1). If the objective is simply to minimize the needs for heating while $H_d=0$. H_n must be less or equal to a fixed value for maximum heating needs, H_{max}.

$$F_1 : \min(abs(H_n - H_d)) \text{ subject to } H_n \le H_{\max} \quad (1)$$

2.1.2. Summer comfort:

The degree-hour *DH*, expressed in the EN15251 version, measure the accumulation of the temperature offset from a comfort threshold per each hour (Figure 1). It is the building thermal zone integral operative temperature degrees T_o higher than a comfort temperature T_c during an hourly simulation period with occupancy *pocc* (2). The comfort temperature depends on the type of building. The objective F_2 is to minimize *DH*. *DH* must be less or equal to a fixed value for maximum degree-hour, DH_{max} (3).

$$DH = \sum \left(\int_{pocc} (T_o - T_c)dt \right) \text{ with } T_o > T_c \quad (2)$$

$$F_2 : \min(DH) \text{ subject to } DH \le DH_{\max} \quad (3)$$

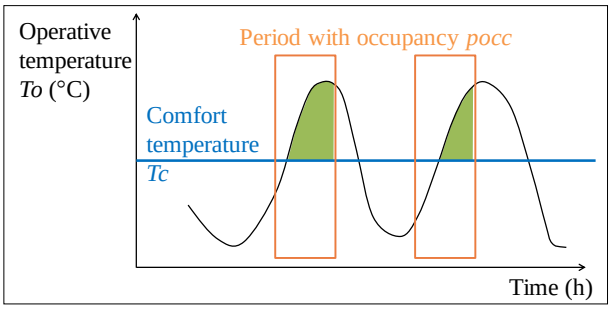

Figure 1: Summer comfort objective calculation

To predict energy needs and thermal comfort dynamic thermal simulation using detailed models are necessary. Such models take into account all of the variables input at the building stage, such as the thermal performance of the materials, yearly weather information, occupation periods of the building and occupant use. Hn and hourly thermal zone operative temperature are computed directly by using *EnergyPlus* 7.2 (DOE: U.S. Department of Energy) software. For a large scale building, as a multi-storey office building, the calculation time required to compute both, Hn and hourly thermal zone operative temperature necessary to compute DH, is about few minutes to hour. An important task is to reduce computation time required to get the optimal solutions from days, weeks, even months to less than one hour. When detailed simulation models are used, the issue may be addressed by meta-modelling techniques, which approximate a simplified function relationship between the simulation results and the input variables. Such functions represent the explanation of links between variables and objectives

for thermal objectives and their generation would be detailed later.

Meta-models may be used instead of main model for the optimisation procedure: more calculations can be made in the available time using a meta-model than a main simulation model that is more detailed. Nevertheless, to surrogate main simulation model, meta-model has to be accurate.

In (Merheb 2013), while the main model requires 200 second to evaluate H_n, use of meta-models allows to evaluate 2056 alternatives in one second. These figures confirm the effectiveness and interest to calculate a meta-model to surrogate a computationally expensive detailed model.

2.2. Mechanical objective and constraints

Structural and environmental objectives, F_3, F_4 and F_5, may be described as follow:

2.2.1. Floor vibration comfort:

Three comfort levels 1, 2, 3 and 4 respectively, very good, good, acceptable and unacceptable are fixed. Comfort level, F_v, have to be minimized.

$$F_3 : \min(F_v) \text{ and } F_v \neq 4 \tag{4}$$

2.2.2. Mechanical constraints

Structural and sizing constraints are:

- **Floor height:**

The floor height is limited to a maximum value defined by the variables.

- **Wall thickness:**

The wall thickness is limited to a maximum value defined by the variables.

- **Structural constraints:**

Solutions must meet the normative requirements of Eurocode 5 (AFNOR 2005a; AFNOR. 2005b) or, for CLT as the recommendations of FPInnovations (FPInnovations 2011). Preliminary design calculations will be performed to check the viability of solutions regarding to the ultimate limit state (ULS) and the serviceability limit state (SLS).

2.3. Environmental objectives

2.3.1. Global warming potential (GWP):

The objective is to minimize de *GWP* related to the envelope during the building life cycle (Pre-Use, Use, Replacement and End of Life). The pre use and replacement emissions of the raw material extraction and materials manufacturing are calculated based on the mass of each material in the building construction. The end of life emission related to the demolition and disposal transportation to landfill and recycling centre are also calculated based on the mass of each material in the building construction. Finally the use emission related to the envelope is determined by first calculating the heating needs during the building life cycle.

Then heating needs are multiplied by the efficiency of the heating system and the local electricity emissions factor.

$$F_4 : \min(GWP) \tag{5}$$

2.3.2. Embodied energy:

The objective is to minimize embodied energy E_m of the envelope during the building life cycle. It is determined similarly to the *GWP*.

$$F_5 : \min(E_m) \tag{6}$$

3. META-MODELLING OF THERMAL FUNCTIONS

3.1. Meta-model generation

To generate a meta-model, three steps are required:

1. Generation of an initial sampling of the dynamic simulation model (the main model)
2. Meta-model calculation
3. Meta-model validation

To define the sampling it is necessary to define its size, parameters, and their range and distribution law for their variation (e.g. Gaussian, Uniform, Log-normal). Then the sampling is carried out by varying the parameters of the model within a range around their baseline value using Monte Carlo method, which randomly selects these samples. Corresponding models are realized and simulated preferably using parallel computation.

From this sample, meta-model based on polynomial chaos (PC) (Wiener 1938) is build. Use of PC from an *EnergyPlus* model was done in (Merheb 2013) to evaluate the spread of uncertainties by coupling with the *OpenTURNS*© tool, which integrate a PC toolbox (Dutka-Malen et al. 2009).

Let a numerical model, f, having n input parameters gathered in an input vector $\underline{X} = (x_1, x_2, \ldots x_n)$, and a scalar output Y:

$$Y = f(\underline{X}) \tag{7}$$

$\underline{X}$ follows the joint probability density function. The polynomial chaos expansion enables to approximate the output random variable of interest Y by the new output random variable of interest $\tilde{Y}$. A truncated polynomial chaos to order k_h is as follows

$$Y \approx \tilde{Y} = \sum_{k=0}^{k_h} \alpha_k \psi_k \circ T(\underline{X}) \tag{8}$$

where T is an isoprobabilistic transformation which maps the multivariate distribution of $\underline{X}$ into the multivariate distribution μ, and Ψ_k is a multivariate

polynomial basis which is orthonormal according to the distribution μ and α_k are the polynomial coefficients to compute in order to minimize the difference between the variable of interest Y and its polynomial approximation using least squares strategy.

Two main parameters characterise PC meta-models:

- The order k_h *of* the polynomial
- The sampling size

To determine the best order the sample is divided into two parts according to learning theory: learning base (90% of the sample) and validation base (10%). The meta-model calculation is done with the learning base and validated or rejected with the validation base.

Mean-squared and relative errors are determined with the validation based, respectively (6) and (7). The order k_h *of* the polynomial is gradually increased until mean squared decrease which means that the sample size is not enough to build higher polynomial order.

$$L^2 = \sqrt{\frac{1}{n_v}\sum_{i=1}^{n_v}\left[f(\underline{X}_i) - \tilde{f}(\underline{X}_i)\right]^2} \quad (9)$$

$$L^\infty = \sup \frac{\left| f(\underline{X}_i) - \tilde{f}(\underline{X}_i)\right|}{f(\underline{X}_i)} \quad (10)$$

After meta-model generation, it is checked on the main model according to the mean-squared error, relative error and residual which is calculated on the learning base (8). If errors and residual are satisfactory according to the designer, the sample size is adequate. Otherwise, sample size has to be increase to obtain a higher order polynomial.

$$r = \sqrt{\frac{1}{n_l}\sum_{i=1}^{n_l}\left[f(\tilde{\underline{X}}_i) - \tilde{f}(\tilde{\underline{X}}_i)\right]^2} \quad (11)$$

3.2. Sensitivity analysis

Meta-models based on polynomial chaos (PC) (Wiener 1938) have the advantage to deduct Sobol indices (Sobol 1993) of the output from its coefficients with almost no additional cost (Crestaux et al. 2009). The Sobol indices are used in global sensitivity analysis as a tool for ranking the input random variables of a model according to their weight in the variance of the model response.

The determination of the Sobol decomposition and sensitivity indices is immediate as soon as the PC expansion of f is known. The Sobol indices S_u of f are approximated by (Crestaux et al. 2009):

$$S_u \approx \tilde{S}_u = \frac{\sum_{k\in k_u} \alpha_k^2 \langle \Psi_k, \Psi_k \rangle}{\sum_{k\in k_h} \alpha_k^2 \langle \Psi_k, \Psi_k \rangle} \quad (12)$$

When generating meta-models, it is possible to extract the total Sobol indices *STi* (10). *STi* express the responsibility of each parameter in its range of variation correlated with the others on the output variation.

$$S_{T_i} = \sum_{u \ni i} S_u \quad (13)$$

Non influent parameters would be fixed according to the designer.

4. MULTI-OBJECTIVE OPTIMISATION

4.1. A mixed integer non linear programming problem (MINLP)

The design of building envelope composition taking into account trade-off between thermal, structural and environmental objectives is a non-linear optimisation problem. Many variables interact with each other and influence several common objectives simultaneously. The optimum value for a variable depends strongly to the value taking by other variables. Two kinds of variables are considered in this optimisation model: continuous variables as insulation thickness and discrete variables as kind of floor. Continuous variables are box constraints with boundary values and discrete variables give a predefined set of alternatives. Each additional variable makes the set of all possible alternatives (the design space) exponentially large.

Metaheuristic algorithms are well adapted to carry out the global optimisation for multi-objective mixed-integer non-linear programming (MINLP) problems, especially when the design space is large.

Developed by Eberhart and Kennedy (1995), PSO, like other metaheuristic methods, finds a set of optimal solutions to a difficult optimisation problem. This method, motivated by the simulation of social behaviour, has proved to be very efficient in hard optimisation problems. The system is initialized with population and searches for optima by updating generations. Kennedy and Eberhart (1997) have introduced a discrete binary version of PSO (DPSO) that operates on binary variables (bit, symbol or string) rather than real number. Thus, they extend the use of PSO optimisation to discrete binary functions as well as to functions of continuous and discrete binary variables at the same time. Michaud et al. (2009) have generalized the discrete binary version of PSO to a discrete n-ary of PSO. Finally, the mixed-integer PSO (MIPSO) technique is especially and fully suitable for our problem where non linear functions have to be optimised with both, continuous and discrete decision variables.

4.2. Multi-Objective Particle Swarm Optimisation algorithm

The original procedure for implementing PSO is simple and easy to implement six steps algorithm (Ndiaye et al. 2009):

1. Initialize a population of particles with random positions and velocities on *n* dimensions in the problem space
2. For each particles calculate the fitness (the function to optimise in *n* variables)
3. Compare particle's fitness with the fitness of its best position ever visited (*pbest*). If current value is better than *pbest*, then it becomes *pbest*.
4. Identify the particle in the neighbourhood with the best fitness; it becomes the leader of the neighbourhood.
5. Change the velocity and position of particles according to velocity and position updating rules (16) and (17).
6. Loop to step 2. Until the end condition is met, usually a sufficiently good fitness or a maximum number of iteration.

For a search in an *n*-dimensional search space where the particles movements are synchronized, at the *t*th iteration, for the *i*th particle, the position and position change (*velocity*) vectors are respectively represented as (14) (15) (Eberhart and Kennedy 1995):

$$X_i^t = (x_{i,1}^t, x_{i,2}^t, ..., x_{i,n}^t) \tag{14}$$

$$V_i^t = (v_{i,1}^t, v_{i,2}^t, ..., v_{i,n}^t) \tag{15}$$

The position and position change (*velocity*) $v_{i,j}^{t+1}$ updating rules are given as below:

$$x_{i,j}^{t+1} = x_{i,j}^t + v_{i,j}^{t+1} \tag{16}$$

$$v_{i,j}^{t+1} = w.v_{i,j}^t + c_1 r_1 (p_{i,j}^t - x_{i,j}^t) + c_2 r_2 (g_j^t - x_{i,j}^t) \tag{17}$$

Where $i = 1,2,\ldots p$, $j = 1,2,\ldots,n$, p is the number of particles (the size of swarm), and n is the dimension of search space; $x_{i,1}^{t+1}$ is the position of the particle i and $v_{i,j}^{t+1}$ its velocity; w is called inertia weight, it is used to control the impact of the previous history of velocity on the current one; r_1 and r_2 are uniformly distributed random numbers between 0 and 1; c_1 and c_2 are positive acceleration constants; $p_{i,j}$ is the value of jth dimension of the best position ever visited by ith particle; g_j is the value of jth dimension of global best position ever visited by all particle in the swarm.

For discrete n-ary variables the difference is in the definitions of velocity updating rules where the position updating rule is based on logistic function as below (Michaud et al. 2009):

$$\begin{aligned} &x_{i,j}^{t+1} = n_k \text{ if } \varphi_{k-1} < S(v_{i,j}^{t+1}) \\ &x_{i,j}^{t+1} = n_l \text{ if } \varphi_{l-1} < S(v_{i,j}^{t+1}) \le \varphi_l \text{ with } 1 < l \le k-1 \\ &x_{i,j}^{t+1} = n_1 \text{ if } \varphi_1 \ge S(v_{i,j}^{t+1}) \end{aligned} \tag{18}$$

where

$S(v_{i,j}^{t+1}) = \dfrac{1}{1+e^{-v_{i,j}^{t+1}}}$ and $\varphi_1,...,\varphi_{k-1}$ are strictly ordered uniformly distributed random numbers between 0 and 1.

With the PSO algorithm, the leader determining that influences the updating of a particle position depends on the established neighbourhood topology. In a multi-objective optimisation problem it is function of the set of leaders already founded in the search space. Set of leaders are stored in a specific memory called extended memory (Hu et al. 2003). When a particle dominates some leaders in the extended memory, it is added to the leaders set and the dominated ones are discarded from the extended memory. The set of leader is reported as the final Pareto optimal set or Pareto front.

4.3. Multi-objective optimisation implementation

Attia et al. (2013), Evins (2013) and Stevanović (2013) underline and conclude on the necessity to develop tools, for sustainable building design, that integrate both, building physic simulation and optimisation process. Such tools have to reduce computation time, to be accurate, and to support decision-making. However, optimisation process can lead to a large computational burden especially when detailed simulation models are used (Wang et al. 2005).

Based on this observation, the optimisation framework consists to a preliminary design tool incorporating thermal meta-models generation, and optimisation process.

The flowchart of optimisation solution toolbox used in this work is illustrated in the figure 2 and is divided into five steps:

1. A multi-storey timber building is defined: architectural geometry, location and use are fixed parameters; constraints and decision variables are identified.
2. Thermal objectives are then modelled on *EnergyPlus* 7.2 for energy and comfort simulation; and corresponding meta-models are generated and used as objective functions
3. A sensitivity analysis is carried out on thermal objectives and non-influent parameters are fixed according to the designer.
4. Structural and environmental objectives are modelled using analytic functions and then implemented in *Ted*© tool (Tool for Ecodesign).
5. The PSO multi-objective optimisation process is then performed using the *Ted*© tool.

5. CASE-STUDY

The case-study building model was made in order to keep calculation time as short as possible. It is a simple rectangular office building without sun protection.

5.1. Description

The case-study (Figure 3) is a three-storey office building with as objective the optimisation of the building envelope composition. Architectural geometry, location and use are fixed parameters. The surface area is about 168 m² and ceiling height about 2,6m. Variables concern the building envelope such as insulation level, glazing, cross laminated timber (CLT) section and panels' thickness.

The building model was built using *OpenStudio* and exported to run in *EnergyPlus*. Each analysis of the model took around 40 seconds to run in *EnergyPlus*. Using such a simple model was judged to be beneficial because the aim of the paper was to set up an optimisation solution toolbox rather than to answer specific building-design questions. Twenty-four decision variables were selected (Table 1).

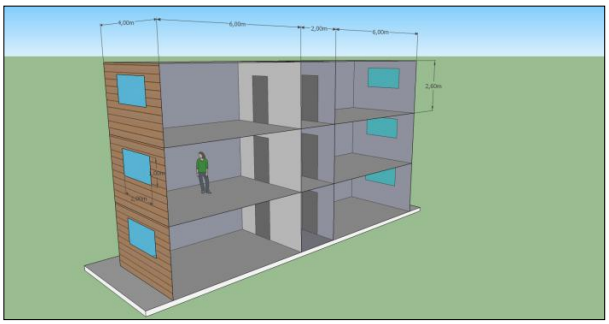

Figure 3: Case-study building

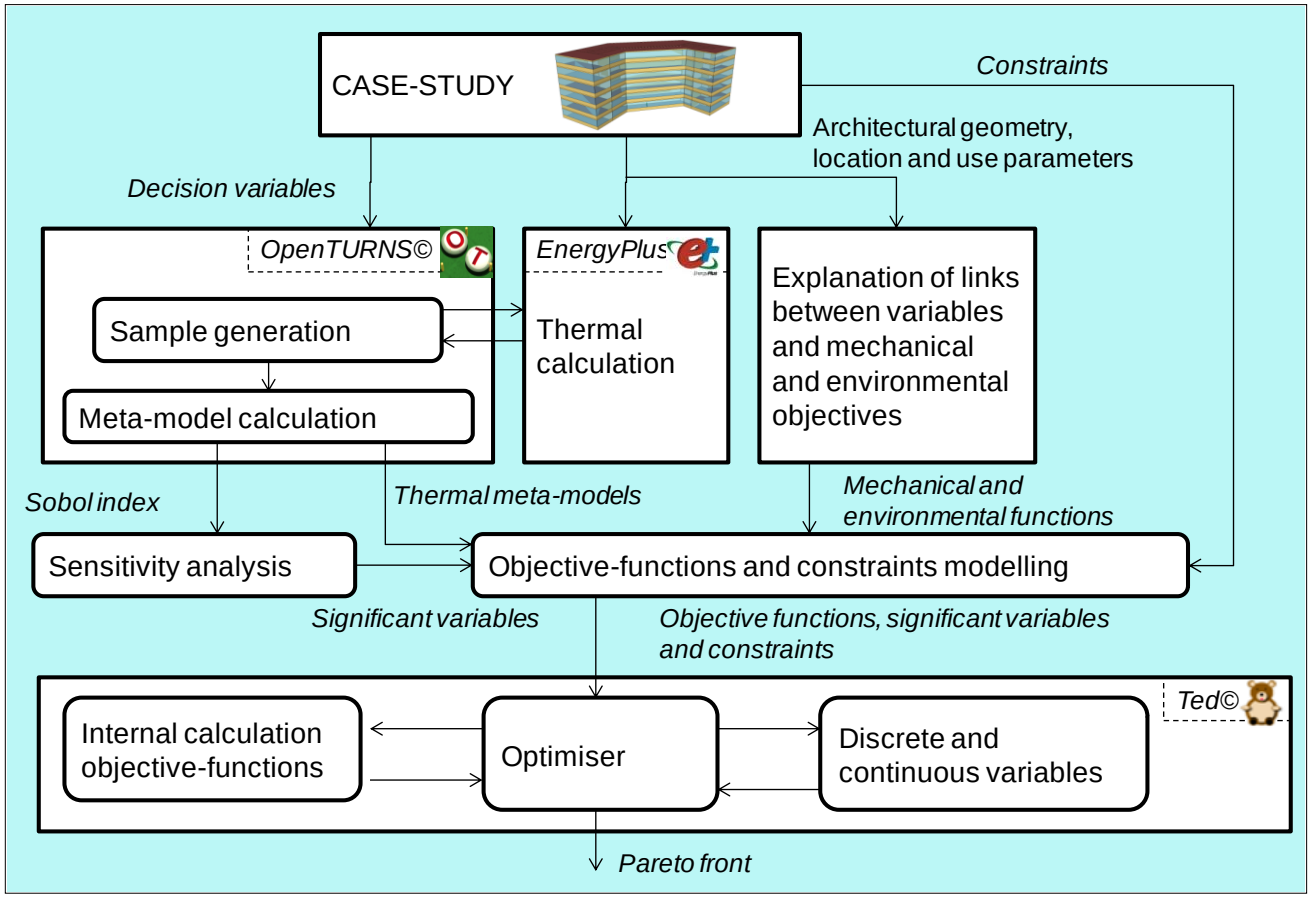

Figure 2: Summer comfort objective calculation

Table 1: Parameters description

xj	Description	Unit	Main relations
x0	Wall insulation thickness	m	$0.04 \leq x0 \leq 0.3$
x1	Wall CLT layers number	-	Discrete variable x1 = {3,5,7,9}
x2	Wall CLT thickness of longitudinal layers	mm	Discrete variable x2 = {20,30,40,50,60,70,80}
x3	Wall CLT thickness of transversal layers	mm	Discrete variable x3 = {20,30,40} and $x3 \leq x2$
x4	Wall CLT thickness	m	$0.06 \leq x4 \leq 0.2$ and x4 = ((x1+1)*x2+(x1-1)*x3)/2000
x5	Wall insulation conductivity	W/(m.K)	$0.03 \leq x5 \leq 0.04$
x6	Wall cover panels thickness	m	$0 \leq x6 \leq 0.04$
x7	Cover and ceiling panels density	kg/m^3	Discrete variable x7 = {800,2200}
x8	North windows U-value	W/(m².K)	$0.6 \leq x8 \leq 2$
x9	South windows U-value	W/(m².K)	$0.6 \leq x9 \leq 2$
x10	North windows solar factor	-	$0.35 \leq x10 \leq 0.6$
x11	South windows solar factor	-	$0.35 \leq x11 \leq 0.6$
x12	Floor insulation thickness	m	Constant x12 = 0.1
x13	CLT density	kg/m^3	$350 \leq x13 \leq 700$
x14	Floor concrete cover density	kg/m^3	Constant x14 = 2300
x15	Roof insulation thickness	m	Constant x15 = 0.2
x16	Roof CLT thickness	m	Constant x16 = 0.5
x17	Roof insulation conductivity	W/(m.K)	Constant x17 = 0.038
x18	Ceiling panels thickness	m	$0.006 \leq x18 \leq 0.04$
x19	Floor CLT layers number	-	Discrete variable x19 = {3,5,7,9,11}
x20	Floor CLT thickness of longitudinal layers	mm	Discrete variable x20 = {20,30,40,50,60,70,80}
x21	Floor CLT thickness of transversal layers	mm	Discrete variable x21 = {20,30,40} and $x21 \leq x20$
x22	Floor CLT thickness	m	$0.2 \leq x22 \leq 0.4$ and x22 = ((x19 + 1) * x20 + (x19 - 1) * x21) / 2000
x23	Floor concrete cover thickness	m	$0 \leq x23 \leq 0.06$
x24	Natural ventilation rate	vol/h	$0 \leq x18 \leq 4$

Table 2: Meta-models characterisation

Meta-model	Sample size	L^2	Linf	r
H_n 2^d order	600	0.5 kWh/(m².year)	9%	0.2 kWh/(m².year)
DH 2^d order	600	12 °C	7%	5 °C

5.2. Results and discussion

Meta-models have been first calculated with *OpenTURNS*® tool. *DH* was calculated only for the warmer zone during the warmer week of the year. H_n and *DH* meta-models have been based on a sampling of 600 data sets that were enough to obtain acceptable second order precision (Table 2). Simulation execution times of 23,1s and 7,7s were necessary to respectively calculate H_n and *DH*; total times of 5 hours and 7 minutes were required for establishing the two meta-models using personal computer (Windows® 8, 2.53 GHz Intel® Core™ processor, 4.00 Go RAM).

Then, a sensitivity analysis has been done using Sobol indices. They where oriented according to meta-model coefficients (Figure 4). Wall insulation thickness, windows U-value and windows solar factor influence both H_n and *DH*. The variations of certain parameters, as roof insulation thickness, do not influence the optimisation process and were implemented as constants (Table 1).

The PSO' parameters *w*, c_1 and c_2 have been respectively settled to 0.63, 1.45 and 1.45. With 300 particles and 100 iterations 38 minutes were necessary to the PSO' program Ted© to calculate a Pareto front of 52 solutions (Figure 5). With this simple case-study, 257 days would have been required to execute the same calculation using the detailed simulation models of the thermal objectives instead of meta-models.

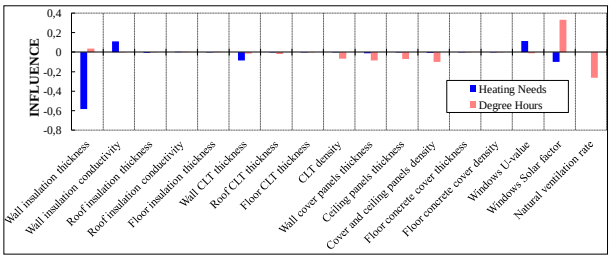

Figure 4: The influences of decision variable on H_n and *DH*

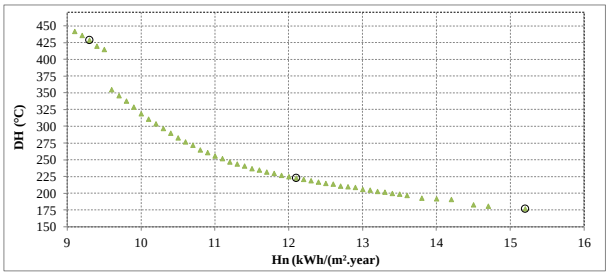

Figure 5: Pareto front for H_n and *DH objectives*

With a Pareto front made from two thermal objectives some parameters as wall insulation conductivity, wall cover panels' thickness and ceiling panels' thickness are constants. By integrating others objectives these parameters would have taken several values.

Table 3 illustrates three solutions in the Pareto front. When windows solar factor is low, insulation and CLT thickness are high; this compensates the deficit of solar gain by a best insulation. On the contrary when solar factor is high, insulation is lower and windows U-value is very low. Solutions on the Pareto front represent the best compromises between insulation and penetration of solar rays.

Table 3: Example of solutions in the Pareto front

Solution	*x0*	*x4*	*x10*	*x12*	*x14*	*x23*	H_n	*DH*
a	0.3	0.2	2200	1.4	0.35	0.03	15.2	177
b	0.25	0.18	2200	0.6	0.37	0.04	12.1	223
c	0.22	0.14	800	0.6	0.58	0.06	9.3	429

6. CONCLUSION

In this paper a methodology to optimise building envelope composition taking into account trade-off between heating needs, summer thermal comfort, floor vibration comfort, global warming potential and embodied energy objectives have been presented.

The optimisation framework which is a preliminary design tool incorporating thermal meta-models generation and optimisation process has been developed. The use of meta-models in state of detailed thermal simulation modelled saves time (from several months to less than one day) and reduces computing resources.

The multi-objective particle swarm optimisation (MOPSO) algorithm enables to calculate a Pareto front for both thermal objective functions. These functions use in the same time continuous and discrete variables.

On-going work on environmental and structural objectives will complete the optimisation process. Also integration of discrete variables concerning the structure type has to be performed.

ACKNOWLEDGMENTS

Appreciations and thanks to Dr. Merheb for useful help on meta-models generation and to Mr. Fernandez for discussion and assistance on optimization computing tool.

This work was performed under the funding of INEF4, research institute for energy transition.

REFERENCES

AFNOR. 2005a. *NF EN 1995-1-2 : Conception et calcul des structures en bois –partie 1-2 : Généralités - calcul des structures au feu*. P 21–712–1 pp.

AFNOR. 2005b. *NF EN 1995-1-1 : Conception et calcul des structures en bois – partie 1-1 généralités règles communes et règles pour les bâtiments*. P 21–711–1 pp.

Attia, S., Hamdy, M., O'Brien, W., Carlucci, S., 2013. Assessing gaps and needs for integrating building performance optimization tools in net zero energy buildings design. *Energy and Buildings* 60: 110–124.

Crestaux, T., Le Maître, O., Martinez, J.-M., 2009. Polynomial chaos expansion for sensitivity analysis. *Reliability Engineering & System Safety* 94 (7): 1161–1172.

Dutka-Malen, I., Lebrun, R., Saassouh, B., Sudret, B., 2009. Implementation of a polynomial chaos toolbox in OpenTURNS and applications to structural reliability and sensitivity analyses. *The 10th International Conference on Structural Safety and Reliability ICOSSAR 2009*.

Eberhart, R., Kennedy, J., 1995. A new optimizer using particle swarm theory. *MHS'95. Proceedings of the Sixth International Symposium on Micro Machine and Human Science*: 39–43.

Eisenhower, B., O'Neill, Z., Narayanan, S., Fonoberov, V. a., Mezić, I. 2012. A methodology for meta-model based optimization in building energy models. *Energy and Buildings* 47: 292–301.

Evins, R., 2013. A review of computational optimisation methods applied to sustainable building design. *Renewable and Sustainable Energy Reviews* 22: 230–245.

FCBA and CSTB, 2009. *Developpement de l'usage du bois dans la construction : Obstacles Réglementaires & Normatifs Bois Construction*. .

FPInnovations, 2011. *CLT Handbook*. .

Gabenisch, A., Maës, J., Mandret, N, 2012. *Marché actuel des nouveaux produits issus du bois et évolutions à échéance 2020. In* Nicole Merle-Lamoot, G. P. (ed.) .

Hu, X., Eberhart, R. C., Shi, Y., 2003. Particle swarm with extended memory for multiobjective optimization. *IEEE Swarm Intelligence Symposium*: 193–197.

Kennedy, J., Eberhart, R., 1997. A discrete binary version of the particle swarm algorithm. *IEEE International Conference on Systems, Man, and Cybernetics* 5: 4104–4108.

Machairas, V., Tsangrassoulis, A., Axarli, K., 2014. Algorithms for optimization of building design: A review. *Renewable and Sustainable Energy Reviews* 31 (1364): 101–112.

Merheb, R., 2013. *Fiabilité des outils de prévision du comportement des systèmes thermiques complexes.* Thesis (PhD). Université de Bordeaux.

Michaud, F., Castera, P., Fernandez, C., Ndiaye, A., 2009. Meta-heuristic Methods Applied to the Design of Wood--Plastic Composites, with Some Attention to Environmental Aspects. *Journal of Composite Materials* 43 (5): 533–548.

Ndiaye, A., Castéra, P., Fernandez, C., Michaud, F., 2009. Multi-objective preliminary ecodesign. *International Journal on Interactive Design and Manufacturing (IJIDeM)* 3 (4): 237–245.

Sobol, I., 1993. On sensitivity estimation for nonlinear mathematical models. *Mathematical Modelling and Computation Experiments* 1 (4): 407–414.

Stevanović, S., 2013. Optimization of passive solar design strategies: A review. *Renewable and Sustainable Energy Reviews* 25: 177–196.

Tresidder, E., Zhang, Y., Forrester, A., 2012. Acceleration of building design optimisation through the use of kriging surrogate models. *Building Simulation and Optimization Conference* (September): 1–8.

Wang, W., Rivard, H., Zmeureanu, R., 2005. An object-oriented framework for simulation-based green building design optimization with genetic algorithms. *Advanced Engineering Informatics* 19 (1): 5–23.

Wiener, N., 1938. The homogeneous chaos. *Amer. J. Math* 60 (4): 897–936.

SIMULATION OF AN ISOLATED WIND HYDRO SYSTEM

R. Sebastián[(a)], J. Quesada[(b)]

[(a)] Department of Electrical, Electronic and Control Engineering (DIEEC), Spanish University for Distance Education, UNED 28040 Madrid, Spain
[(b)]University of the Basque Country UPV/EHU, E.U.I. Vitoria-Gasteiz, Nieves Cano 12, 01006 Vitoria-Gasteiz, Spain

[(a)]rsebastian@ieec.uned.es, [(b)]jeronimo.quesada@ehu.es

ABSTRACT
In this paper it is presented the modeling and the dynamic simulation of a Wind Hydro isolated Power System (WHPS) consisting of a Hydraulic Turbine Generator (HTG), a Wind Turbine Generator (WTG), the consumer Load and a Dump Load. The models of the hydraulic turbine along with its penstock and the wind turbine are presented. The Synchronous Machine of the HTG provides the isolated system voltage waveforms so the HTG must be always running. The used hydraulic turbine speed governor is isochronous so that the isolated system frequency will be kept in its rated value. The WTG provides active power to the isolated system when enough wind is available and its induction generator consumes reactive power. The WHPS is simulated for a positive load step and a positive wind speed step and graphs for the main system variables: system frequency and voltage and active powers of each component of the WHPS are presented. The simulations show how the WTG induction generator increases the system stability.

Keywords: Wind Turbine Generator, Hydro Turbine Generator, Isolated microgrid, Power systems Simulation

1. INTRODUCTION

Remote microgrids (RMG) are microgrids [Lasseter 2002] and [Basak et al. 2012] deployed in remote geographical areas either isolated from the distribution grid or with an intermittent or low-reliability connection to it. Isolated power systems are traditionally based on diesel generators (DG) but when combined with renewable energy sources and energy storage [Sebastian 2013], they acquire the characteristics of a microgrid. Wind power and Hydro power are two sources of renewable energy. Both types of renewable energy are site dependent, enough available wind is needed for wind power and a river and the possibility of building a dam is needed for hydro power. Fig.1 shows a Hydraulic turbine (HT) driving a Synchronous Machine (SM) forming a Hydraulic Turbine generator (HTG) and a Wind Turbine driving an Induction Generator (IG) forming a Wind Turbine Generator (WTG). Both HTG and WTG are combined to form an isolated Wind Hydro Power System (WHPS) to supply the isolated community electric load. Also a DL is in Fig.1 to balance active power when an excess of generating power exists.

In the WHPS of Fig. 1 the HTG is always running since the SM generates the voltage waveform of the isolated grid. The WTG will be connected to the isolated grid when enough wind is available. Two operation modes are possible in the WHPS of Fig.1: Hydro Only (HO) mode where the HTG supplies all the demanded active and reactive power (WTG is disconnected) and Wind Hydro (WH) mode where in addition to HTG the WTG also supply active power.

2. THE ISOLATED POWER SYSTEM

The hydraulic turbine (HT) converts water pressure into mechanical shaft power (Paish 2002). As Fig. 1 shows the HT drives the Synchronous generator SM. The hydraulic turbine is modeled with a nonlinear turbine model. Non-linear turbine models are required when speed and power changes are large during the hydraulic turbine operation which is the case of this article. The mechanical power produced by the HT $P_{h\text{-}mec}$ is proportional to the product of the effective pressure head of water above the turbine H, the volume flow rate passing through the turbine Q and the hydraulic efficiency of the turbine η:

$$P_{h\text{-}mec} = \rho g H Q \eta \quad (1)$$

where ρ is the density of water and g is the acceleration due to gravity. Another way to take into account the hydraulic efficiency η if it is assumed constant and independent of Q, is to consider in eq. (1) an effective flow which is the difference of actual flow Q from the no load flow Q_{nl}:

$$P_{h\text{-}mec} = (Q - Q_{nl}) \rho g H \quad (2)$$

The mechanical power produced by a HT is varied to meet variations in load demand by regulating the turbine flow rate Q. For this aim a needle valve is used in impulse type turbines and a wicket gate is used in

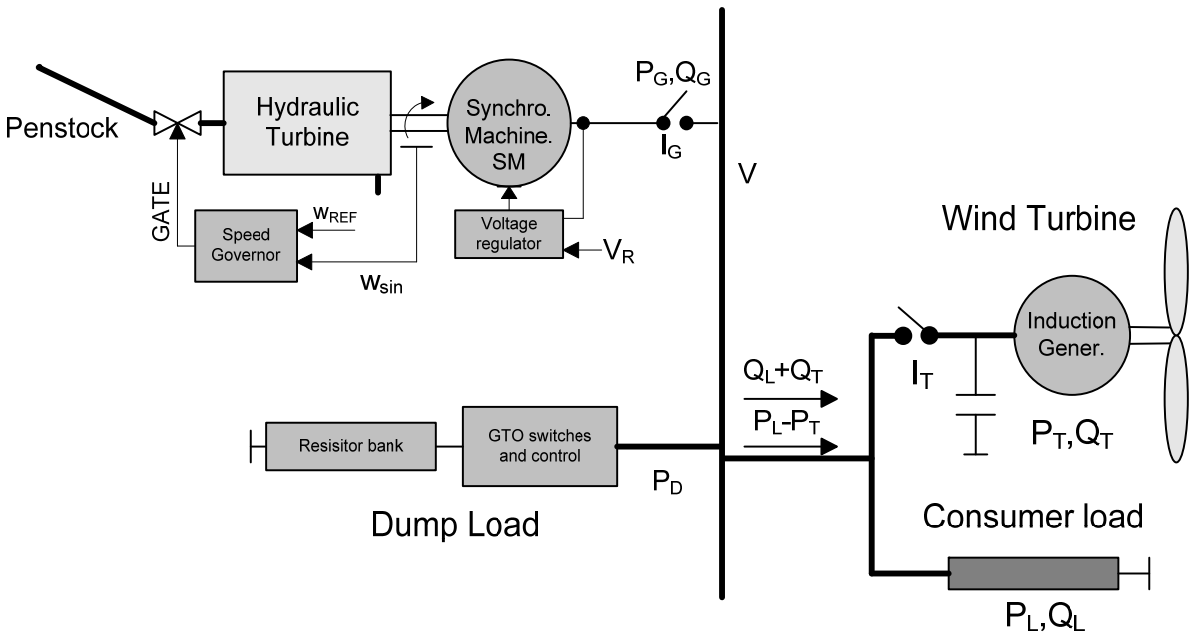

Fig. 1. Layout of the Wind-Hydro isolated Power System

reaction type turbines (Lucero 2010). The pressure head above the turbine per unit h is related to the per unit flow rate q by assuming that the turbine can be represented by the valve characteristic:

$$q = yh^{1/2} \quad (3)$$

where y is the turbine gate opening position, which has values from 0 (fully closed) to 1 fully open, $q = Q/Q_{base}$, where Q_{base} is the turbine flow rate with the gate fully open and $h=H/H_{base}$, where H_{base} is the total available static head above the turbine (Mello et al. 1992).

Equation (2) in per unit power on SM rated power base and taking into account a speed deviation effect which is a function of the gate opening y can be expressed as (Mello et al. 1992):

$$p_{h\text{-}mec} = A_t(q - q_{nl})h - K_D y(\omega\text{-}1) \quad (4)$$

where q_{nl} is the no load flow rate per unit, (ω-*1*) is the difference between the actual HT speed in per unit ω and the rated turbine speed 1 pu, K_D is the damping torque coefficient and A_t is a proportionality factor and is assumed constant. A_t is calculated using HT active rated power and SM apparent rated power (Mello et al. 1992).

The penstock is a pressure pipe that conveys the water to the turbine. The penstock is modeled assuming an inelastic conduit and incompressible fluid. Also the traveling pressure wave effects are neglected, so that this penstock model is valid only for short-medium lengths penstocks. If the penstock has length L (m), an area A (m^2), H_o and H are the static heads of water column at the beginning and end of the penstock respectively and the H_f is head loss due to friction in the penstock, the second Newton´s law applied to the penstock gives (Mello et al. 1992):

$$\frac{dQ}{dt} = \frac{gA}{L}(H_o - H - H_f) \quad (5)$$

Eq. (5) expressed in per unit values becomes:

$$\frac{dq}{dt} = \frac{1}{T_W}(1 - h - h_f) \quad (6)$$

where T_W is the water time constant or water starting time (secs) defined as:

$$T_W = \frac{L}{Ag}\frac{Q_{base}}{H_{base}} \quad (7)$$

In the simulations ahead the penstock friction losses H_f in eq. (5) and the damping torque coefficient K_D in eq. (4) are considered null, so that the system stability of the WHPS simulated will be worse since these natural damping are not taking into account.

The SM of Fig. 1 generates the voltage waveform of the isolated grid and its automatic voltage regulator controls the system voltage to be within the prescribed levels. For this reason the SM must be always running close to its rated speed. The SM has a rated power ($P_{SM\text{-}NOM}$) of 300 kVA, it receives the HT mechanical output power and converts it in electrical power. The SM electrical part is represented by a sixth-order model. An IEEE type 1 Voltage regulator plus an exciter regulates the voltage in the SM terminals.

The WTG in Fig.1 consists of a Wind Turbine (WT) driving an Induction Generator (IG) directly connected to the autonomous grid conforming a constant speed stall-controlled WTG (no pitch control).

The mechanical power produced by a WT (Sebastian and Peña 2011) is:

$$P_{T-MEC} = \frac{1}{2}\rho A v^3 C_P \quad (8)$$

where ρ is the air density, v is the wind speed, A is the area swept by the turbine blades and C_P is the power coefficient. C_P is a function of the Tip Speed Ratio (TSR=$R\omega_r/v$, where R is the blade length and ω_r is the WT shaft speed) and the blade pitch. Since the WTG used in this paper has no pitch control, C_P is only a function of TSR. In addition, the IG speed range variation in the WTG is very limited and thus C_P can be considered in first approximation as a function only of the wind speed. As the wind speed is quasi-random there is no way to control the active power that the WTG produces, so the WTG behaves as an uncontrolled source of active power. The IG consumes reactive power so a capacitor bank has been added in Fig. 1 to compensate the power factor. The simulated constant speed stall controlled WTG model follows the one in (Gagnon et al. 2002) and has an Induction Generator (IG) of 275 kW (WTG rated power $P_{T\text{-}NOM}$ = 275 kW) and the Wind Turbine (WT) block described later. The electrical part of the IG is represented by a fourth-order model. Typical inertia constant H_W values for WTGs are between 2 and 6 seconds (Knudsen and Nielsen 2005). As the WTG used in the article is a low power one, the low limit of the previous range, 2 seconds, is assigned to H_W.

The Dump Load (DL) of Fig.1 consists of a set of semiconductor power switches and a bank of resistors. By closing/opening these power switches, the DL consumed active power can be controlled behaving as a controlled sink of active power. The DL of (Sebastián and Peña 2010) is used and consists of eight three phase resistors connected in series with GTO switches. The resistors values follow an 8 bit binary progression so that the power consumed by the DL, assuming that the voltage in the isolated grid is nominal, can be expressed in the form:

$$(I_0+I_1\cdot 2^1+..+I_7\cdot 2^7)\cdot P_{STEP} = X_{D\text{-}REF}\cdot P_{STEP} \quad (9)$$

(9) means that the power can be varied discretely from 0 to $255\cdot P_{STEP}$, where P_{STEP} is the power corresponding to the least significant bit and I_J is "1" when the associated GTO is turned on and "0" when the GTO is turned off. For this article P_{STEP} = 1.4 kW and therefore $P_{D\text{-}NOM}$ = 357 kW. The DL is used in the isolated WHPS to consume power when there is an excess of generated power. This active power consumption is temporary until the HTG has adjusted its produced power to the needed power. In other isolated hydro power systems (Paish 2002) the HTG always run at full power and speed control is achieved by adjusting the DL consumed power instantly so that the sum of the powers consumed by the load and the DL is equal to the HTG generated power.

2.1. The HT speed governor system

The isolated power system frequency f is regulated by maintaining an instantaneous balance of the active power consumed and produced. The HT/SM shaft speed ω (rad/s) is related with the system frequency (frequency of the voltage waveform) f (Hz) by:

$$\omega = 2\pi f/p \quad (10)$$

with p the number of pole pairs of the SM. The used SM in this article has p=16 and the isolated system frequency is f= 60 Hz, so the HTG rated speed is 187.5 rpm.

The HT speed governor modulates the HT produced power in order to accomplish active power balance, so the HT behaves as a controlled source of active power. To vary HT produced power, the HT governor regulates the inlet of water into the turbine through the gate variable as explained previously.

The speed control of the HT used in this article is isochronous, so the HT will run at constant speed provided that the HT demanded load is in the range spanning from 0 to its rated power. The HT governor consists of a PID speed regulator and a servo which converts the speed regulator output in the corresponding GATE opening. As the speed control is isochronous, the speed controller does not include permanent speed droop, which can help to improve the power system stability in isolated operation. The PID K_p, K_i and K_d parameters are calculated according to (Hagihara et al. 1979):

$$K_p = 1.6H/T_W \quad (11)$$

$$K_i = 0.48Kp/(3.33T_W) \quad (12)$$

$$K_d = 0.54H \quad (13)$$

where H is the HTG inertia constant (secs) and T_W is the previously defined water time constant. For a low speed HTG (< 200 rpm) as the present case H is between 2-3 seconds (Kothariand and Nagrath 2003). The first figure of the previous range is applied to H, as the HTG used in the article is a low power one. For the penstock it is assumed a short length one with T_W= 1 sec. With H=2 secs for the HTG and T_W= 1 sec for the penstock, the parameters in (11)-(13) are calculated conforming the PID speed controller used in the described simulations below.

3. SIMULATION RESULTS

The isolated WHPS of Fig.1 were simulated using the MATLAB-Simulink multipurpose simulation software [Matlab 2014]. The WHPS Simulink schematic can be seen in Fig. 2. Some of the components described previously and shown in Fig.2, such as the IG, the SM and its voltage regulator, the consumer load, etc. are blocks which belong to the SimPowerSystems library for Simulink. The Hydro Turbine block implements all the equations (1) to (7) that described the HT, gate and penstock behavior. It receives as inputs the constant 1

pu speed reference, the current HTG speed ω and deviation speed $d\omega$ and outputs the mechanical power $P_{h\text{-}mec}$ to take the HTG speed to 1 pu speed reference.

The WT block of Fig. 2 contains the wind turbine power curves which define the mechanical power in the WT shaft $P_{T\text{-}MEC}$ as a function of the wind speed and the WT shaft speed as it is described in eq. (8). This $P_{T\text{-}MEC}$ is divided by the WT speed to calculate the mechanical torque applied to the WTG-IG.

For sake of clarity the DL is not shown in Fig.2 as the DL is not needed throughout the tests presented ahead (the HTG accommodates it output power to the consumer load and WTG power variations) so the DL does not actuate and its consumed active power is zero.

The results of the simulation are shown with the following variables: the frequency per unit (fpu) and WTG-IG speed per unit (Fig 3), the RMS voltage per unit (Fig 4) and the active powers for the WTG, HTG, and consumer load (Fig 5) in kW. In Fig. 5 the active power is considered positive if produced and negative if consumed. At the test starting point the wind speed is 7 m/s, the WTG and HTG are producing active powers of 50 kW and 200 kW respectively and the load is consuming active power of 250 kW being the system at steady state.

In t=1 s the extra 30 kW resistive load is connected to the system (10% of the HTG rated power) by closing the 3 phase breaker of Fig. 2 as it can be observed in the load active power curve in Fig. 5. Fig. 5 also shows that the load power oscillates due to the voltage variations (minimum-maximum: 0.9806-1.0074 pu) observed in Fig. 4 after the connection of this extra load (main and extra loads are purely resistive). Additionally Fig. 5 shows that the wind power presents a transient due to the 30 KW positive load step. Fig. 3 shows that the system frequency reduction after the load step contributes to increase sharply the difference between the WTG-IG speed and the fpu (IG slip). The WTG active power is approximately proportional to the IG slip, so the IG slip increase makes the WTG to instantaneously increase power production at expense of its kinetic energy as Fig 5 shows. This is a desirable effect since counter acts the frequency dip by providing more power to the grid, increasing the damping and therefore the isolated power system stability. In steady state the wind power has the same value as the initial one in t=0, since the wind speed has not changed. Fig. 3 shows that the IG speed is greater than the fpu (IG slip positive) during the load step transient so that the WTG behaves as a generator the whole transient. The fpu/IG speed minimums and maximums are 0.9743 (-2.57%)/0.9772 and 1.0043/1.0072, and both responses are lightly over oscillating. Fig. 5 shows that the power in the HTG increases with oscillations at the beginning of the load step and at steady state reached at t= 28,268 s, the HTG assumes the increase of load with a final power of 230 kW.

In Fig. 3 it is also plotted the system fpu response to the +30 kW extra load in HO mode, i.e. with only the HTG supplying the consumer load (WTG disconnected). It can be seen that the fpu minimum and maximum are 0.9529 (-4.71%) and 1.0145 respectively and the fpu response is over oscillating. If the HO fpu response it is compared with the previous fpu in WH mode, it is demonstrated that when the WTG also supplies power, the WTG adds damping so that the isolated power system stability is greater.

In t = 41 s the wind speed changes suddenly from its initial value of 7 m/s to 8 m/s. Fig 3 shows that the IG slip increases, but its variation is smoother than in the load step case since in this case the system frequency increases and part of the captured wind power is converted in WTG kinetic energy. Fig. 5 shows the corresponding increasing in the WTG power

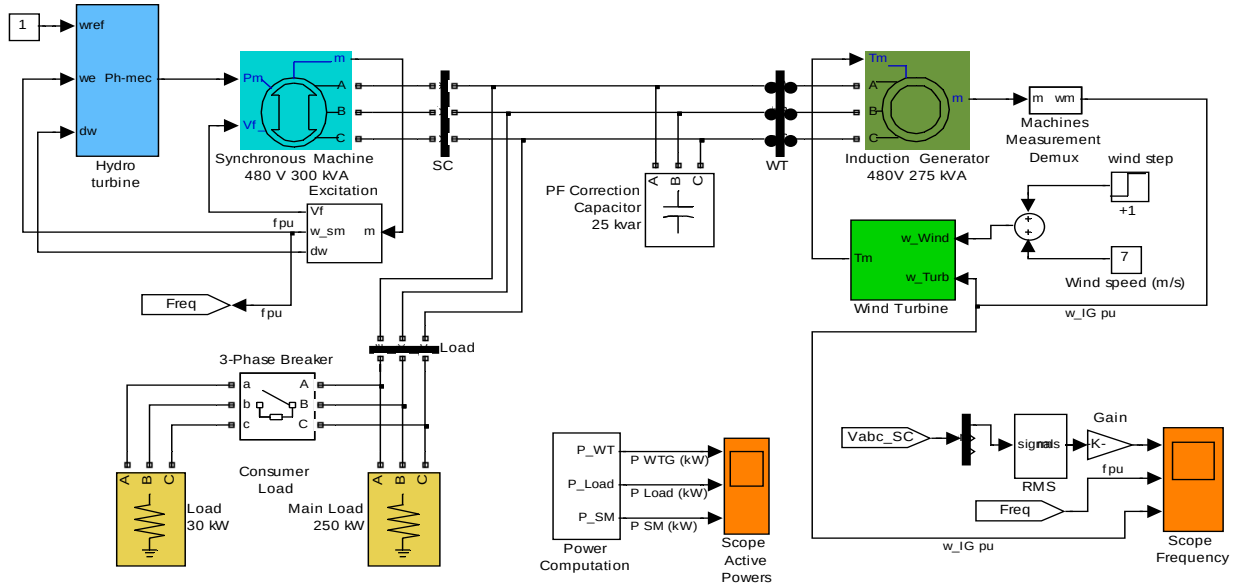

Fig. 2. Wind-Hydro isolated Power System Simulink schematics

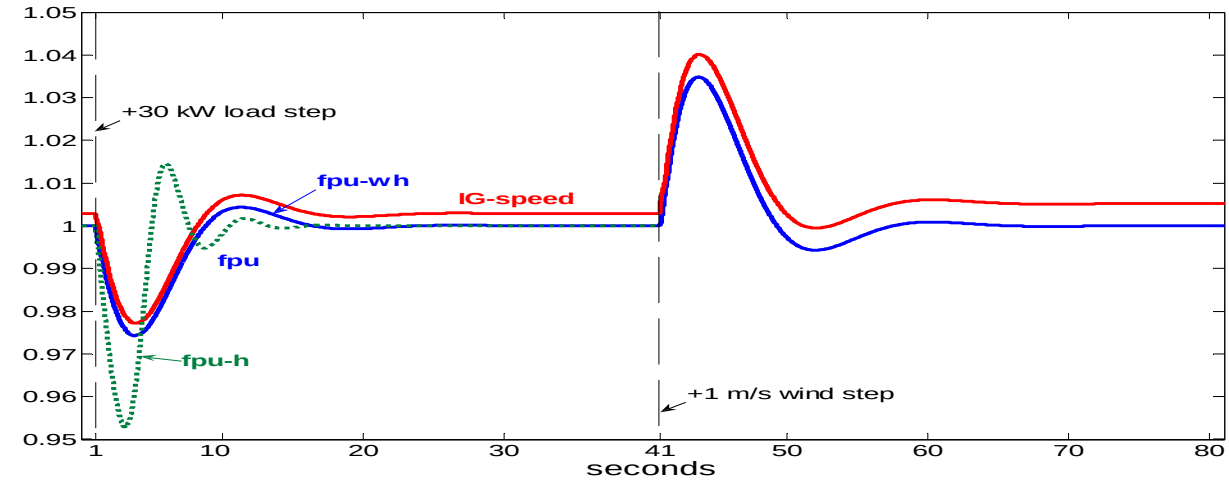

Fig. 3. Frequency and IG generator speed per unit

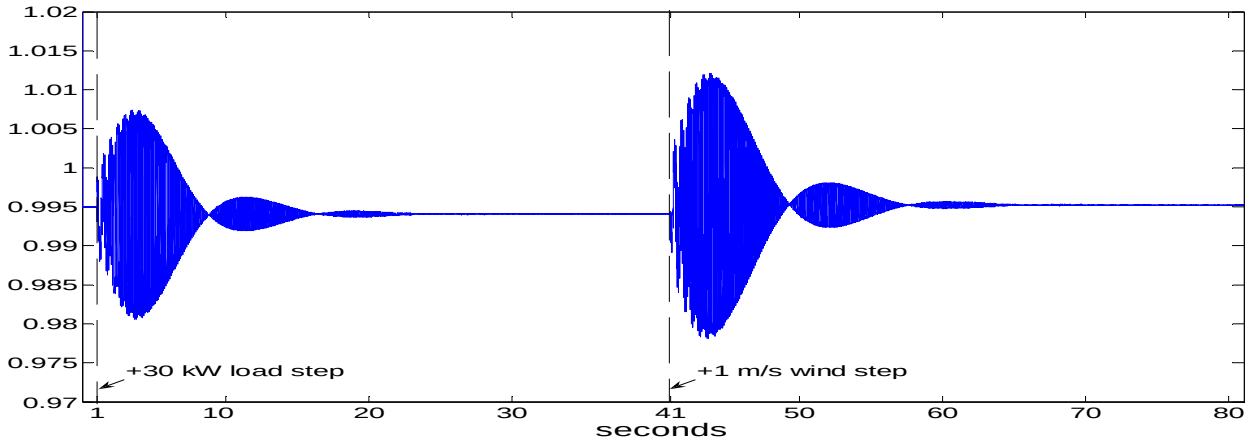

Fig. 4. RMS Voltage per unit

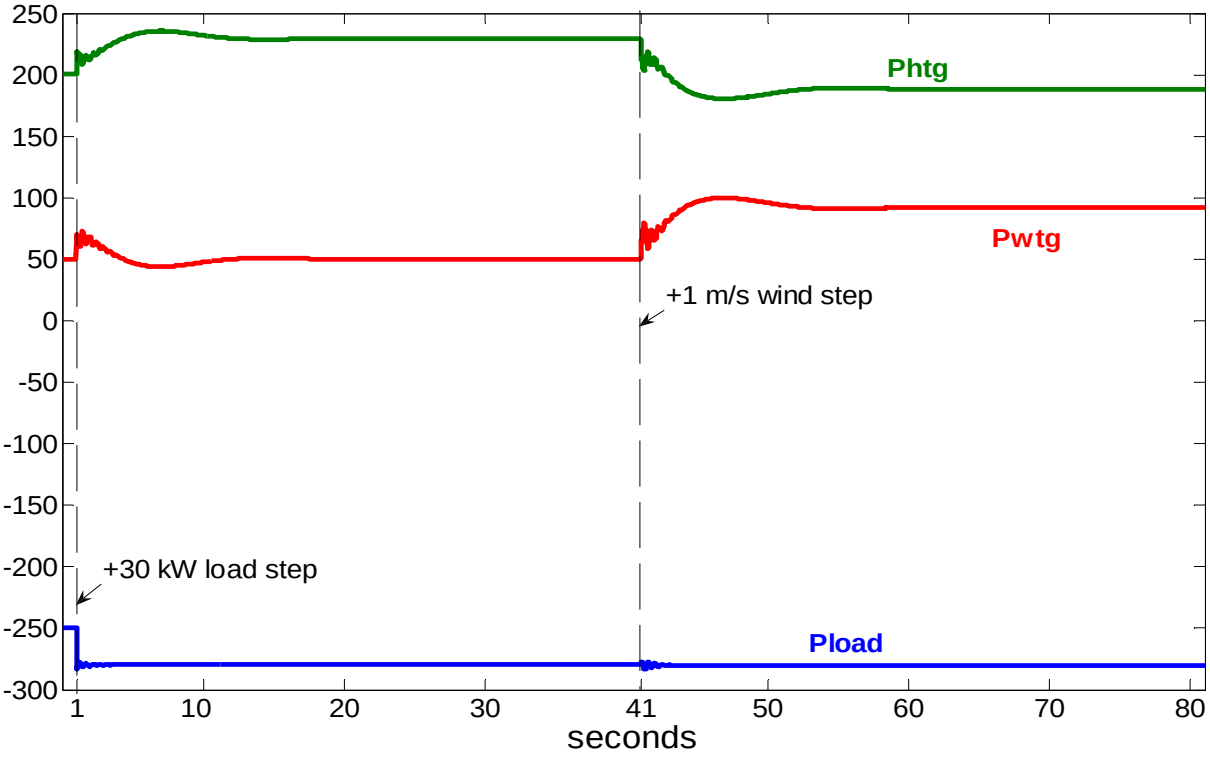

Fig. 5. Generated(+)/consumed(-) active Powers (kW) by the WTG, HTG and Load

from its initial 50 kW value to 92 KW in steady state. Fig. 3 shows fpu/IG speed maximums of 1.0348 (+3.48%)/1.0402 being in addition both responses under oscillating. The minimum–maximum voltages during this wind step are 0.9781-1.0121pu. Fig. 5 shows that the HTG active power decreases with oscillations at the beginning of the wind step. In steady state, reached at t = 59.188 s the HTG accommodates its output power to the new situation generating 188 kW.

4. CONCLUSSIONS

The WDPS model has been presented and tested for positive load and wind steps. The detailed models of the HT and its penstock and the WT have been described. The simulations show the damping that the WTG adds to the isolated system increasing the power system stability.

ACKNOWLEDGMENTS

The authors would like to thank the DIEEC-UNED for supporting partly the attendance to the conference.

REFERENCES

Basak P., S. Chowdhury, S. Halder nee Dey, S.P. Chowdhury, A literature review on integration of distributed energy resources in the perspective of control, protection and stability of microgrid, Renew. Sustain. Energy Rev. 16 (2012) 5545–5556.

Gagnon, R.; Saulnier, B.; Sybille, G.; Giroux, P.: "Modelling of a Generic High-Penetration No-Storage Wind-Diesel System Using Matlab/Power System Blockset", 2002 Global Windpower Conference, April 2002, Paris, France

Hagihara, S. et al, 1979, Stability of a Hydraulic Turbine Generating Unit Controlled by P.I.D. Governor, Power Apparatus and Systems, IEEE Transactions on, 1979.PAS‐98(6): p.2294‐2298.

Knudsen H., Nielsen J. N., Introduction to the modeling of wind turbines, In *Wind Power in Power Systems*, T. Ackermann, Ed. Chicester, U.K. Wiley, 2005, pp. 525–585

Kothari, D. P. , Nagrath I. J., Modern power system analysis**,** Tata McGraw-Hill Education, 2003

Lasseter R., Microgrids, in: Proceedings of the IEEE PES Winter Meeting, vol. 1, 2002, pp. 305–308.

Lucero L.A., 2010. Hydro Turbine and Governor Modelling: Electric - Hydraulic Interaction, Master Thesis, June 2010, Norwegian University of Science and Technology

Matlab 2014, The MathWorks Inc., "Matlab –Simulink documentation", available in: http://www.mathworks.es/es/help/index.html

Mello F.P. et al, Hydraulic turbine and turbine control models for system dynamic studies. Power Systems, IEEE Transactions on, 1992. 7(1): p. 167‐179.

Paish O., 2002. Small hydro power: technology and current status, Renewable and Sustainable Energy Reviews, Volume 6, Issue 6, December 2002, Pages 537-556, ISSN 1364-0321, http://dx.doi.org/10.1016/S1364-0321(02)00006-0.

Sebastián R., Peña Alzola R., 2010 , Effective active power control of a high penetration wind diesel system with a Ni–Cd battery energy storage, Renewable Energy, Volume 35, Issue 5, May 2010, Pages 952-965, ISSN 0960-1481, http://dx.doi.org/10.1016/j.renene.2009.11.029.

Sebastian R., 2011, Modelling and simulation of a high penetration wind diesel system with battery energy storage, International Journal of Electrical Power & Energy Systems, Volume 33, Issue 3, March 2011, Pages 767-774, ISSN 0142-0615, http://dx.doi.org/10.1016/j.ijepes.2010.12.034.

Sebastián R., Peña Alzola R., 2011. Simulation of an isolated Wind Diesel System with battery energy storage, Electric Power Systems Research, Volume 81, Issue 2, February 2011, Pages 677-686, ISSN 0378-7796, http://dx.doi.org/10.1016/j.epsr.2010.10.033.

Sebastián R., 2013. Reverse power management in a wind diesel system with a battery energy storage, International Journal of Electrical Power & Energy Systems, Volume 44, Issue 1, January 2013, Pages 160-167, ISSN 0142-0615, http://dx.doi.org/10.1016/j.ijepes.2012.07.029.

NUMERICAL INVESTIGATION OF BOUNDARY LAYER DETACHMENT BY ACTIVE FLOW CONTROL

Karunakaran Hemrijicks[(a)], Tonino Sophy[(b)], Julien Jouanguy[(c)], Arthur Da Silva[(d)], Luis Lemoyne[(e)]

[(a)] [(b)] [(c)] [(d)] [(e)]DRIVE – ISAT EA 1859, 49, Rue Mademoiselle Bourgeois, 58000 NEVERS, FRANCE

[(a)]joe.karna90@gmail.com , [(b)]tsophy@u-bourgogne.fr , [(c)]julien.jouanguy@u-bourogne.fr , [(d)]arthur.da-silva@u-bourgogne.fr , [(e)]luis.le-moyne@u-bourgogne.fr .

ABSTRACT

After decades of investigations have failed to produce a positive outcome on flow control technologies that requires complex devices and micro-plumbing, recent technologies like synthetic jets, DBD (Dielectric Barrier Discharge) seems to be promising and these technologies can overcome limitations of the old ones. Our work mainly deals with delaying boundary layer detachment of over an aerodynamic body (Air foil). In this paper we produce our study of an active flow control device over the BL detachment point over a circular cylinder by the aid of simulations. Results from the uncontrolled flow seem to be in accordance with literature and the presence of the jet has an effect on the boundary layer.

Keywords: Detachment point control, Flow control technologies, Synthetic jets and Boundary layer.

1. INTRODUCTION

Boundary layer is formed when a fluid is obstructed by the body. This thin layer is formed due to the viscous friction of the adjacent layers of the fluid. This boundary layer detaches from the body when the pressure gradient is adverse (Prandtl 1904). Adverse pressure gradient and its effect on the detachment are explained in fig 1.

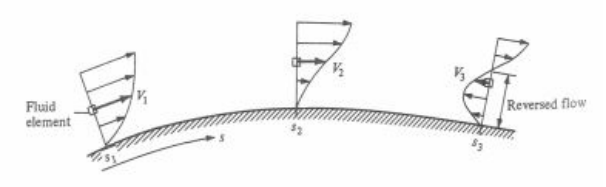

Figure 1 Pressure gradient and BL detachment

This detachment may be avoided or delayed when the transition occurs from laminar to turbulent boundary layer. Since turbulent boundary layer creates more friction drag than laminar, there is a need for new technologies for manipulating detachment of this boundary layer (David C Hazen 1962). The manipulation may be done by mixing or reenergizing a boundary layer. In other words low momentum bottom layers are replaced by higher momentum fluid streams so that the boundary layer detachment is delayed or avoided.

Though for nearly a century has been spent to improve the energetic of automobiles and aircrafts. Many innovations and technologies have been developed to make the vehicle more energy efficient. The detachment occurs due to the shape of the body (a sharp edge or rear end). In commercial vehicles like trucks body have improved aerodynamically to reduce the drag (Ola Logdberg 2008). In motorsport aerodynamics is more crucial to push the vehicle ahead of current performance. In aviation apart from these aerodynamic developments in the body there is a need for technologies like flow control devices that induces primary vortex that energizes boundary layer and delays the detachment. These devices are classified in to two categories:

1. Passive devices (fig 2) are mechanical devices or alterations made on the exterior body of the vehicle. These devices create stream wise vortices that convert the low momentum fluid layers with free stream so that to influence adverse pressure gradient and delay BL detachment. Rigidity in the control and drag penalty are the drawbacks.

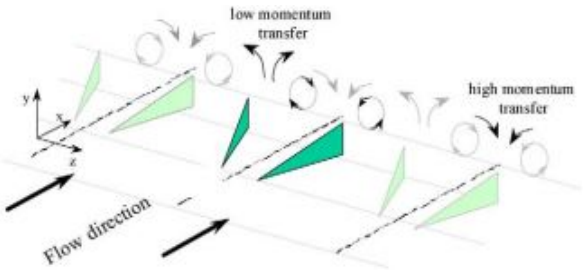

Figure 2 Passive Vortex Generator

2. Active devices are technologies integrated on the body.

Recent experiments show that passive devices have better performances than active devices but they have drag penalties and they are not controlled according to the requirement (Godard *et al* 2006a, b and c).

Active devices that are type of momentum inducing devices (reciprocating piston type or jet type) were commonly investigated early the past decades. But these devices need complex plumbing, wiring and are inefficient in terms of energy required to generate jets. Recently synthetic jets (Zero Net Mass Flow Jets), a new type of flow control device which has been widely investigated by researchers. They are called as Zero Net Mass Flow Jets because unlike former jets they induce momentum (energy) and more energy is saved here. Piezoelectric jets (Fig 3) and Dielectric barrier discharge jets are common synthetic devices (Widjanargo et al 2012). Their research and investigation has its significance not only in commercial automobile and aviation but also extends in unmanned micro aerial vehicles.

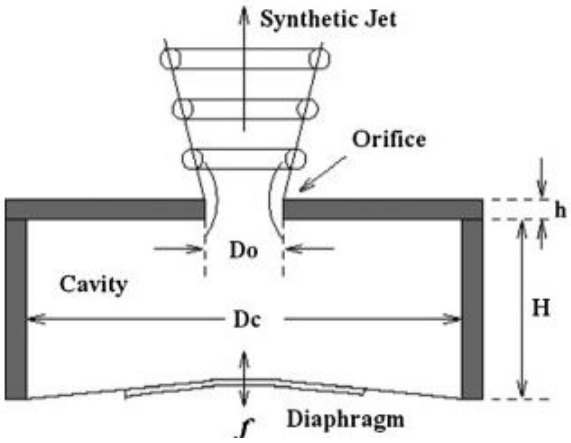

Figure 3 Piezo-electric synthetic jet

Our concentration is in delaying the separation and to begin with our work we chose to study the separation of boundary layer on a circular cylinder by computer aided numerical simulation. Our first phase deals with creating a basic computational model of a cylinder and validating the model by comparing the results (Mean velocity profiles and pressure coefficient curve). Results are compared with verified computational and experimental with results that are extracted from literature (Muddada 2010). Final phase will be introducing a simple flow control device (jet) and analysing the outcome.

2. SIMULATION PROCEDURE

Though 3D simulations are possible although due to cost and time constraints we chose 2D computational simulations with the aid of a computational solver called Star-ccm+. A finite volume approach is followed in these simulations. Moreover a URANS model easily allows a statistic representation of the flow

2.1. Mathematical models

Classical methods such as DNS (Direct Numerical Simulations) and LES (Large Eddy Simulaitons) are available and very accurate. But as said before RANS and URANS are able to predict experimental result on flow statistics with low computational cost. So we chose to go with Unsteady Reynolds Averaged Navier Stokes model (URANS) equations (1&2).

$$\frac{\partial \overline{U_i}}{\partial t}+\frac{\partial\left(\overline{U_i U_j}\right)}{\partial x_j}=-\frac{1}{\rho}\frac{\partial \overline{P}}{\partial x_j}+\nu\frac{\partial^2 \overline{U_i}}{\partial x_i \partial x_j}+\frac{\partial \overline{U_i' U'}_j}{\partial x_j} \quad (1)$$

$$\frac{\partial \overline{U_i}}{\partial x_i}=0 \quad (2)$$

The k-ε model is the turbulence model, in which the first equation (3) models the turbulent energy k and the second equation (4) models the turbulence dissipation ε.

$$\frac{\partial(\rho k)}{\partial t}+\frac{\partial\left(\rho k \overline{U}_i\right)}{\partial x_i}=\frac{\partial\left[\left(\mu+\frac{\mu_t}{\sigma_k}\right)\frac{\partial k}{\partial x_j}\right]}{\partial x_j}\ldots \quad (3)$$

$$\ldots+P_k+P_b-P_\varepsilon-Y_M+S_k$$

$$\frac{\partial(\rho\varepsilon)}{\partial t}+\frac{\partial\left(\rho\varepsilon \overline{U}_i\right)}{\partial x_i}=\frac{\partial\left[\left(\mu+\frac{\mu_t}{\sigma_{k\varepsilon}}\right)\frac{\partial \varepsilon}{\partial x_j}\right]}{\partial x_j}\ldots \quad (4)$$

$$\ldots+C_{1\varepsilon}\frac{\varepsilon}{k}\left(P_k+C_{3\varepsilon}P_b\right)-C_{2\varepsilon\rho}\frac{\varepsilon^2}{k}+S_\varepsilon$$

2.2. Grid details and meshing

The (2.56 × 1.28) 2D domain is meshed using the integrated Starccm+ meshing tool.The cylinder centred at (x,y) = (0.64,0.64) is 0.08 diameter. Fig 4 shows the quadric refined 2D mesh grid we created for this simulation. Prism layer mesher, Trimmer and Surface remesher are the other models used in here. The base size of the mesh is chosen to be 0.02 m to get an accurate model. The refinement near the cylinder is modelled to be very smooth (at least 10 layers at each level). The extended refinement (trimmer wake) at the back of the cylinder allows a better numerical resolution of the vortices detaching from the body because these vortices are considered to affect the flow even after shedding.

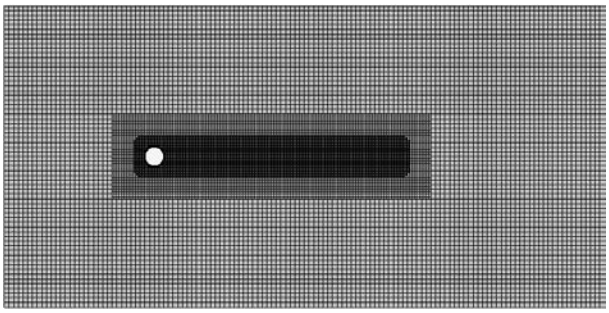
Figure 4 2D mesh grid

Table 1 shows the mesh specifications that we followed for our computational model.

Table 2 shows the solver criterion that was followed. We have chosen these settings from the convergence of residuals and the periodic stability

obtained by parameters of the model like drag coefficient and frequency of the simulation.

Table 1: Mesh details

Specifications	
No.of.cells	18220
No.of faces	36434

Table 2: Simulation details

Specifications	
Residuals	$\varepsilon<10^{-5}$
No.of.Iterations per time steps	50
No.of.Time steps	1000

2.3. Physical and boundary conditions

Incompressible flow and a Reynolds number of 3900 was selected. A velocity flow inlet, pressure outlet, wall boundary for cylinder and slip walls (zero stress walls) are the boundary conditions applied to the model (fig 5). In other words slip walls are free stream velocities which means no physical boundary is formed by the slip walls. The velocity of the flow is calculated from Reynolds number (Re) 3900. The pressure outlet is modelled to maintain relative pressure zero at the outlet so that the flow leaves the boundary to maintain the atmospheric conditions at the outlet. On the cylinder no slip boundary conditions are applied.

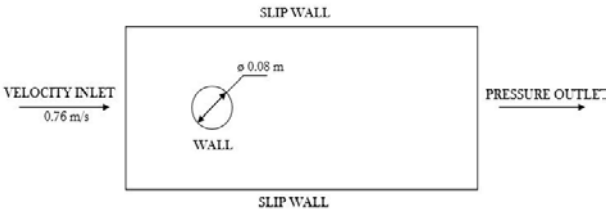

Figure 5 Boundary conditions

3. SIMULATION AND RESULTS

3.1. Simulation and validation of cylinder model

Many researchers have chosen many shapes of model like a bump or a backward facing step but we chose cylinder because it is a model that exhibits a wide range of compartment and has both favourable and adverse (unfavourable) pressure gradient which will be interesting to study. Availability of several experimental results for example in (Muddada 2010) was also a motivation.

3.1.1. Results

To validate our control free model we have to compare our various outputs like mean velocities, pressure coefficient curve, vorticity field and velocity field to reference results.

Fig. 6 which represents the evolution of the pressure forces coefficient for Re = 3900, shows that the periodic flow is reached at our simulation final time. The main frequency of 2 Hz corresponds to a Strouhal number $St = \frac{Freq \cdot D}{V_0} = 0.21$.

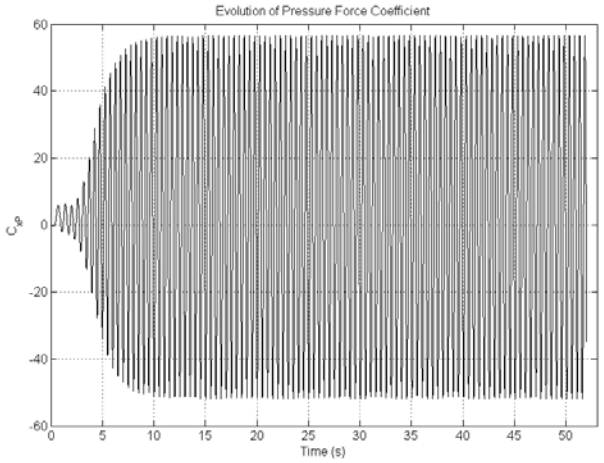

Figure 6 C_{xp} evolution without control

Comparison with some Strouhal numbers mentioned in (Muddada2010) is related in table 3. Standard k-ε numerical model of Muddada *et al.* and experimental results of Kravchenko *et al.* (Kravchenko2000) are mentioned.

Table 3: Strouhal numbers

Strouhal number for Re = 3900	
Present study	0.21
Muddada2010 k-ε	0.22
Kravchenko exp.	0.21

The obtained result seems to be in accordance with reference Strouhal number.

3.1.1.1. Pressure Coefficient

Pressure coefficient is a parameter to quantify the velocity distribution over a body.

$$C_p = \frac{P - P_0}{0.5 \cdot \rho \cdot V_0^2} \quad (5)$$

Where:
P – Static pressure at point of interest
P0 – Static pressure at free stream
ρ – Free stream density
V0 – Free stream velocity

In Fig 7 shows the comparison of pressure coefficient curve of our simulation with experimental and simulation result extracted form reference literature. From the Cp curve, we can witness the detachment point around 90° of theta. Regarding fig 7 in the case of uncontrolled flow, our 2D U-RANS solution seems to be a few closer to the experimental results of Kravchenko *et al.* (Kravchenko2000) than k-ε numerical results of Muddada *et al.* (Muddada 2010).

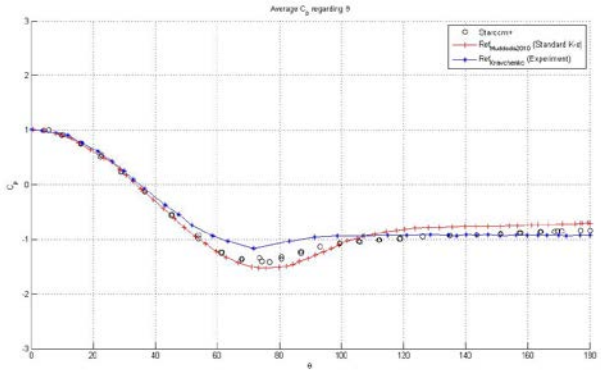

Figure 7 C_p comparison

3.1.1.2. Vorticity fields

Fig 8 shows the comparison of our vorticity fields with the reference at times allowing similar vortical structures. The Von-Karman street can be observed as the rotating cells are dropped along the flow behind the cylinder.

(a)

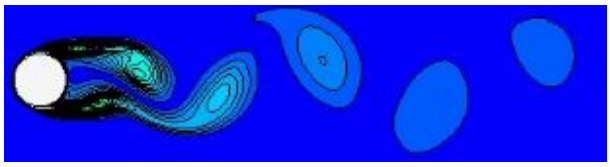

(b)

Figure 8 Vorticity fields: refrence (a) & our model (b)

3.1.1.3. Velocity fields

Fig 9 shows our velocity streamlines representing VON-KARMAN street.

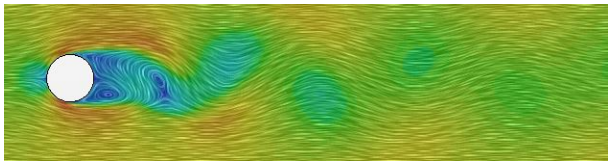

Figure 9 Re = 3900 streamlines, Von-Karman street.

3.1.1.4. Mean velocities

U represents velocity in the X direction, V represents velocity in the Y direction and D represents diameter of the cylinder. U_{ref} is the inlet free stream velocity 0.76 m/s. Figures 10 and 11 show the mean velocities V and U measured respectively at various positions (X/D = 1.06, 1.54 & 2.02) at the wake region of the cylinder in our model.

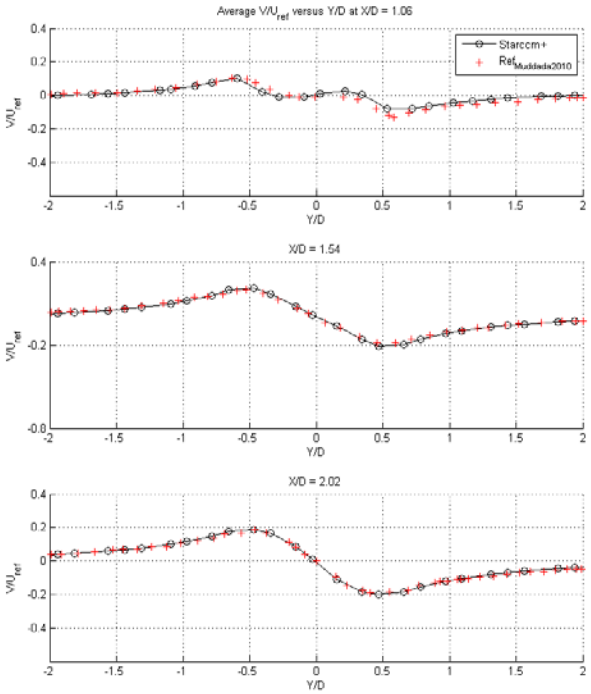

Figure 10 Mean velocity (V/Uref) vs Y/D comparison (a) X/D = 1.06 (b) X/D = 1.54 (c) X/D = 2.02

Figure 10 shows the V mean velocities in comparison with literature simulation results. It seemed to be accurate.

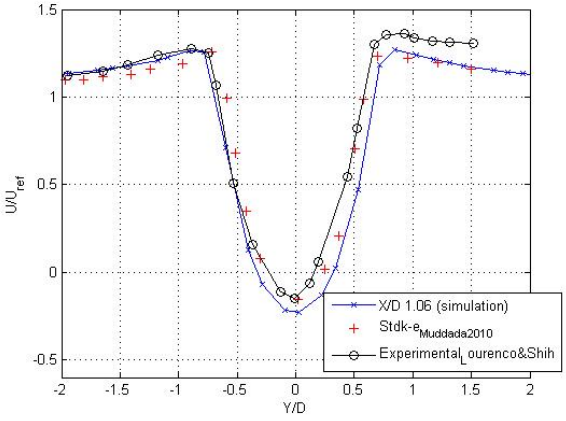

(a)

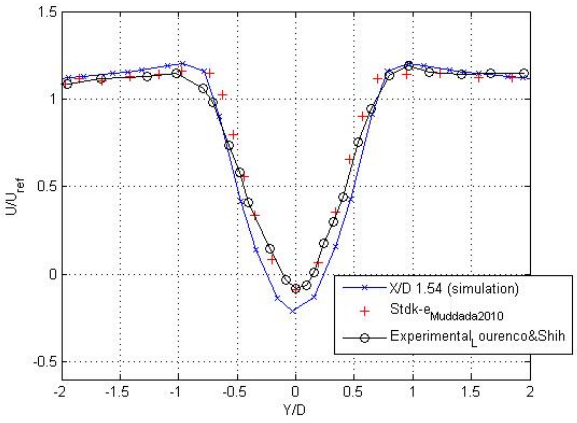

(b)

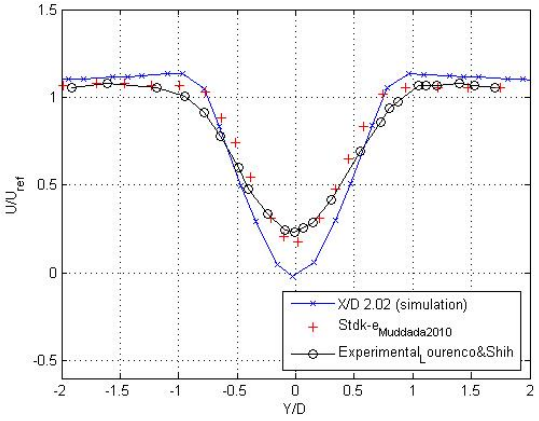

(c)

Figure 11 Mean velocity (U/Uref) vs Y/D comparison
(a) X/D = 1.06 (b) X/D = 1.54 (c) X/D = 2.02

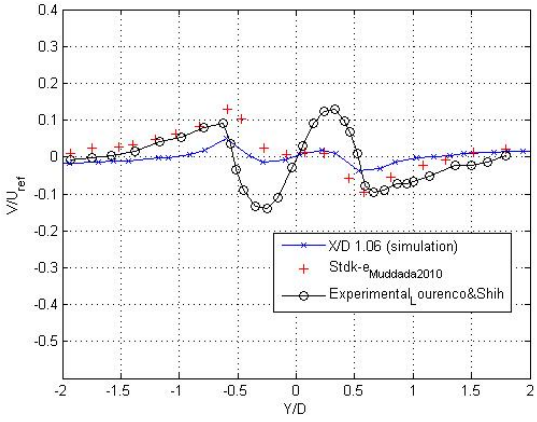

(a)

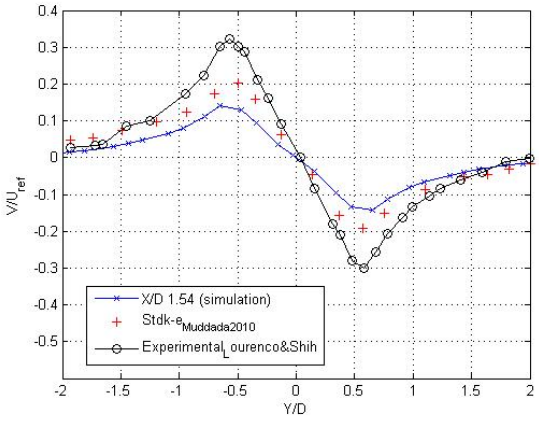

(b)

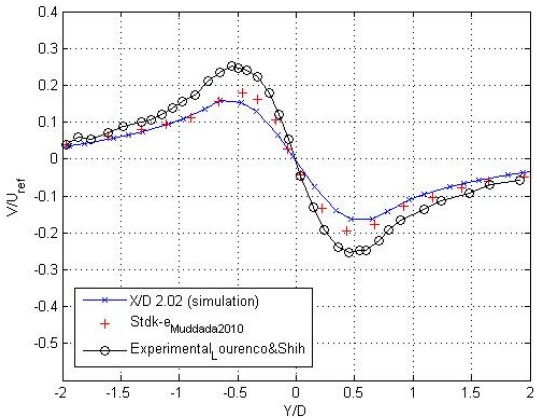

(c)

Figure 12 Mean velocity (V/Uref) vs Y/D comparison
(a) X/D = 1.06 (b) X/D = 1.54 (c) X/D = 2.02

These plots say that our model behaves correctly with simulations and experiments of publications. The X axis in the plots represents U/ Uref in fig 11 and V/ Uref in fig 12 respectively whereas the Y axis represents the non-dimensional Y/D ratio.

3.1.2. Comments

Our simulation results such the Cp curve, velocity fields and vorticity fields are proved to behave close to Standard k-ε models and the experimental results used in the publication (Muddada2010).

There are some differences in experimental curve due to unavoidable external disturbance during experiments (as observed in Muddada 2010).

Mean values of the velocities are taken as the instantaneous velocities around the cylinder and are non-symmetrical due to vortex shedding at the wake.

From the three U mean velocities (Fig 11) we can witness the accuracy of our model to the publication. As we see our results at X/D = 2.02 are quite different from Std K-ε model than X/D =1.06 and 1.54. These inaccuracies can be corrected further making some improvements like using finer mesh or another wall model. The shape of the U mean velocities is due to the recirculation at the wake of the cylinder. The minimum value of the velocity increases from X/D = 1.06 to X/D = 2.02 due to the dissipation of vortices. We can also witness the same mechanism in the V mean velocity curve. From V mean velocity curve for X/D = 1.06 we can see that there is a region of flat zero velocity after the positive bump. This null velocity region is produced as a result of suction produced by wake.

3.2. Implementing a flow control device

A simple flow control device is introduced to affect BL detachment. We created a normal jet at θ = 90° with a velocity of 7.6 % of the maximum flow velocity. This jet can be seen in Fig. 13 placed on top of the cylinder.

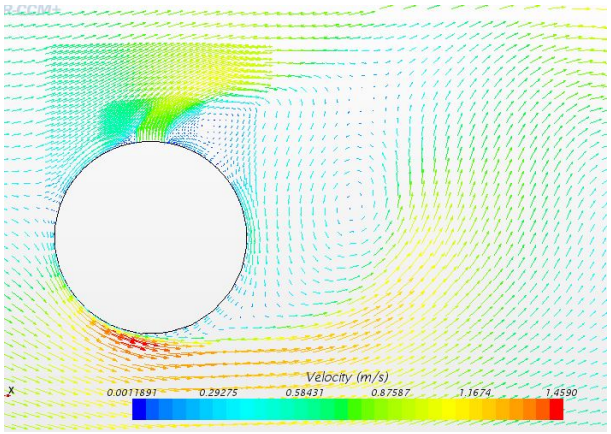

Figure 13 Velocity Vector in presence of jet

Fig. 14 which represents the evolution of the pressure force coefficient shows that the periodic flow is reached. The main frequency is 1.63 Hz, corresponding to a Strouhal number of 0.17.

Thus, all the average values are calculated on one unique period.

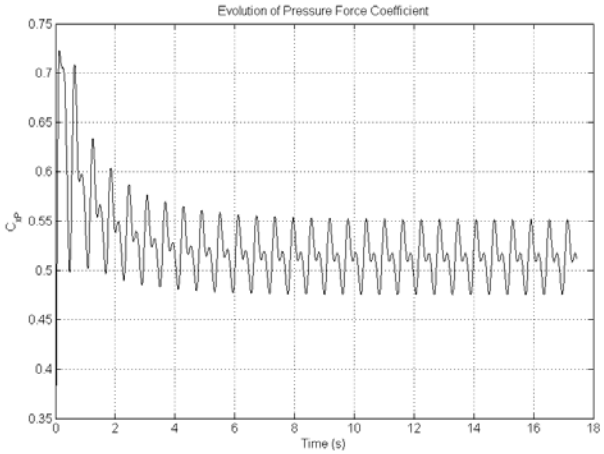

Figure 14 C_{xp} evolution with top jet

Fig 15 compares our Cp curve for the model with jet with the model which has no jet. The jet introduction seems to alter the condition here. First we can see that Cp curve is no longer symmetrical. The jet introduction at the top of the cylinder involves a separation between the upper and lower sides. So, one can see two Cp curves in case of jet introduction. For the upper side of new curve the Cp deviates from previous case by, at a first time, reaching a lower value.

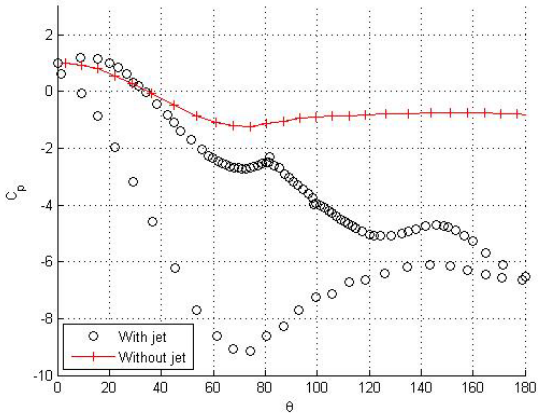

Figure 15 Cp curve with jet vs without jet

This is due to the increase in momentum caused by the increment of the velocity due to the jet. Even if the curve tends to reach the original one, one can see near 90°, the presence of the discontinuity make it decrease again. As a result the pressure is generally lower with the jet. This is the sign of delay in detachment. The second Cp curve is the pressure coefficient at the bottom of the cylinder. The bottom Cp curve is much decreased and it is linked to the acceleration occurring at the bottom of the cylinder. This can be witnessed in Fig 13 showing a fluid acceleration just at the bottom of the circular object. Moreover, the stagnation point is shifted above (Fig 15). This non-symmetry is due to the presence of a single jet at the top. This drawback can be corrected during future works by introducing another jet at the bottom or a periodic pulsed jet.

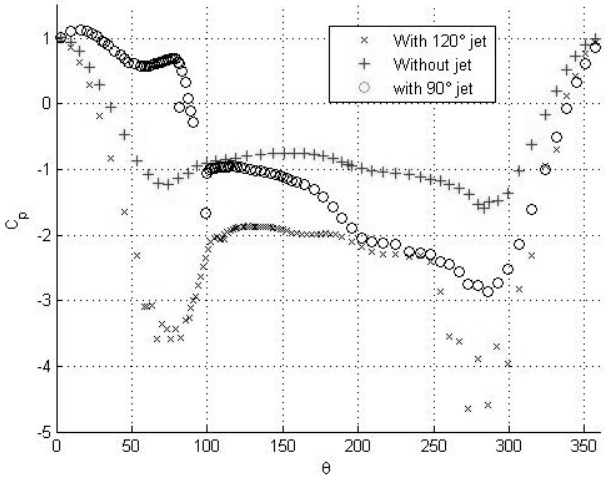

Figure 16 Cp curve with jet vs without jet

As the 90° jet creates the effects of a virtual wall, it was decided to test a new position at 120°. In figure 16 instead of superposing the upper and lower Cp between 0° and 180°, the curves are now deployed until 360°. The new jet at 120° tends to accelerate the flow compared to the 90° jet, and discontinuities are attenuated. Further works will treat the case of 2 opposite jets, to respect cylinder symmetry.

4. CONCLUSION

A 2D numerical study on the effect of flow control over a circular cylinder has been conducted using URANS Starccm+ CFD software model.

A validation test on the flow without control is performed at Re = 3900. Results seem to be accurate compared to numerical and experimental data from the literature. The detachment point figures to be near 90° which is a value close to theoretical angle of 80°.

Then a normal velocity jet is introduced at the top of the cylinder. Several effects are observed due to the presence of jet. Detachment point is moved from its original location. This outcome is encouraging for future work. A control of the detachment point is similar to controlling drag or lift in the flow. Repercussions on energy consumption could be figured. Next work can introduce a second jet at the bottom of the cylinder permitting the flow symmetry. The direction of the inlet fluid jet can also be improved and more generally a parametrical study on the jet characteristic can be conducted.

REFERENCES

Godard, G., Stanislas, J.M, 2006a. Control of a decelerating boundary layer. Part 1: Optimization of passive vortex generators. *Aerospace science and technology*, 10, 181–191.

Godard, G., Stanislas, M., Foucaut, J.M, 2006b. Control of a decelerating boundary layer. Part 2: Optimization of slotted jets vortex generators. *Aerospace science and technology*, 10, 394–400.

Godard, G., Stanislas, J.M, 2006c. Control of a decelerating boundary layer. Part 3: Optimization of round jets vortex generators. *Aerospace science and technology*, 10, 455–464.

Hazen C David, 1965. *Boundary layer control*. Princeton, Princeton University.

Kravchenko, A.G., Moin, P., 2000. Numerical studies of flow over a circular cylinder at Re_D = 3900. *Physics of Fluids*, 12 (2), 403–417.

Muddada, S and Patnaik, B.S.V, 2010. An assessment of turbulence models for the prediction of flow past a circular cylinder with momentum injection. *Journal of wind engineering and industrial aerodynamics*, 575-591.

Ola, L., 2008. Vortex generators and turbulent boundary layer separation control. *Technical reports from Royal Institute of Technology*, KTH Mechanics, Stockholm, Sweden.

Prandtl, L, 1904. Boundary layer theory. *Verhandlungen des dritten internationalen Mathematiker-Kongresses*, Heidelberg, GERMANY.

Widjanarki, M.D., Geesing, J.A.K, Vries H, Hoeijmakers, W.M., 2012. Experimental/Numerical investigatin airfoil with flow control by synthetic jets. *28th International congress of the Aeronautical science*.

AUTOMATIC GRID GENERATION FROM A NUMERICAL PICTURE FOR TRANSIENT FLOW SIMULATION OVER A CAR SHAPE OBSTACLE

Tonino Sophy[(a)], Julien Jouanguy[(b)], Luis Le Moyne[(c)]

[(a)] DRIVE – ISAT EA 1859, 49, rue Mademoiselle Bourgeois, 58000 NEVERS, FRANCE.

[(a)] tsophy@u-bourgogne.fr , [(b)] julien.jouanguy@u-bourgogne.fr , [(c)] luis.le-moyne@u-bourgogne.fr

ABSTRACT

Computer assists numerization of a domain, requires several engineers or scientists during considerable time. Thus, meshing automatization process has been developed using heavy devices like LASER metrology. It can sometimes be more convenient to use simple devices.

Image processing field, reveals many works concerning object detection. Applications concern medical field, automotive, face detection or national defense.

This paper aims proposing a simple, but accurate enough, tool to generate 2D domain meshing from a numerical picture that can be used with a transient Finite-Volume CFD code. A car shape object is chosen. From the original picture, edge detection and threshold techniques are applied and then, the object contour points' gird is provided.

Another process is applied to generate a refined Finite-Volume mesh compatible with Gerris Flow solver. Transient simulations are conducted at different Reynolds numbers. Results, in terms of pressure fields or velocity evolutions, are shown. Von-Karman alley flow is detected.

Keywords: Flow simulation, Object Recognition, Complex shape, Image processing, Mesh generation, Drag coefficient.

1. INTRODUCTION

Numerical simulation is widely used in advanced technology studies especially in engineering field. Indeed, it is necessary to use adapted numerical method to produce convincing simulations of physical phenomenom such as fluid flow or thermal diffusion. Even if direct experimentations are essential, the observation of physical phenomenon is more convenient using numerical simulation.

Numerization of the considered domain (often called meshing), that is usually achieved with computer assisted conception software, can require one or more engineer or scientist during a considerable amount of time. Thus, automatization of meshing process has been developed using heavy devices like LASER metrology. Nevertheless, it can be more convenient to use a simple device, like a commercial digital camera, to run simple numerical tests.

Image processing scientific field, reveals many works done concerning object detection or reconstruction. Main applications concern medical field, automotive comfort or security, face detection (Viola 2001, Li 2002, Sochman 2004) or national defense department. Muñoz-Salinas et al. used image processing to detect and track people with multiple stereo cameras (Muñoz-Salinas 2009). Cao et al. used image treatment to reconstruct surface using bivariate simplex splines on Delaunay configurations (Cao 2009).

The aim of this paper is to propose a simple, but accurate enough, tool to generate a 2D domain meshing from a numerical picture that can be used with a transient FV (Finite Volume) CFD code. A car shape object is chosen. A description of the grid generation process, from the original picture to the object contour points' gird, is first provided. Then, the process to load these contour points and to generate a refined Finite Volume mesh compatible with the Gerris Flow solver is rapidly described. The tool is validated using a car shape object. The known Von Karman alley phenomenon can be observed. Thus, transient simulations are conducted at different Reynolds numbers. Results, in terms of pressure fields or velocity versus time evolutions, are shown. This type of results can allow evaluating the drag or lift coefficient of the car or the fundamental vortexes' drop frequency. The influence of the Reynolds number on the vortexes' drop frequency is depicted.

2. METHOD DESCRIPTION

The main purpose of the proposed tool is using a simple commercial digital camera picture to build a 2D mesh in order to run a numerical simulation. When an image is acquired by a camera for another vision system, it is rarely directly ready for use. Thus, a first image processing should be applied for noise reduction for instance. Then, the real image processing can take place to obtain the points cloud representing the picture. At last, this points cloud has to be modified to be load in our numerical simulation software. The obtained mesh is so ready for the simulations.

2.1. Image processing

In this section we show different used methods for image treatment. A brief description will be given for these methods. Our code development is based on C++

language using an Open source Computer Vision library (OpenCv) (Bradski 2008). To achieve the points grid generation, the captured image has to be smoothed by filtering. This is necessary for edge detection then pixel classification.

2.1.1. Mathematical tool

To perform image preprocessing and processing several mathematical tools are required like linear discrete convolution or derivative filters.

- Linear convolution

Consider an image I[x, y] and a two-dimensional filter h [x, y]. The 2D discrete convolution sum is then given by equation 1.

$$g[x,y]=\sum_{k=-\infty}^{\infty}\sum_{l=-\infty}^{\infty}I[k,l]h[x-k,y-l] \quad (1)$$

Then g [x, y] is the new obtained image after convolution.

- Derivative filter

In practice, to work with discrete gradients it is necessary to approach them. It is usual to see a Finite Difference scheme calculated by a convolution with simples kernels as an approximation of directional derivative. For example, the approximation $\frac{\partial I}{\partial x}$ of the derivative of a continuous signal I(x) is obtained by convolution with the simple kernel [0 -1 1]:

$$\frac{\partial I}{\partial x}\approx\frac{\Delta I}{\Delta x}=\frac{I(x+\Delta x)-I(x)}{\Delta x} \quad (2)$$

If the signal I is an image we have two derivatives at each point (pixel). The vertical and horizontal derivatives are respectively Iy and Ix. Then, the gradient image is defined as the sum of a two components

$$\Delta I=|I_x|+|I_y| \quad (3)$$

ΔI gives an indication of the intensity of the gradient in the current pixel.

2.1.2. Image Preprocessing

When an image is acquired by a camera or other imaging system, often the vision system for which it is intended is unable to use it directly. The image may be corrupted by random variations in intensity, variation in illumination, or poor contrast that must be dealt with in the early stages of vision processing. So, good image smoothing should be able to deal with different types of noise. In this paper, some image smoothing filters are used.

In this paper, non-linear and linear filters are the two types of smoothing methods used.

- Linear filter

The Gaussian filter is an example of linear filter.

It is used as a linear filter. Its operator is given by equation 4.

$$h_{Gauss}(x,y)=\frac{1}{2\pi\sigma^2}e^{\frac{x^2+y^2}{2\sigma^2}} \quad (4)$$

The kernel of a Gaussian filter with a standard deviation σ = 1.4 is expressed in equation 5.

$$h_{Gauss}=\frac{1}{159}\begin{bmatrix}2&4&5&4&2\\4&9&12&9&4\\5&12&15&12&5\\4&9&12&9&4\\2&4&5&4&2\end{bmatrix} \quad (5)$$

The obtained filter hGauss[x,y] is applied to the image I [x, y] in term of h [x, y] in the Eq.(1).

- Non-linear filter

The median filter is an example of a nonlinear digital filtering technique, often used to remove noise. Instead of simply replacing the pixel value with the mean of neighboring pixel values, it takes the median of those values after they have been sorted. The median is calculated by first sorting all the pixel values from the surrounding neighborhood into numerical order and then replacing the pixel being considered with the middle pixel value.

For example, let's consider a matrix M as expressed Eq. 6.

$$M=\begin{pmatrix}124&126&127\\120&150&125\\115&119&123\end{pmatrix} \quad (6)$$

Considering the pixel M(3,3) to be filtered, all the 9 neighbors of this pixel (including the pixel itself) are sorted in a table.

1	2	3	4	**5**	6	7	8	9
115	119	120	123	**124**	125	126	127	150

So the median value, corresponding to the index 5 of the table, replace the value of the M(3,3) pixel and the obtained matrix M_{Median} is expressed in equation 7.

$$M_{Median}=\begin{pmatrix}124&126&127\\120&\mathbf{124}&125\\115&119&123\end{pmatrix} \quad (7)$$

Figure 1 shows an example of original image and the results obtained with a Gaussian linear filter and a Median non-linear filter which is very effective in removing salt and pepper and impulse noise while retaining image details.

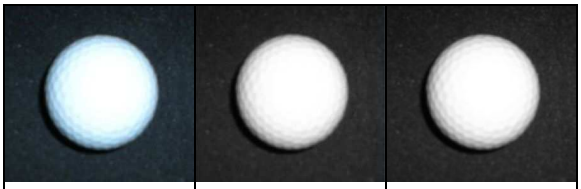

(a) Original image | (b) Gaussian filter | (c) Median filter

Figure 1: Smoothing filters

2.1.3. Edge detection

As seen before the contour points of the object are needed by the CFD code. Edge detection is a fundamental tool used in most image processing applications to obtain information from the frames as a precursor step to feature extraction and object segmentation. This process not only detects boundaries between objects and the background in the image, but also the outlines within the object. To detect edges, many operators such as Sobel operator or Canny detector can be applied. The OpenCv library gives an important function that can detect contours. This function is called cvFindContours (Bradski 2008).

During our work many detection operators like Sobel or Canny have been tested. The OpenCv CvFindContour function and the Hough operator emerge from the list (figure 2).

- Sobel operator:

It is a discrete differentiation operator computing an approximation of the opposite of the gradient of the image intensity function. The Sobel operator measures two components. The vertical edge component is calculated with kernel Sy and the horizontal edge component is calculated with kernel Sx. The intensity of the gradient at the pixel is then calculated with the derivative filter. These two kernels are calculated using a simple convolution of [−1 0 1] and $\begin{bmatrix} -1 \\ 0 \\ 1 \end{bmatrix}$ with a smooth filter [1 2 1] (or its transpose):

$$S_x = \begin{pmatrix} -1 & 0 & +1 \\ -2 & 0 & +2 \\ -1 & 0 & +1 \end{pmatrix} \quad S_y = \begin{pmatrix} -1 & -2 & -1 \\ 0 & 0 & 0 \\ +1 & +2 & +1 \end{pmatrix} \quad (8)$$

- Canny operator:

Canny's aim is to find the optimal edge detection algorithm (Canny 1986) based on three criteria:

– Good detection: the algorithm should mark as many real edges in the image as possible

– Good localization: edges marked should be as close as possible to the edge in the real image

– Minimal response: a given edge in the image should only be marked once, and where possible, image noise should not create false edges.

The canny algorithm is built in 5 steps:

– Smoothing: Blurring of the image to remove noise

– Finding gradients: The edges should be marked where the gradients of the image has large magnitudes

– Maximum suppression: Only local maxima should be marked as edges

– Double thresholding: Potential edges are determined by thresholding

– Edge tracking by hysteresis: Final edges are determined by suppressing all edges that are not connected to a very certain (strong) edge

- cvFindContours:

The function cvFindContours retrieves contours from the binary image and returns the number of retrieved contours. The pointer firstContour is filled by the function. It will contain pointer to the first most outer contour or NULL if no contours is detected (if the image is completely black). Other contours may be reached from firstContour using h_next and v_next links.

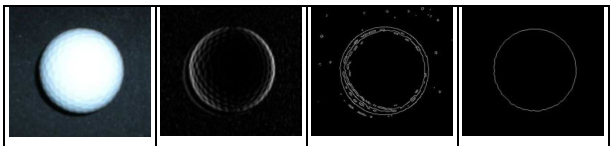

(a) Original image | (b) Sobel detector | (c) Canny detector | (d) Find Contour

Figure 2: Edge detectors

- Hough transform:

The Hough transform is a feature extraction technique used in image analysis, computer vision and digital image processing (Shapiro 2001). It is a method to reconstruct lines, circles, or other simple shape in an image. In our work, as the validation object has a circular shape, we used Hough to reconstruct the circles contour's (Kimme 1975). The Hough circle reconstruction technique highlights in the image the potential centers of a r radius circle (figure 3-a). The center being detected, one can reconstruct the circle's contour (figure 3-b) or the entire object (figure 3-c).

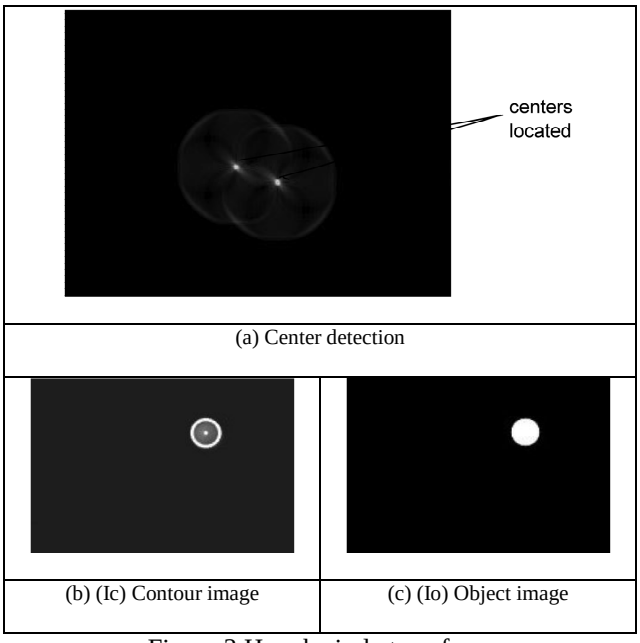

(a) Center detection

(b) (Ic) Contour image

(c) (Io) Object image

Figure 3 Hough circle transform

2.1.4. Car edge detection:

The initial picture (Figure 4a) used for this study is a 500×222 pixel picture acquired with a Sony DSC-W510 camera. A 72 ppp low resolution have been chosen. The exposition time is 1/250 second.

For the case of the car shape obstacle, the cvFindContours function is used to detect the contour of the car after an accurate pre-processing (regulating the brightness, contrast and Gamma of the picture). Then a contour points grid can be built (Figure 4b) using a threshold level technique.

(a)

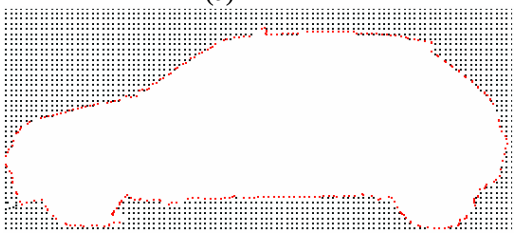

(b)

Figure 4: (a): Complex shaped object, (b): Automatic generated grid.

2.2. CFD code mesh import

The Finitie Volume CFD code chosen is the Open Source Gerris Flow solver. This software is licensed under the Free Software Foundation's GPL and is written is C language. As Gerris only deals with 3D calculation, the 2D mesh have to be extruded limited to one cell (intersecting z = 0).

2.2.1. Grid transfer

Our process requires exportation in STL format which is convertible in Gerris object format. CATIA software has been use for the conversion of the text coordinates file to an STL format file. One has to pay attention to the dimensions of the object (aspect ratio) to respect the non dimensional number further.

Finally, the STL format file has to be converted in a Gerris format file (GFS format) using an internal Gerris command. An option (“revert”) can be added to this command to swap the localization of the fluid in or out of the object.

2.2.2. Meshing

Unlike most flow solvers which uses structured or unstructured meshes, Gerris implements a deal between both types by using a tree data structure. For this study, a quadtree data structure has been used to mesh our 2D case. First, 4 quadric volumes of dimension 1 are defined. Then each volume is divided in four new smaller quadrics and the process start again. The volume division process continues until a previously fixed dimension is reached. User has just to precise the number of “level” nlevel to be applied. The volumes size will be $\frac{1}{2^{n_{level}}}$.

Gerris also allows local refinement of the mesh using a wall vicinity technique. In this case, a new level number (nrefine) is required. Near the object, a successive volume division will be applied layer by layer. At the end, the layer closest to the object will have a dimension of $\frac{1}{2^{n_{refine}}}$.

Figure 5 shows an example of refined mesh used in the incompressible 2D Gerris Navier-Stokes’ solver.

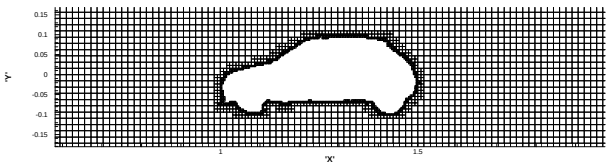

Figure 5: Example of quadric refined mesh representing the car shape obstacle

3. RESULTS

The two dimensional incompressible Navier-Stokes equations are directly solved with Gerris software. All data are adimensionned so that simulations results are only function of dimensionless Reynolds number.

The objective of this preliminary work is to examine whether the method is able to represent the flow over the car in a 2D configuration. Simulation will thus be ran for several intermediate Reynolds numbers ($250 < Re < 500$), for which transient regime is observed without turbulence. The expected

phenomenon is the development, in such a configuration, of a vortex drop behind the car called Von Karman Street which appears behind several geometrical forms with 2D circular or squared sections (Lübcke 2001), (Muddada 2010).

3.1. Simulations configuration

At the inlet, a velocity-step profile is imposed with a single component in the x-direction and convective outflow boundary condition is set to ensure the flow rate conservation. Lateral zero gradient boundaries conditions are also imposed and we checked that their distance from the car is enough to neglect their effect into simulation domain.

Different kind of output data are available such as the pressure field in figure 6 , streamlines on figure 7 or vorticity module on figure 8. These results are obtained from simulations carried out at Re=250 with cells of size 0.0156 (n_{level}=6). The qualitative observations indicate that the transient regime is obtained especially from figure 8 where the vorticity indicate presence of contra-propagative vortexes. On Figure 7, it is also possible to see a recirculation zone behind the car object which is a characteristic of the Von Karman street. For a quantitative study of this regime (detachment frequency and Strouhalt number), it is important to be sure that the grid convergence is reached.

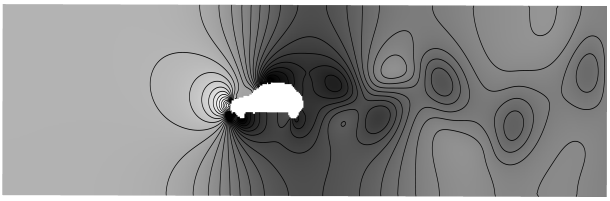

Figure 6: Pressure field for dimensionless time t = 10 and Re=250 . The maximum value in black is 0.7 Pa and the minimum value is -1.6 Pa

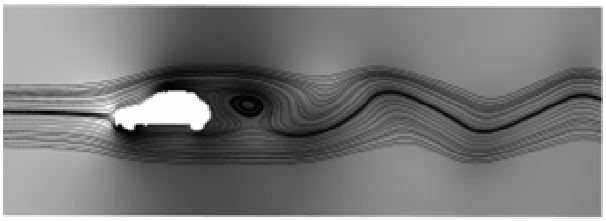

Figure 7: Flow Streamlines at dimensionless time t=10 and Re=250

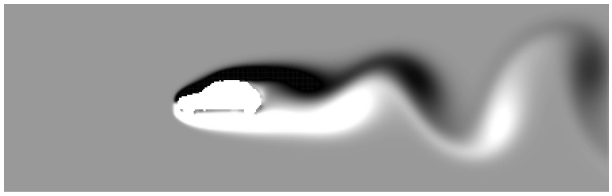

Figure 8: Vorticity module at dimensionless time t=10 and Re=250. Maximum value (+10) is in black and minimum value (-10) is in whit

3.2. Grid convergence

While solving the Navier-Stokes equations, the chosen option is to use a regular grid without distinguishing flow region. The several grid chosen are defined according to the resolution given by the nlevel value and the near object refinement is always given by nrefine=8. The name of the tested grid and their crrespondance to resolution are given in the following table.

Table 1: Different used grid

name	grid1	grid2	grid3	grid4
n_{level}	5	6	7	8

To evaluate the spatial grid convergence we plotted the time evolution of components of the velocity field at position (x=0.125, y=0) at Re=250.

The dimensionless frequency of the signal was also computed from periodicity of the signal after regime stabilization (5<t<10). The convergence is reached when the frequency became independent of the resolution. An example of visualizations is presented on figure 9. On this figure, it is obvious that the grid is very important as it can change the frequency of vortex detachment near the vehicle and also the amplitude of the signal. This can be explained by the fact that Von Karman street is created by boundary layer detachment on the car object. The optimal resolution is thus the one which solve the boundary layer thickness and the whole development of vortexes. The table 1 shows computed frequency for different grids.

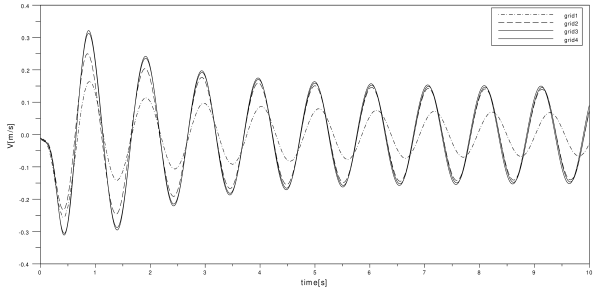

Figure 9: Time evolution of vertical component of velocity V at point (x=0.125,y=0) and Re=250 for several grid resolutions.

Table 2: Frequency of vortex detachment for the different grid tested

Grid n°	1	2	3	4
frequency	1.13	1.16	1.16	1.16

The convergence based on frequency is obtained for grid 2. However, on figure 9 it can be observed that the convergence for amplitude is only reached for grid 3, after the dimensionless time t=3 which is necessary to get a stabilized regime. For the other parts of this study, we will use the same approach to ensure the spatial convergence, especially when the Reynolds

number is increased which may change the boundary layer thickness, and thus the resolution needed for convergence.

3.3. Reynolds number study

Another specific result observed in literature for a transient flow regime behind an object is the relation between Reynolds number and vortex detachment frequency. We thus inquired about this relation with the same procedure as before. The signal of vertical component of velocity in time at point (x=0.125,y=0) is thus analyzed and plotted on figure 10.

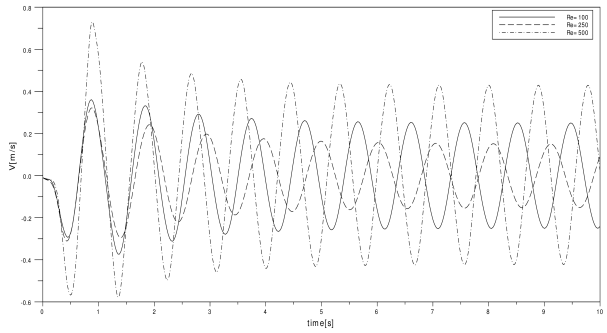

Figure 10 Time evolution of vertical component of velocity V at point (x=0.125,y=0) for several Reynolds number.

The frequency Reynolds dependence can be qualitatively observed. The trends obtained by studies of flow behind other object are also obtained in this configuration, i.e. augmentation of frequency with Reynolds number. The value of the frequencies of different Reynolds numbers can be found in table 2.

Table 3: Frequency of vortex detachment for several Reynolds number

Reynolds number	250	350	500
frequency	1.15	1.22	1.28

3.4. Potential studies with the method

The results of simulation show that this approach, coupled with a CFD code can predict qualitatively the flow comportment behind a vehicle. As the method we used for the flow solver is Direct numerical simulation, the turbulent cases can not be simulated, as a third dimension is needed to get a solution in accordance with experiments. Several option are thus available:

- Extend the method to 3D object description
- Use other CFD aprroach like RANS or URANS with this configuration.

The advantage of this method is that lots of output variables are available and allow computing classical coefficients and forces used to evaluate the aerodynamics of vehicle. For example, Pressure and viscous forces can be obtained and influence of several parameters such as car geometry and Reynolds number can be inquired. An example of such output is presented on figure 11 with evolution of pressure forces that acts on the vehicle. We can see the periodic evolution of these forces in time.

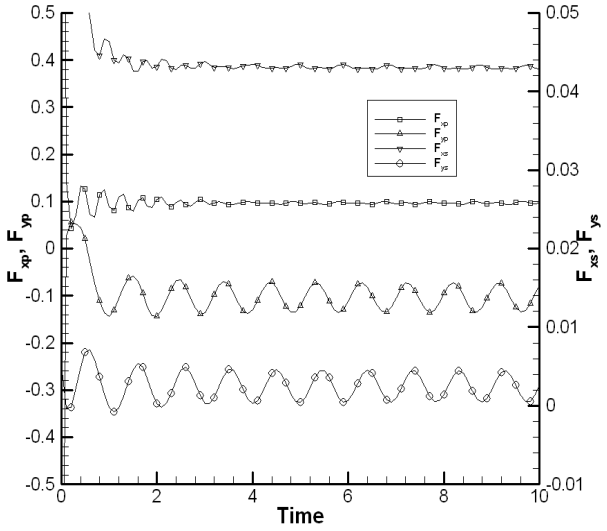

Figure 11 Time evolution of pressure and shear forces on the vehicle

To see if the obtained mesh is robust, 2D high Reynold number simulation is conducted. The purpose is then so see if the Finite Volume mesh leads to convergence of the simulation. The Reynolds number is then fixed to Re = 2.10^5. All other simulation's parameters are kept unchanged. The grid2 is the used.

Figure 12 and 13 respectively show the pressure field at time t = 5 and the evolutions of the components of the velocity at the point (x,y) = (1.625,0) located behind the car shape object for times up to t = 10.

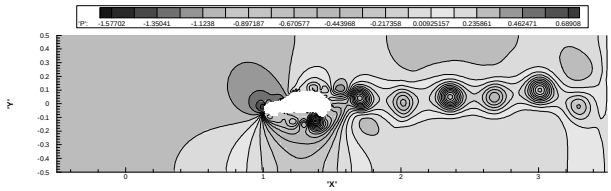

Figure 12: Pressure field for dimensionless time t = 5

Figure 12 reveals that the automatic meshing method is able to generate a mesh compatible with high Reynolds numbers as a converged result is obtained. One can clearly see the iso-pressures corresponding to the vortex drop.

Figure 13 shows that a periodic flow is clearly reached and a dimensionless frequency of 1.9 is found.

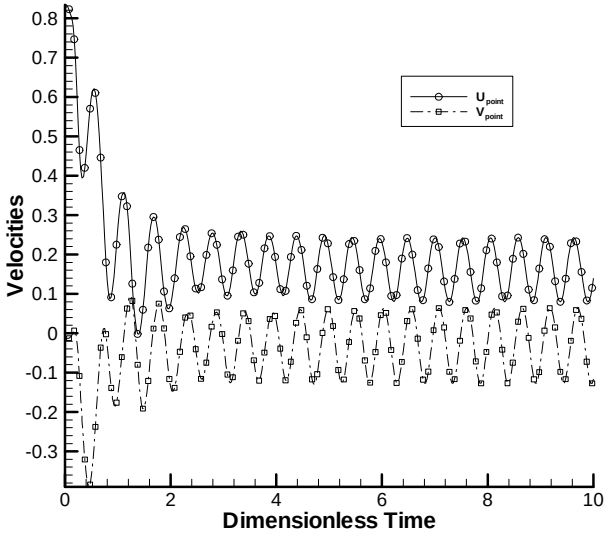

Figure 13: Evolution of U and V velocity component at the point (x , y) = (1.625 , 0)

4. CONCLUSIONS

A light and easy to use automatic grid generation tool as been developed. The idea is to build from a numerical picture, took with a simple commercial digital camera, a realistic 2D numerical simulation mesh. It seems to construct suitable grids for complex shaped object as this work used a car picture as initial picture. The obtained point clouds have been processed to obtain a Finite Volume mesh compatible with Open Source 2D incompressible Navier-Stokes flow solver on transient forced convection problems. Results are in agreement with the physical phenomena as, for several Reynolds numbers, the well known Von Karman Street flow is obtained.

This method potentially allows the study of the optimization of the vehicle flow lift and drag coefficients as the evolutions of the pressure and shear forces are obtained.

Finally, it has been shown that the 2D realistic mesh obtained, does not lead to divergence when high Reynolds numbers are involved.

REFERENCES

Bradski, G.-R., Kaebler, A., 2008. Learning OpenCV,Computer. *Vision with OpenCV Libarary*, O′Reilly Media, Inc., 234-244.

Canny, J., 1986. A Computational Approach To Edge Detection. *IEEE, Trans. Pattern Analysis and Machine Intelligence*, 8 (6), pp. 679-698.

Cao, J., Li, X., Wang, G., Qin, H., 2009. Surface reconstruction using bivariate simplex splines on Delaunay configurations. *Computers&Graphics*, 33, 341-350.

Kimme, C., Ballard, D. H., Sklansky, J., 1975. Finding circles by an array of accumulators. *Communications of the Association for Computing Machinery*, 18, 120-122.

Li, S., Zhu, L., Zhang, Q., Blake, A., Zhang, H. J., and Shum, H., 2002. Statistical learning of multi-view face detection. Proceedings *of the 7th European Conference on Computer Vision*, Copenhagen, Denmark.

Lübcke, H., Schmidt, S., Rung, T., Thiele, F., 2001. Comparison of LES and RANS in bluff-body flows. *Journal of Wind Engineering and Industrial Aerodynamics*, 89, 1471-1485.

Muddada S., Patnaik B.S.V., 2010. An assesment of turbulence models for the prediction of flow past a circular cylinder with momentum injection. *Journal of Wind Engineering and Industrial Aerodynamics*, 98, 575-591.

Muñoz-Salinas, R., Medina-Carnicer, R., Madrid-Cuevas, F. J., Carmona-Poyato, A., 2009. People detection and tracking using stereo vision and color. *Journal Vision Commun. Image R.*, 20, 339-350.

Shapiro, L., Stockman, G., 2001. *Computer Vision*. Prentice-Hall, Inc.

Sochman, J., Matas, J., 2004. AdaBoost with totally corrective updates for fast face detection. *Proceedings of the 6th IEEE International Conference on Automatic Face and Gesture Recognition*, 445-450.

Viola, P. and Jones, M., 2001. Rapid object detection using a boosted cascade of simple features. *Proceedings of the IEEE Computer Society Conference on Computer Vision and Pattern Recognition (CVPR '01)*, 1, 511-518.

ADAPTION OF MULTI-PHYSICS PEM FUEL CELL MODEL USING SENSITIVITY ANALYSIS

Raaj Ganesh SAMIKANNU RAMESH, El-Hassane AGLZIM, Daniela CHRENKO, Luis LE MOYN

DRIVE ID-MOTION, EA 1859, Institut Supérieur de l'Automobile et des Transports
University of Burgundy, 49 rue Mlle Bourgeois, 58027 Nevers, France
Email: raaj-ganesh_samikannu-ramesh@etu.u-bourgogne.fr, (el-hassane.aglzim, daniela.chrenko, luis.le-moyne)@u-bourgogne.fr

ABSTRACT
This paper presents the adaption of an existing multi-physics 1D fuel cell model to an existing PEM fuel cell system. The input parameters of the model are separated into system properties, linked to physical values, and running conditions. On the 40 system properties required, a sensitivity analysis was applied in order to identify that only four membrane properties have the most influence on the stack voltage. These parameter values were identified by optimization. The prediction accuracy with the new parameter values decreased to 1.48%.

Keywords: PEM fuel cell, multi-physics 1D model, sensitivity analysis

1. INTRODUCTION

In the pursuit of a sustainable future with regard to energy production and transportation, fuel cells are among the most promising solutions to produce electric energy whenever and wherever needed in an environmentally friendly way. This is due to the fact that most fuel cells can run on hydrogen and hydrogen can be produced from renewable sources without the need of fossil fuel and the emission of greenhouse gases as CO_2. The potential of fuel cells has already been identified, but their commercialization has not yet developed as expected. In order to push the development of PEM fuel cells for different applications, it is very useful to dispose of a complete and viable fuel cell system model that is able to reproduce fuel cell systems precisely. There is a great number of fuel cell models available that respond to different demands (Chrenko, Péra, Hissel, & Geweke, 2008; Grasser & Rufer, 2006; Rodatz, 2003). There are electro-chemical models, which are able to describe in detail the mechanisms occurring inside a cell allowing to understand and improve electro-chemical processes (Famouri & Gemmen, 2003). There are also system models, providing information about the overall system. Those global models might be zero dimensional (Miotti, Di Domenico, & Guezennec, 2005), which offer little information and are only interesting in cases without faults. One dimensional models consider the propagation of electrons and protons through the cell and offer an interesting compromise between calculation time and accuracy (Gao, Blunier, & Miraoui, 2009) and three dimensional models, which can describe the behaviour at every point of the cell, but need considerable calculation time (Cheddie & Munroe, 2008). The most important output parameter is the cell or system voltage, which is crucial for the utilization of the fuel cell inside a system (Miotti et al., 2005). Moreover it is important to describe the fluidic domaine behaviour of the fuel cell, including not only the hydrogen consumption, but also the influence of air stoichiometric ratio and aspects of humidification (Van Nguyen & Knobbe, 2003). Finally, it is important to consider the thermal aspects of the system, because fuel cells have to be kept in a narrow window of acceptable working temperatures and the system behaviour has big influence on the cell temperature.

Among the big number of available fuel cell models, the 1D three domain models of Gao et al. is remarkable, as it provides high accuracy in the three domains of modelling (electric, fluidic and thermal) and furthermore it is capable to provide results in real time (Gao et al., 2009). Unfortunately this model requires a large number of forty system properties, next to twenty different input parameters. Moreover, this model was only trained and validated for one type for fuel cell system. In order to open the model for a wider range of applications, it has to be adapted for different fuel cell systems. This article presents a method to adapt the existing model to a Bahia system, including the identification and evaluation of the most important system properties using sensitivity analysis.

In the following section the Bahia fuel cell system is presented. This system is used as baseline for the new model. Thereafter, basic aspects of the reference model are presented in section 3. The identification of most important system properties and their evaluation is presented in section 4. Results from the initial model, measurement and adapted model are presented in section 5. The article ends with conclusions and perspectives.

2. BAHIA FUEL CELL SYSTEM

The Bahia Fuel Cell System is a complete 1kW fuel cell system for research and education provided by Helion/Areva (Helion/Areva, 2014). This system has been sold widely throughout universities in France and Europe.

It consists of the complete hardware, including not only the fuel cell and its accessories (pumps, valves, cooling system), but also the electric load and the supervision software, installed in a dedicated computer (Figure 1), the package is completed by a software interface module - Bahia Fuel Cell Simulator – which can be used both in testing and simulation mode.

Figure 1 Bahia Fuel Cell System

The Bahia fuel cell system is a proton exchange membrane (PEM) fuel cell and contains 24 cells connected in series to provide a maximum power of 1kW. The system is connected to the software module, allowing system control and supervision, offering the possibility to visualize and save a big number of system parameters, like cell and stack voltages, gas flows and temperatures. Figure 2 shows a schematic representation of the system on the Bahia software module.

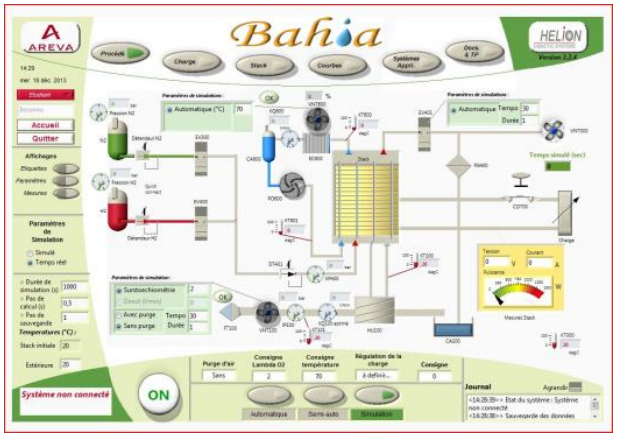

Figure 2 Schematic of the Bahia Fuel Cell System [9]

The fuel cell system was tested for a ramp up polarization curve with a temperature limit of 70°C. Results are shown in Figure 3.

3. 1 D, THREE DOMAIN FUEL CELL MODEL

3.1. Model Objective

The multi physics model by F.Gao et al. (Gao et al., 2009; Gao, Blunier, & Miraoui, 2012) contains electrochemical, fluidic and thermal domain respectively. It has been created to run in real time on a fuel cell emulator and to provide the complete set of system parameters of a fuel cell system.

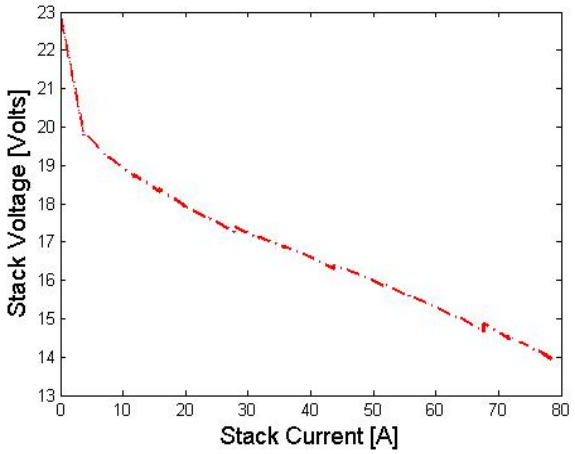

Figure 3 Polarisation curve of Bahia FC System at 70°C

These parameters contain not only the voltage response of the system, but also temperatures at different locations as well as gas and water flows. It is important to know all those parameters as temperature and humidity influence the fuel cell voltage considerably.

3.2. Model Structure

The model presented by Gao et al. (Gao et al., 2009, 2012), describes the behaviour of an entire fuel cell stack.

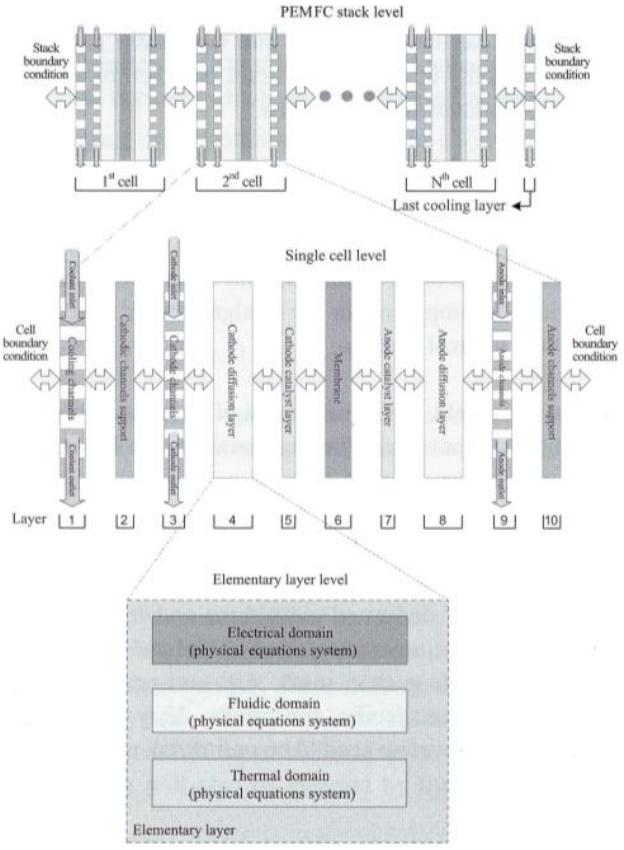

Figure 4 Structure of FC stack, cell & layers model presented by Gao et al. (Gao et al., 2009) (Gao et al., 2012).

In order to be precise on the entire stack, the system is broken down to the individual cells, all connected in series and linked by temperature and gas flow. Each of the fuel cells is than divided into 10 different layers containing membrane, cathode and anode, gas layers and cooling layers. For every layer the electric, thermal and fluidic behaviour is calculated and the results are linked. The structure is presented in Figure 4.

3.3. Model Parameters

There are two types of inputs to the model, which have to be treated.

3.3.1. System Properties

The system properties include properties of the fuel cell system that have to be known by the model in order to work properly. These parameters include number of cells and their surface, membrane properties, gas diffusion layer properties, bipolar layer properties, cooling system, anode and cathode properties respectively. There are in total 40 system properties that have to be defined.

3.3.2. Running Conditions

The running conditions represent the ambient conditions at the fuel cell, including temperature at different positions of the system, ambient pressure, and pressure at cathode and anode, cooling channel mass flow rate, etc. In total 20 running conditions are required to model the fuel cell system. The parameters are measured from the Bahia fuel cell system and then given as input to replicate the same conditions as in the experiment.

4. IDENTIFICATION OF MAIN SYSTEM PROPERTIES

In order to represent the Bahia fuel cell stack using the same approach that has been used by Gao et al., the system properties and running conditions have to be known. Even though the running conditions can be measured or approximated, the system properties are very specific and partly confidential data, which are not available.

Methods exist to identify parameters for non-linear, multi-input systems, but their calculation time and the complexity to identify parameters increases with the numbers of parameters to identify (Deb, 2001). Therefore, the sensitivity of the result with regard to the system parameters was analysed, before the most important parameters were identified numerically.

4.1. Sensitivity Analysis procedure

The objective of sensitivity analysis is to find system properties that affect the output stack voltage of PEM fuel cell model most. Knowing the most important system properties allows focusing and identifying their accurate values.

The procedure followed is Multi-parametric sensitivity analysis (MPSA) as introduced by Correa et al. (Correa, Farret, Popov, & Simoes, 2005), (Correa, J M, Borello, F. Santarelli, 2011) and used by Gao et al. (Huangfu, Gao, Abbas-Turki, Bouquain, & Miraoui, 2013). The main steps are as follows:

1. Select the set of the parameters to be analysed: *40 parameters (i.e. system properties) selected.*
2. Set the numeric variation range of each parameter: *This is set to be ±30% from base value for all 40 parameters.*
3. For each selected parameter, generate a series of 500 iteration steps.
4. Run the PEM model using the selected series of 500 numbers for each parameter and then calculate the corresponding objective function value using Eq. (1), for different PEM current values.

$$f_{(i)} = \sum_{k=1}^{500} \left(V_{cell(i),typical} - V_{cell,(i)}(k) \right)^2 \quad (1)$$

5. Evaluate the relative sensitivity criteria at different SOFC current values of each parameter by using Eq. (2).

$$\phi_{(i)} = \frac{f_{(i)}}{V_{cell,(i),typical}} \quad (2)$$

6. Evaluate the sensitivity index value (overall relative sensitivity criteria) of each parameter by using Eq. (3)

$$\theta = \sum_{i=0}^{i_{max}} \phi_i \quad (3)$$

4.2. Sensitivity Analysis Results

The sensitivity analysis on the given system leads to the conclusion, that a large number of parameters have low influence on the output voltage. The most important parameter is the membrane section area, which seems to be crucial, followed by the membrane dry density and the membrane thickness and to a lesser degree the membrane equivalent mass. It has to be noted, that the most important parameters are all linked to membrane properties. Gas diffusion layer (GDL), anode and cathode seem to have less influence on the results. The result of the analysis is shown in Table 1. In the following we will concentrate on the four most important parameters.

Table 1 Sensitivity Analysis Results

Rank	Parameters (System Properties)	Sensitivity Index
1	**Membrane Section Area**	**1416.3177**
2	**Membrane Dry Density**	**476.1759**
3	**Membrane Thickness**	**223.0769**
4	**Membrane Equivalent Mass**	**77.4765**
5	Catalyst Section Area	10.0850
6	GDL Porosity	9.7113

7	GDL Tortuosity	9.0120
8	GDL Section Area	6.2642
9	GDL Thickness	5.8449
10	Cathode Channel Thickness	5.2944
11	Cathode Channel Fluid Section Area	2.8557
12	Cathode Channel Length	1.8520
13	Bipolar Plate Solid Density	1.0434
14	Bipolar Plate Solid Cp	1.0434
15	Cathode Channel Number	0.4526
16	Cooling Channel Solid Section Area	0.3809
17	Cooling Channel Thickness	0.3374
18	GDL Solid Density	0.3107
19	GDL Solid Cp	0.3107
20	Anode Support Thickness	0.3082
21	Anode Channel Solid Section Area	0.3062
22	Cathode Channel Solid Section Area	0.3035
23	Cathode Support Thickness	0.2792
24	Catalyst Solid Lambda	0.2636
25	Catalyst Thickness	0.2586
26	Anode Channel Fluid Section Area	0.2568
27	Membrane Solid Lambda	0.2564
28	Bipolar Plate Solid Lambda	0.2561
29	Membrane Solid Cp	0.2554
30	Anode Channel Thickness	0.2548
31	Bipolar Plate Height	0.2537
32	Cooling Channel Length	0.2532
33	Cooling Channel Number	0.2532
34	Bipolar Plate Emissivity	0.2529
35	Anode Channel Length	0.2525
36	Catalyst Solid Density	0.2525
37	Catalyst Solid Cp	0.2525
38	Cooling Channel Fluid Section Area	0.2524
39	GDL Solid Lambda	0.2524
40	Anode Channel Number	0.2523

4.3. Parameter Identification

As shown before, there is a strong difference with regard to the sensitivity for different parameters. Unfortunately very little information is available for the system, neither from system manufacturer nor from other researchers. Therefore the parameters have to be identified numerically (Laffly, Pera, & Hissel, 2007). Hence, a non-linear, constrained approach based on least-squares method is applied in Matlab Software (Deb, 2001). The initial and optimized parameter values are presented in Table 2.

Table 2 Initial and Final Values of Parameter

Parameter	Unit	Default Value	Final Value
Membrane Section Area	[m2]	0.01476	0.01
Membrane Dry Density	[kg/m2]	1970	858.596
Membrane Thickness	[mm]	0.1279	0.0517
Membrane Equivalent Mass	[kg/mol]	1.0	0.5055

5. COMPARISON OF RESULTS

Figure 5 shows the results of the model with default, improved model and measurement results, it can be seen, that the identification of the four most influencing parameters leads to a significant improvement of the model with regard to measurement values. The mean error for a polarization curve dropped from 9.58% to 1.48%.

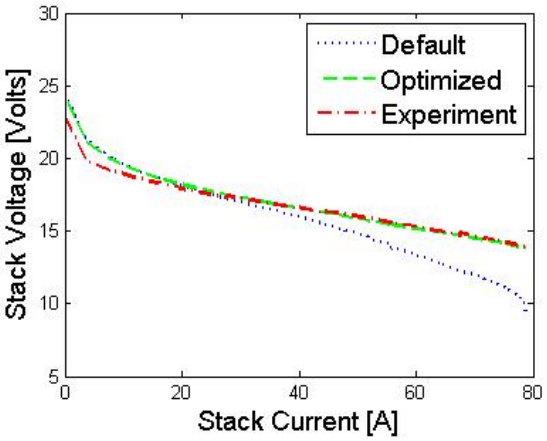

Figure 5 Modelling and Experimental Results

In order to validate the solution, the optimized system properties were used on a more dynamic current profile. This profile is based on the power demand that might occur in a fuel cell vehicle (based on Renault Zoé vehicle) on the new European driving cycle (NEDC).

This power demand was scaled down so that the peak power demand is within the working limits of the Bahia fuel system. Figure 6 shows the measured and simulated voltage profile. It can be seen that improvements have to be made with regard to the open cell voltage. As seen from figure 5 at low currents the open cell voltage is higher than experimental voltage and in NEDC there many idling / no load and low load phases, the same effect is reflected on the NEDC.

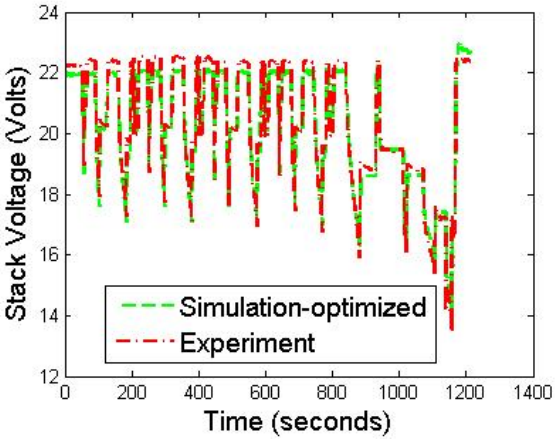

Figure 6 Comparison of Experimental and Simulated voltage in NEDC

The parameter identification is done with initial temperature of cathode, anode and cooling channels at 60.8°C. However, for NEDC the same was 30.5°C. The difference in initial temperature reflects on the NEDC simulation. Thus at the beginning of NEDC the experimental voltage is higher and towards the end the theoretical voltage is higher than experimental voltage. This can be attributed to warming up the Bahia Fuel System as the whole driving cycle lasts 1220 seconds.

6. CONCLUSION AND PERSPECTIVES

A precise model is a very important tool in order to complete the research portfolio of a fuel cell system. Even though the Bahia fuel cell system is useful for experiments with regard to different applications, it does only provide a very limited number of technical data. In order to use a physical model, instead of a black box model, an existing multi-physics model - capable of doing real time evaluation - was chosen and its forty system properties were analysed with regard to their sensitivity on the model result. The sensitivity analysis showed that only few system properties have a big influence on the stack voltage and that all the most influencing parameters are linked to membrane. Afterwards, the four most influencing parameters are identified with the help of a non-linear constrained parameter identification based on least squares method. Those results are re-injected into the model and show considerable improvement of the model results in comparison to the measurement values.

In the following the four most important system properties have to be identified more accurately, for different working temperatures. With improved parameters, the model will be used for different applications, which may contain real time application.

REFERENCES

Cheddie, D. F., & Munroe, N. D. H. (2008). Semi-analytical proton exchange membrane fuel cell modeling. *Jounal of Power Sources*, *183*, 164–173. doi:doi:10.1016/j.jpowsour.2008.04.067

Chrenko, D., Péra, M.-C., Hissel, D., & Geweke, M. (2008). Macroscopic Modeling of a PEFC System based on Equivalent Circuits of Fuel and Oxidant Supply. *ASME Journal of Fuel Cell Science and Technology*, *5*, 11015. doi:DOI: 10.1115/1.2786471

Correa, J. M., Farret, F. A., Popov, V. A., & Simoes, M. G. (2005). Sensitivity analysis of the modeling parameters used in Simulation of proton exchange membrane fuel cells. *Energy Conversion, IEEE Transactions on*, *20*(1), 211–218. doi:10.1109/TEC.2004.842382

Correa, J M, Borello, F. Santarelli, M. (2011). Sensitivity Analysis of Temperature Uncertainty in an Aircraft PEM Fuel Cell. *Internaltional Journal of Hydrogen Energy*, *36*, 14745 – 14758.

Deb, K. (2001). *Multi-Objective Optimization Using Evolutionary Algorithms*. John Wiley & Sons.

Famouri, P., & Gemmen, R. S. (2003). Electrochemical circuit model of a PEM fuel cell. In *Power Engineering Society General Meeting*.

Gao, F., Blunier, B., & Miraoui, A. (2009). A multiphysic dynamic 1D model of a proton exchange membrane fuel cell stack for real time simulation. *IEEE Transactions on Industrial Electronics*. doi:10.1109/TIE.2009.2021177

Gao, F., Blunier, B., & Miraoui, A. (2012). *Proton Exchange Membrane Fuel Cell Modelling* (p. 239). Wiley & Sons.

Grasser, F., & Rufer, A. C. (2006). A fully analytical PEM fuel cell system model for control applications, *00*(c), 2162–2168.

Helion/Areva. (2014). Bahia Bench Overview. Retrieved April 13, 2014, from http://www.areva.com/EN/operations-4576/bahia-bench-overview.html

Huangfu, Y., Gao, F., Abbas-Turki, A., Bouquain, D., & Miraoui, A. (2013). Transient dynamic and modeling parameter sensitivity analysis of 1D solid oxide fuel cell model. *Energy Conversion and Management*, *71*, 172–185. doi:10.1016/j.enconman.2013.03.029

Laffly, E., Pera, M.-C., & Hissel, D. (2007). Polymer Electrolyte Membrane Fuel Cell Modelling and Parameters Estimation for Ageing Consideration. In *IEEE International Symposium on Industrial Electronics, ISIE 2007*.

Miotti, A., Di Domenico, A., & Guezennec, Y. G. (2005). Control-Oriented Model for an Automotive PEM Fuel Cell System with Imbedded 1+1D Membrane Water Transport. In IEEE (Ed.), *Vehicle Power and Propulsion, 2005 IEEE Conference* (pp. 611–618). IEEE.

Rodatz, P. H. (2003). *Dynamics of the Polymer Electrolyte Fuel Cell: Experiments and Model-Based Analysis*. Eidgenoessische Technische Hochschule (ETH) Zuerich.

Van Nguyen, T., & Knobbe, M. W. (2003). A liquid water management strategy for PEM fuel cell stacks. *Journal of Power Sources*, *114*(1), 70–79. doi:10.1016/S0378-7753(02)00591-8

AUTHORS BIOGRAPHIES

Raaj Ganesh SAMIKANNU RAMESH was born in Tamil Nadu, India in 1988. He received Bachelor of Engineering degree in Automobile Engineering in 2005 at PSG college of Technology affiliated to Anna University, Chennai, India. He worked in Automotive Transmission engineering, research, design and development division of Maruti Suzuki India Limited, New Delhi India for 3 years. He is currently pursuing Masters in Automotive Engineering for Sustainable Mobility jointly conducted by École d'ingénieurs Polytech Orléans affiliated to University of Orleans, Orleans, France and Institut Supérieur de l'Automobile et des Transports (ISAT) affiliated to University of Burgundy, Nevers, France. He is now working as a research intern at Laboratory DRIVE, affiliated to ISAT & University of Burgundy. He is currently working on the modelling of low temperature fuel cell systems.

El-Hassane Aglzim was born in Morocco February 13, 1981. AGLZIM received in 2004 the "DESS" degree (specialized graduate degree) degree in embedded electronics systems from the University of Metz, France. In 2005, AGLZIM received the M.Sc. degree science engineering, from the University of Nancy, France. After that, he joined the Instrumentation and microelectronics Group of the LIEN Laboratory LIEN), University of Nancy, France, in October 2009 AGLZIM obtained the Ph.D. degree in the Instrumentation and Microelectronics (IM) Science at the University of Nancy. His Ph.D. thesis was entitled 'Characterization by electrochemical impedance spectroscopy method of the complex impedance of a fuel cell - evaluation of the influence of humidity'. From 2009 to 2010, he completed a Postdoc in the System and Transportation Laboratory (SeT) in Belfort, France. He joined the Energetic team of the ISAT in September 2010 as an associate professor. He works in the field of fuel cells and has published several articles in the domain. His current research interests the diagnosis of fuel cells by using the Impedance Spectroscopy method. In parallel to his research works, he teaches electrical engineering, signal acquisition, electrical motors and hybrid vehicles.

Daniela Chrenko was born in Germany in June 1978. She received the Dipl-Ing. FH degree in applied physics of the university of applied sciences in Wedel, Germany in 2002, the MSc of process engineering at the university of applied sciences in Hamburg Germany in 2006 and the PhD for the study of on-board hydrogen production for low temperature fuel cell systems at the university of Franche Comté in Belfort, France in 2008. Her research is linked to technologies for automotive applications, namely hybridization, battery technology and fuel cell systems. She worked on Stirling engines in combination with high temperature fuel cell systems. The aim of her current research is to increase energy efficiency in transportation applications, including studies of energy demand, energy management and main system components as batteries and fuel cell systems. She is now working as associate professor at the University of Burgundy and teaching electrical engineering, signal acquisition, electrical motors and hybrid vehicles..

Luis Le Moyne was born in Mexico City, on April 24, 1969. He received in 1992 the Engineer degree from the Ecole Nationale Supérieure d'Arts et Métiers (Paris tech), in 1993 the D.E.A degree in Energy Conversion, from the University of Paris 6, France. He developed advanced modelling of Diesel engines for airborne. After that, he joined the Physics & Mechanics lab, University Pierre and Marie Curie (Paris VI), France, where he started his Ph.D. thesis under the supervision of Pr. J. Jullien. In 1997 he obtained the Ph.D. degree in the Energy Conversion Science at the Ecole Nationale Supérieure des Arts et Métires (Paris Tech). His Ph.D. thesis was entitled 'Air/Fuel excursions reduction in transient functioning of S.I Engines)'. From 1998 to 2008, he was an associate lecturer in the University Pierre and Marie Curie (Paris VI). In September 2007, he was awarded the «Habilitation à Diriger des Recherches» (HDR) from University Pierre and Marie Curie (Paris VI) for his research on 'Reactive mixture formation studies in internal combustion engines'. In September 2008 he joined ISAT University of Burgundy where he founded the energy, propulsion, electronics and environment department, and in February 2011 was nominated director of institute.

INFLUENCE OF PROBABILISTIC WIND FORECAST ACCURACY IN THE OPERATIVE MANAGEMENT OF RENEWABLE ENERGY SYSTEMS WITH STORAGE

Azcárate C[(a)], Mallor F [(b)], Blanco R[(c)]

[(a) (b) (c)]Public University of Navarre, Spain

[(a)]cazcarate@unavarra.es, [(b)]mallor @unavarra.es, [(c)]rosa.blanco@unavarra.es

ABSTRACT

A key feature in the management of wind energy systems with storage is the probabilistic wind speed forecast. In this paper we consider a mathematical model to determine the operative management of a wind energy system with storage. The model includes all the important elements of the energy system. Decisions take into account data concerning to the structure of selling prices and penalties as well as updated probabilistic wind speed forecast. The main focus of this work is to study the influence of the probabilistic wind forecast accuracy in the operative management of a wind energy system with storage. A simulation based optimization methodology is proposed to conduct the computational study.

Keywords: Energy, storage management, simulation, optimization

1. INTRODUCTION

Renewable energy provides valuable benefits for the environment, health and economy (produces little or no CO2 emissions, stabilizes energy prices, provides an inexhaustible energy supply, etc.). Nevertheless common problems to all renewable sources of energy are high variability in its availability; uncertainty in its forecast and then difficulty in matching production and demand. As a consequence in geographic areas with high wind energy penetration energy plants based on fossil fuels are necessary to support the network (in cases of low wind energy production), which increase the cost of the energy. In periods of high wind energy production the wind-driven generators could be disconnected because the network could not absorb all the electricity.

The storage of energy would allow solving most of the problems posed by the wind energy generation. It makes possible the management of the generated energy leading to better selling prices in the electricity market. Furthermore, the stored energy increases the reliability of the renewal energy system since it enables to correct forecasting errors by matching the output energy to the forecasted production. Lastly, it increases the wind energy penetration index: energy can be stored in periods with higher production than requirements, and then released in low production periods.

Different energy storage systems are nowadays available: lead-acid and sodium-sulfur batteries, compressed air energy storage, pumped hydro, electrolysis combined with fuel cells, and others, with different properties related with response time, storage efficiency and costs. Comprehensive technical reviews on energy storage systems can be found in (Ibrahima et al, 2008; Beaudin et al, 2010; Hedegaard and Meibom, 2012). In this work we consider hydrogen (H2) as the energy storage system, although the analysis carried out in this paper could be easily adapted to other storage systems. The hybrid wind-hydrogen energy system comprises electricity-generating wind turbines, electrolysers and hydrogen compressors to convert electricity into hydrogen (the conversion process), an H2-tank with finite hydrogen storage capacity and various energy-conversion technologies for the process of turning hydrogen into electricity (the recovery process).

Energy prices follow similar rules to the stock market. They vary with demand, and fluctuate throughout a given day while also showing variations for the same time across different days. Furthermore, prices depend on whether (or not) the amount to be sold has been pre-committed (the day before). In the case of a pre-commitment, the price is higher, but if the agreed amount is ultimately not supplied, then a penalty has to be paid. When more than the agreed amount is supplied then the surplus has a lower price. Thus, to obtain full benefit from the participation in the electricity market it is necessary to commit the electricity to be sold one day ahead.

Due to the stochastic nature of renewal sources, like wind, the exact amount of renewal energy produced cannot be known in advance. The commitments of energy have to be done by using wind speed forecast. Wind speed forecast errors lead to a mismatch between commitments and generated energy. Magnitude of errors increases as prediction horizon moves away. Probabilistic forecast becomes the most appropriate way of estimating forecast uncertainty. It provides forecast of the probability distribution of wind speed for each look-ahead time (Gneiting and Larson 2006).

A probabilistic wind speed forecast at time *t* is a set of *m* predicted wind speed trajectories for the coming future (Moehrlen 2004). They are obtained from

different and coherent physical parameterizations of the meteorological model utilized. Usually, meteorological forecasts have a forecast resolution of one hour for look-ahead times up to 48 hours (Pinson and Madsen, 2009).

Storage operative management involves deciding when to use the stored energy to meet the pre-commitments. Decisions should take into account data concerning to the structure of selling prices and penalties, as well as updated wind speed forecast.

A main issue is to determine the amount of energy that should be committed one day ahead to maximize the profit. In (Aguado et al, 2009) the committed energy was obtained as solution of a sequence of linear integer programming problems which use as input data the expected wind speed in the look-ahead period. This analysis does not consider the uncertainty in the wind speed forecast and the operative management of the H2-tank is addressed in a naïve way: At time *t*, if more energy than committed is produced, then store the surplus; if the generated energy is less than commitments, then use the stored energy to correct deviations. The model provided an economic analysis of the viability of such systems and was valid as a first approximation to solve a dimensioning problem related with the facilities and necessary equipment. Nevertheless, the model was not appropriate for the system management. As a solution to those drawbacks, managers suggested a class of management policies based on a more regular and dynamic use of the tank. The new strategy, named peaking strategy, is based on the conversion of electricity into hydrogen during price troughs and the use of the stored hydrogen to produce electricity during the day's demand (thus price) peaks. These loading and unloading periods are denoted by H2-storage (valley) and H2-release (peaking) periods, respectively. Strictly speaking, peaking strategy dictates to store energy in valley hours and to release it in the peaking hour, giving no further use to the tank. However, the possibility of using the stored energy to fulfil the energy committed by correcting deviations is attractive and worthy to be investigated. This additional use for the stored energy requires making new decisions at each hour concerning with whether release energy when generated energy is below the committed energy and whether store energy in the opposite case, that is, the generated energy exceeds the committed energy. The computational implementation of the peaking strategy (Azcárate et al, 2012) allowed the capability of use the tank to match the delivery commitments but the operative decisions needed to manage the tank were fully assumed by the decision maker.

In this work, we provide the decision maker with an optimized strategy to operate the tank. Two objectives are considered: an economic one, aiming at maximizing the profit from the energy selling and a reliability one by maximizing the number of hours in which the energy commitments are fulfilled.

2. MATHEMATICAL MODEL

Optimal management policies have to make full use of the available information at the decision times. We propose operative policies for the storage management that benefit from an updated probabilistic wind speed forecast, $W(t_0)$, and take into account the structure of electricity prices, the hourly committed electricity, penalties for mismatch the commitments and the current amount of stored energy.

Two types of scenarios are considered to define an operative management policy for the tank:

- Shortage scenario (A): at time *t* the generated wind energy (*G(t)*) is less than the committed energy (*C(t)*). In this case, should the stored energy in the tank be used to match the committed energy?
- Surplus scenario (B): at time *t* the generated wind energy is greater that the committed energy. In this case, should the surplus of energy be stored in the tank for its future use?

Optimal management policies are obtained as solution of a sequence of rolling horizon stochastic optimization problems. At each time t_0, an optimization problem with decision variables $g_T(i), g_R(i),\ i = t_0, t_0+1, \dots, t_p-1$ is formulated, where t_p represents the peaking hour. In a shortage scenario, decision variable $g_R(i)$ represents the amount of energy recovered from the tank to match the committed energy in hour *i*. In a surplus scenario, $g_T(i)$ represents the amount of energy stored in the tank for its future use.

Variables *T(i)* represents the amount of energy stored in the tank in hour *i*. Deviations d_i^+ and d_i^- are introduced for modeling purposes and defined by: $G(i) - d_i^+ + d_i^- = C(i)$.

The objective function includes both economical and reliability criteria. The economical objective is composed by two terms. The first one assesses the profit in time interval $[t_0, t_p]$, under management policy g, $B(t_p, g)$, by using the probabilistic forecast $W(t_0)$ and the energy prices. Energy prices include different values for commitments, surplus sales (above commitments) and penalties for shortfalls in the pre-committed energy. The second term in the economical objective function $V\left(T\left(t_p^+\right), g\right)$, is an assessment of the energy that could remain stored in the tank at the end of the peaking hour, and is expressed as follows:

$$V\left(T\left(t_p^+\right), g\right) = \gamma_V * P\left(t_p^*\right) * T\left(t_p^+\right)$$

where t_p^* represents the peaking hour of the next peaking cycle, $P\left(t_p^*\right)$ the selling price of committed energy at that peaking hour and γ_V is a parameter.

The objective function can be expressed as

$$\max_g \ E_{W(t_0)}\left[\, B(t_p, g) + V\left(T\left(t_p^+\right), g\right)\right]$$

where g is the vector of decision variables, $W(t_0)$ is the probabilistic wind speed forecast and $E_{W(t_0)}[.]$ stands for the expected value of the compound benefit function.

The consideration of only economic criteria leads to use the tank for correction of errors when these corrections provide a profit. In order to improve the reliability, the tank should be used to correct errors even with no direct economic benefit. Reliability objective function $R(t_p, g)$ aims to maximize the number of hours at which the energy commitments are fulfilled.

The constraints of the optimization problem consider the capacity of the H2-tank, the H2-tank update and the efficiencies of the H2-conversion and recovery processes.

3. PROBABILISTIC WIND SPEED FORECAST

A key feature in this management strategy model is the updated probabilistic wind speed forecast. The main focus of this work is to study the influence of the probabilistic wind forecast accuracy in the operative management of a wind energy system with storage. To conduct the computational study our model simulates the probabilistic wind speed forecast at each hour through the simulation of *m* wind forecast trajectories. The model handles prediction errors as follows. Historical wind speed data are used to simulate meteorological predictions by adding an error to each item of real energy data. The error is obtained by combining an absolute error and a relative error. The maximum relative error depends on the prediction horizon and is represented by a set of non-decreasing polynomial functions limited by the initial and final maximum relative errors. In order to smooth the predicted energy curve, we keep a record of past errors to generate an auto-correlated error series. The parameters in this error forecast simulation model are used to represent the accuracy of the meteorological forecast.

Concretely, we use the following model:

$$forecast\_wind(t) = \max\left\{\begin{array}{l} 0, true\_wind(t) + \\ + \max\{relavive\_error(t) * true\_energy(t), absolute\_error\} * \\ * (2 * pred\_error(t) - 1)\} \end{array}\right.$$

We consider different non-decreasing functions representing *relative_error(t)*. Specifically, an initial *(IRE)* and a final *(FRE)* relative error are introduced as parameters of the model, and a set of order-two polynomial non-decreasing functions *(relative_error(t) = A+Bt+Ct²)* limited by both *IRE* and *FRE* values are obtained as solutions of the following system of equations, where *t=1,…,T* represents the forecast time horizon:

$$\begin{cases} A + B + C = IRE \\ A + BT + CT^2 = FRE \\ B + 2Ct > 0, \forall t = 1,...,T \end{cases}$$

As an example, Figure 1 shows a set of functions, with *IRE=5*, *FRE=40* and *T=60*. For more details about this wind speed forecast simulation model, the reader is referred to (Mallor et al, 2009).

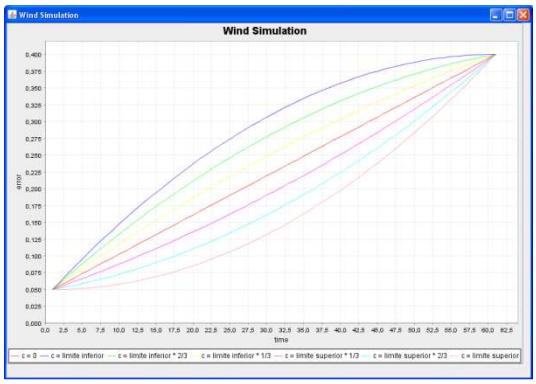

Figure 1: Relative error functions

An example illustrating the simulation of the probabilistic wind speed forecast from hour t_0 to hour t_p (band 1) and an updated probabilistic forecast at hour t_i (band 2) is shown in figure 2. The variability of the errors in probabilistic wind speed forecast decreases as the updated prediction gets closer the peaking hour.

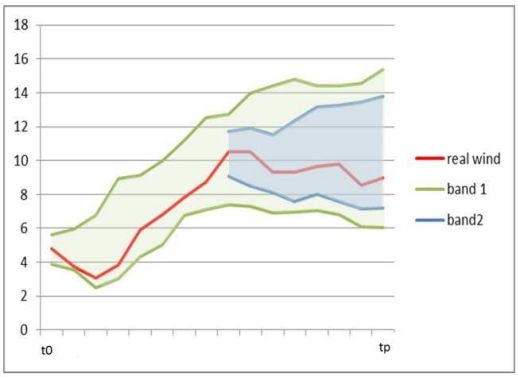

Figure 2: Probabilistic Wind Speed Forecast

4. USEFULLNESS OF THE SIMULATION-OPTIMIZATION MODEL

A simulation based optimization methodology is proposed for the assessment of the management. We develop a discrete event simulation model for a real inspired renewable energy system with H2-based storage, moving the simulation clock in 1-hour steps. The simulation model incorporates the important equipment that compose the wind-H2 energy system and the random elements of the stochastic environment in which the energy system evolves. The wind farm is

characterized by its power capacity and its wind-power conversion curve; the hydrogen tank is described by its capacity; and the electrolysers, compressor and the different technologies involved in the recovery process are described both by their capacities and their efficiency curves. Our study assumes the availability of a long series of historical data containing hourly wind speed. A detailed description of such real energy systems can be found in (Aguado et al, 2009). The model allows the determination of different peaking strategies.

At each hour *t*, we simulate the wind speed forecast and then the amount of energy generated. Taking into account this amount of energy, the hydrogen stored in the tank and the pre-committed supply for this hour, the amount of energy to be stored or released into the grid is determined. This decision is made according to the optimization problem described in section 2, implying the simulation of the updated probabilistic wind speed forecast. When the simulation clock reaches the time at which the energy supply commitments for the following day must be announced, these values are determined by the cost and probability strategy described in (Azcárate et al, 2011).

Global system assessment is made by considering two objective functions: reliability and profit. Economical objective function is calculated considering energy prices for commitments, energy prices for surplus sales (above commitments) and penalties for shortfalls in the pre-committed energy. In order to compare the effect of the use of the tank to correct errors, we consider as economical objective function the ratio between the expected profit obtained with the operative management strategy and the expected profit obtained without using the tank to correct errors. Reliability objective function is measured as the percentage of hours in which commitments have been accomplished.

This proposed simulation based optimization methodology allows the assessment of the management strategy considering different price structures and efficiencies of the whole storage system. Preliminary results show that price structures with very high penalties for shortfalls in commitments and surplus with almost no value make economically attractive the use of the tank to correct errors in normal hours. This also depends on the efficiency of the whole storage system and on the probabilistic wind forecast accuracy.

5. CONCLUSIONS

In this paper we have mathematically modelled the problem of optimally operating the storage of a renewal energy system. This mathematical model describes all important elements of the energy system and, furthermore, it incorporates the variability of both energy prices and renewable resource availability. Main features of this model are the incorporation of a probabilistic forecast for the renewal energy which is dynamically updated and the simultaneous consideration of economical profit and reliability objectives.

The variability in the structure of the energy prices and penalties influences the commitment strategy and, together with the system efficiency, the cost of correcting errors. The degree of uncertainty in the renewal forecast affects the reliability of the system as provider of energy. And, of course, differences in the amount and variability pattern of the renewal resource impact in the global performance of the energy system. The consideration of all these elements together requires an extensive design of simulation experiments to assess the influence of each one of them.

ACKNOWLEDGMENTS

This work has been in part supported by grant MTM2012-36025.

REFERENCES

Aguado, M., Ayerbe, E., Azcárate, C., Blanco, R., Garde, R., Mallor, F., Rivas, D. 2009. Economical assessment of a wind-hydrogen energy system using WindHyGen® software, *International Journal of Hydrogen Energy*, 34, 2845-2854.

Azcárate, C., Blanco, R., Mallor, F., Garde, R., Aguado, M., 2012. Peaking strategies for the management of wind-H2 energy systems, *Renewable Energy*, 47, 103-111.

Beaudin, M., Zareipour, H., Schellenberglabe, A., Rosehart, W., 2010. Energy storage for mitigating the variability of renewable electricity sources. An updated review, *Energy for Sustainable Development*, 14,302-314.

Gneiting, T., Larson, K., Westrick, K., Genton, M.G., Aldrich, E., 2006. Calibrated probabilistic forecasting at the state-line wind energy center. The regime-switching space-time method. *Journal of the American Statistical Association*, 101, 968-979.

Hedegaard, K., Meibom, P., 2012. Wind power impacts and electricity storage - a timescale perspective. *Renewable Energy*, 37, 318-324.

Ibrahima, H., Ilincaa, A., Perronb, J., 2008. Energy storage systems. Characteristics and comparisons. *Renewable and Sustainable Energy Reviews*,12,1221-1250.

Mallor, F., Azcárate, C., Blanco, R., 2009. Including risk in management models for the simulation of energy production systems. *Proceedings of the 39th International Conference on Computers & Industrial Engineering*, pp. 1821-1826. July 6-8, Troyes (France).

Moehrlen, C., 2004. *Uncertainty in wind energy forecasting*. Thesis (PhD). University College Cork.

Pinson, P., Madsen, H., 2009. Ensemble-based probabilistic forecasting at Horns Rev. *Wind Energy*, 12, 137-155.

FERMÍN MALLOR studied mathematics at the University of Zaragoza, Spain. He received his doctorate in mathematics from the Public University of Navarre, in 1994. Currently he is a Professor in statistics and operations research. In addition to having taught for more than 20 years university courses in simulation, operations research and statistics, he has successfully applied his knowledge in simulation and statistical modeling to the analysis of complex real problems arisen in several industrial companies and institutions. His research interests are simulation modeling, queuing theory, functional data analysis and reliability. His email address is mallor@unavarra.es.

CRISTINA AZCÁRATE studied mathematics at the University of Zaragoza, Spain. She received her doctorate in mathematics from the Public University of Navarre, in 1995. Currently she is an Associated Professor in statistics and operations research. She teaches optimization and simulation to civil engineers. Her research interests are simulation modeling and optimization with simulation. Her email address is cazcarate@unavarra.es.

ROSA BLANCO is an assistant professor in the Department of Statistics and Operations Research at the Public University of Navarra. Her research interest lies in the area of supervised classification and optimization by means of Bayesian networks with medical applications. Nevertheless, she starts with a new research interest in combinatorial optimization and simulation.

ELECTRICITY CONSUMPTION PATTERNS IN HOUSEHOLDS

Fermín Mallor[(a)], José Antonio Moler[(b)] and Henar Urmeneta[(c)]

Departamento de Estadística e Investigación Operativa, Universidad Pública de Navarra. Pamplona, Spain

[(a)] mallor@unavarra.es, [(b)]jmoler@unavarra.es, [(c)]henar@unavarra.es,

ABSTRACT

Obtaining patterns for electricity consumption in a particular household is a key point to simulate and to dimension the electricity supply needed in an isolated house. Electricity consumption profile of a user is a function that indicates the electrical consumption in a dwelling over a period of time, usually one day. When this function is considered as a datum and some days are observed, a sample of functions is obtained. Functional Data Analysis (FDA) provides procedures and techniques to analyze this kind of samples. In particular, usual estimators and some procedures of the classical statistical analysis are extended to this context. In this paper we make use of the FDA to analyze the variability in the electricity consumption profiles to obtain consumption patterns useful for simulation of electricity demand in individual households.

Keywords: electricity consumption pattern, functional data analysis, electricity demand simulation.

1. INTRODUCTION

Electrical demand modeling is quite usual in the study of electrical consumption because this analysis is crucial for making decisions about electrical production.

End-user models describe the electrical consumption of a particular household. Depending on relevant characteristics of the consumers, different demand models can be considered. A careful aggregation of the consumer models provides the conventional global electrical demand curve. This procedure is known as bottom-up demand modeling approach. The main difficulty of this procedure is to obtain enough information, in some cases with a high level of detail, from the individual users to design accurate models. Several approaches have been considered in the specialized literature to provide realistic models, see, for instance, Paatero and Lund (2006) or Muratori et al. (2012) and the references therein.

On the other hand, top-down models use global information, say, macro-economic variables joint with global estimates of the energy consumption and structural characteristics of the dwellings, to assign a pattern of the electrical consumption in a particular household. Econometric models have usually been used in this approach. An interesting review about top-down and bottom-up models is presented in Swan and Ugursal (2009) where pros and cons for each methodology are analyzed.

This work is a part of a more ambitious project that aims at obtaining a simulation model of the individual household electrical consumption. This is needed in order to properly dimension the energy supplies that an isolated household may need to cover its necessities. Both methodologies, bottom-up and top-down will be used to reach this goal. On the one hand, big national surveys carried out by statistical agencies are used to establish several profiles of electrical consumers about the total energy in a year. In this work we make an exploratory analysis to identify which general characteristics cluster properly the population with respect to the consumption of energy. On the other hand, data are taken from individual households to establish individual profiles, and observe how to deal with these information in order to determine which aspects explain better the consumption of electrical energy in a particular household. A datum now is the vector of dimension 1440 which contents daily electrical consumption minute by minute of a user and, from the mathematical point of view, these are the values that take a function in points equally spaced on the interval [0,1440]. This function is the daily individual profile load curve of a user. For each user, we observe N days, so we have a sample of N individual profile load curves. In order to handle this kind of data, we appeal to a specific statistical technique which is Functional Data Analysis (FDA) and becomes the natural way to handle this kind of data, see Ramsay and Silverman (2005).

The classical techniques to deal with electricity prices and loads are time series models, see, for instance, an overview in Weron (2006). FDA is seldom applied in this context, however, some papers have appeared in the recent literature that use it with different goals to the one considered here. In the seminal paper by Hyndman and Ullah (2007) FDA is introduced to forecast time series data, even though they illustrate the methodology with demographic data, the extension to other contexts is immediate. In Andersson and Lillestøl (2010) two FDA techniques are presented, functional analysis of variance (FANOVA) and a functional autoregressive model (FAR), in order to make, respectively, data exploration and forecasting electricity

consumption. The former helps to study seasonalities and the latter focuses on the time-series nature of the consumption. They consider that FDA is a promising way to search for the data-generating mechanisms in the electricity market. In Goia et al. (2010) FDA is also used for short-term peak load forecasting. They have hourly observations of the aggregate consumption in a district-heating during 198 days in four different years. A basic model is to consider a functional regression model where the response is the daily peak of heating and a functional regressor which is the load curve of the previous day. The forecasts are improved when load curve are clustered with a FDA technique and the basic regression model is applied in each cluster that concentrates load curves that exhibit similar consumption. Recently, in Liebl (2013), FDA is used to model and forecast electricity spot prices but, as stated there, the techniques to model and forecast spot prices are more complex than those needed for modeling and forecasting electricity demand.

In this paper, as stated before, we deal with general surveys on the consumption habits of the population, as the HBS in Spain, see INE (2010), which provides household profiles with respect to the electric consumption. Then, individual load curves for representative dwellings of each profile are sampled where observational points of the daily load curve are taken every minute with a smart meter. In the previous references, aggregated data are used in the applications and this entails smoother curves than individual ones. The variability of individual load curves require some treatment of the sample information in order to apply FDA techniques. In Chaouch (2014) the goal is short-term forecasting of the household-level intra-day electricity load curve so the setting is quite similar to this work but nor the goal neither the statistical techniques used are equal. Guardiola et al. (2014) is an important methodological reference for this paper, although the setting is quite different to ours.

A common conclusion in the previous references is that FDA allows making an integral treatment of the daily consumption and avoids the separate treatment that classical techniques require for the observational points in the same day. FDA also allows us to establish daily patterns depending on the consumer and some environmental characteristics.

This paper is organized as follows. In section 2 a description of the procedure used to collect and organize the sample information is given. In section 3, statistical methodology applied to sample data is briefly explained. In section 4, some results are outlined for a particular household in order to illustrate the technique applied.

2. COLLECTION OF DATA

As a preliminary step, a study to determine typologies of households depending on their consumption of energy has been carried out. This study considers a huge amount of data provided by the Spanish Statistical Institute in the Household Budget Survey (HBS), see the methodology followed in this Survey in INE (2010) . This survey is made every year on 24000 dwellings randomly selected. Each household provides detailed information of their consumption expenditure during two consecutive weeks in each of the two years of their participation. They also fill a form where the consumption of goods which are periodically paid, as the energy, is reflected, therefore, Spanish Statistical Institute publishes every year the annual consumption of each type of energy in the sampled households.This survey considers several classifications to understand the different typologies of households and the classification that shows the best ability to distinguish profiles of total consumptions among households is taken as a benchmark. In fact, a household representative of each class is considered in order to make an individual study. The goal now is not so much to know the total daily consumption, but to be able to simulate consumption curve minute by minute of the day.

For this individual study an energy meter has been installed in several dwellings. The global electricity consumption in the house is saved every minute. So that, not distinction among the appliances used in the household is collected. The information was recorded for one year. The information provided by the device is given in an excel file with two main columns: date and time of the record (DD/MM/YYYY HH/MM) and kwh consumed.

Considering a day as a natural period of time we have a sample of size 365 where each datum is a vector of 1440 components (the electrical consumption of each minute of the day). This sample of functional data is the basis for the study in each household.

The excel file is read by the R software. Date and time information is used to obtain several factor variables: day of the week, month and period of the day.

A new file is built where each day becomes a column (or row) with 1440 observations which represent the kw consumed each minute of the day. The fda package for R fda.usc, see FebreroBande and Oviedo de la Fuente (2012), is used to make an exploratory analysis of these data.

First of all, we should refine the file because some days show extremely low consumption levels. This can be produced because the family leave the house for a long period, for instance, holidays but the most disturbing situation is when some accidental failures of the energy monitor produce large sequences of zero consumption which distort dramatically the analysis. In order to do this refinement, two procedures are followed

a) The routine implemented in fda.usc to detect outliers.
b) A particular routine is implemented in order to detect those days with a high percentage of minutes without consumption that has not been large enough to be considered as an outlier.

This refinement must be careful because we do not have to punish households with efficient appliances that save energy.

3. STATISTICAL METHODS

Data are collected as n observed digitized curves $\{x_i(t_j): j=1, ..., p\}$ with $i=1, ..., n$. The observation points, t_j ,are equidistant. In our case $n=365$ and $p=1440$. This entails a large amount of observations for which classical statistical techniques are not designed to cope with. FDA fills this gap.

The first task in FDA is to convert these data to a function x_i with values $x_i(t)$ computable for any desired argument t. Two approaches are possible: interpolation or smoothing. The latter is better when the target is to clustering data. This is our case because different behaviors of the individual electricity consumption are expected depending on the weekday, the month or other characteristics associated to each day. See, Hitchcock et al (2007).

In this work, the smoothing procedure consists of representing the function $x(t)$ as a linear combination of K known basis functions. This functions are polynomial segments jointed end-to-end at certain argument values called knots. This technique is computationally intensive but, as stated in the previous section, appropriate algorithms have been implemented in the statistical package R to ease the application of the FDA.

An outlier technique implemented in the fda.usc package has been used to eliminate from the sample those days which reflect failures in the energy meter, see more technical details in Febrero-Bande and Oviedo de la Fuente (2012).

There is also a natural extension of the classical summary statistics mean and standard deviation in the FDA framework.

We can also consider with FDA a technique similar to the multivariate technique of principal components, this is called with the acronym PCA. In this case, each functional datum (each day) is written as a linear combination of a basis of splines. The size of the basis is chosen with an optimization function included in the fda.usc package. Then, the role of the components is taken over by the harmonics. Each harmonic is a function which collects some essential characteristic of the electrical usage in a household. Each day can be written as a lineal combination of the harmonics. The coefficients are called scores. The technique is useful when two or three harmonics are enough to capture a high percentage of the variability of the whole data. The harmonics are ordered depending on the percentage of variance that contain. Then, we can represent each day in a plane attending at their scores in the two main harmonics. The goal is to cluster the whole sample of days depending on the harmonic that best represent them. A similar procedure is followed, in another context, in Guardiola et al. (2014) where the interested reader can find technical details.

Finally, smoothing methods, not necessarily based on splines, are considered in order to distinguish in each daily curve a fixed behavior in the individual electrical consumption and the peaks generated by the use of some appliances in the house as dishwasher, washing machine, iron, microwave…. These peaks account for a large part of the data variability. A good understanding of both processes is a basic step for designing a good simulation model.

4. RESULTS

Here we present a short overview of some graphical and numerical results that can be obtained with FDA techniques.

We consider the sample of a user. First an outlier detection technique is applied and n=216 curves (days) are finally considered for the study.

In Figure 1, mean and standard deviation functions are plotted over the profile generated after drawing the 216 curves. We observe that this user presents the most homogeneous behavior from the minute 1200 (20:00 CET) until midnight and wee hours because the mean function takes greater values than the standard deviation. Besides this, some load curves present large peaks, far away from the mean behavior. These peaks of consumption produces the high variability in the data which is so typical in individual load curve, something that gets mitigated when data are aggregated in hours, see Figure 2 f or this user.

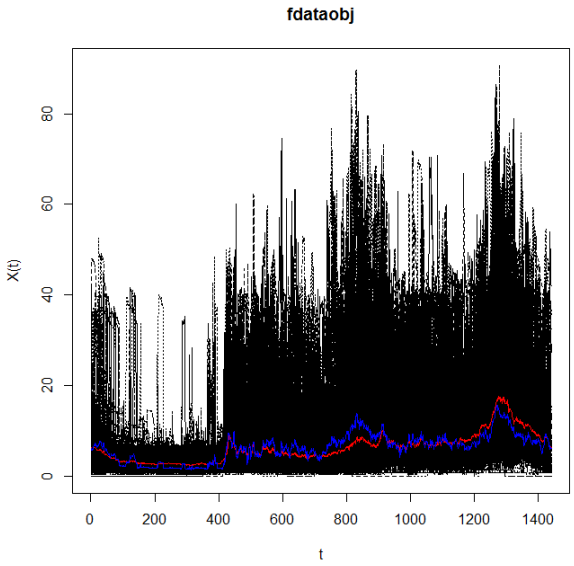

Figure 1. Mean function in red, deviation function in blue. Consumption profile for the 216 curves in black.

A PCA exploratory analysis is applied with the fda.usc package. Unfortunately, the three main harmonics are not able to capture a 30% percent of the variability of the data for any of the households under study. We modify our data file as follows. We consider for each day the electricity consumption ordered in a decreasing way. Now, the graph of each functional data does not represent the amount of consumption at each minute of the day. But it gives the amount of minutes for which the electricity consumption was larger than a

specific value, we will call it ordered load curve. This graphic can be obtained for several tracks in the same day. Figure 3 shows in the left panel the ordered load curve when the day is divided in 1 period, and in the right panel, when there is no division in periods.

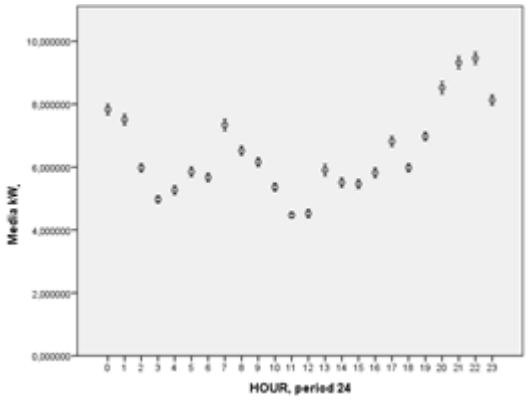

Figure 2. Confidence interval (95%) of the mean consumption per hour

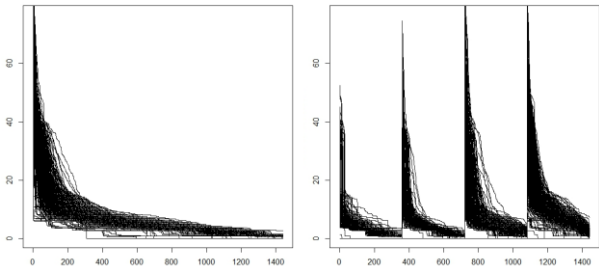

Figure 3. Left panel, Pareto grafic of the electric consumption for the 216 load curves. Righ Panel, Pareto graphic of the consumption for each of the four periods of the day (0,6) (6 , 12), (12, 18) (18, 24)

An analysis of principal components for these new data files provides, for the three first harmonics, an explanation of the total variability that increases, see Table 1, when the ordered load curve only consider one period.

Table 1. Total variability collected by the harmonics.

Data file	Harm 1	Harm2	Harm3	Sum
Load curve	0.1384	0.0817	0.0558	0.2759
Ordered Load curve in four periods	0.4317	0.2352	0.0931	0.76
Ordered Load curve in one period	0.7706	0.091	0.0486	0.9102

The improvement of the power explanation of the harmonics comes from the fact that the ordered load curve in one period does not take into account the exact time when, for instance, one appliance has been used, only takes into account the level of consumption whatever the time of the day. So that, the possible shifts in the habits of a particular household do not affect the ordered load curve, and then a source of variability that is present in the load curve disappears in ordered load curves.

In Figure4 a two dimensional representation of the data is drawn. Days are represented with different colors depending on the weekday. First harmonic distinguishes week-end days from labor days. Similar analysis can be done with other factor variables as month or bank-holidays.

Finally, in figure 5, several smoothing methods are presented with the aim of capturing a basal behavior in the electronic consumption of this family. The peak process becomes, per each day, the values over the smoothed line. Criteria to establish the best smoother are needed.

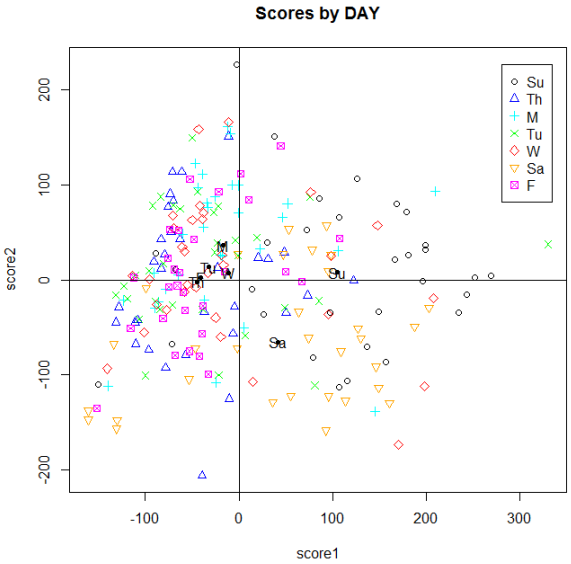

Figure 4. Two axis representation of the functional data distinguished by the weekday.

The HBS classifies households according to some typologies widely accepted by the statistics agencies, see pg. 39 in INE (2010). The main variables that determine a particular typology is the number of people in the dwelling and their age. Attending to the typology D.1.3. , Figure 2 corresponds to a household with a couple with three or more children dependent. On the other hand, Figure 6 shows the sane graphic for a household where the inhabitants are a couple where both are older than 65. Their profiles are quite different because their habits are different.

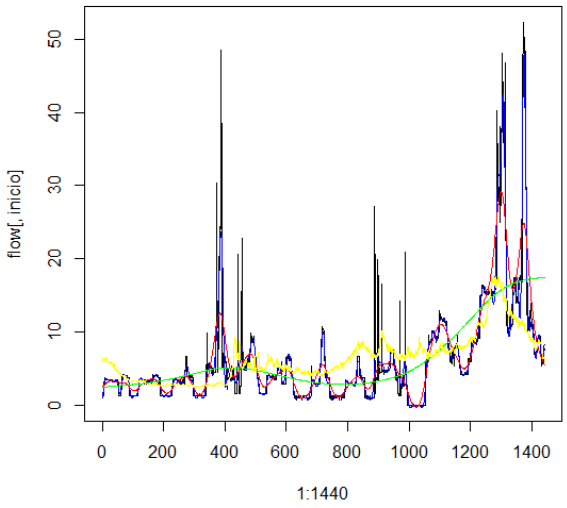

Figure 5. Smoother of a consumption electrical curve for a particular day (black), mean function (yellow), smothers for different parameter for the smoothing algorithm (blue, red, green)

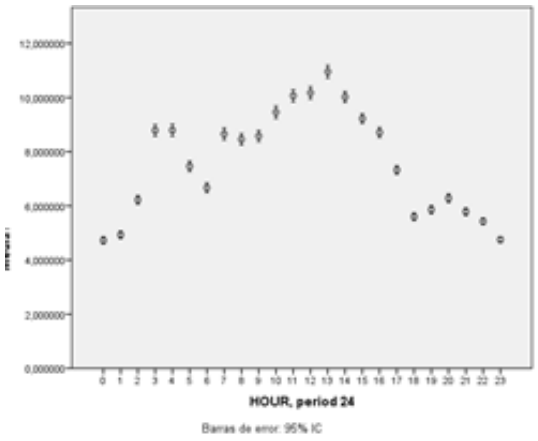

Figure 6. Confidence interval (95%) of the mean consumption per hour in a household of a couple where both are older than 65.

The HBS allows the study, with explanatory goals, of the behavior of the population with respect to the consumption of several sources of energy and the main variables that influence this behavior are the location, the existence of heater and the typology of the household.

REFERENCES

Andersson, Jand Lillestøl, J., 2010. Modeling and forecasting electricity consumption by functional data analysis. *The Journal of Energy Markets*, 3 (1), 3–15.

Chaouch, M. 2014. Clustering-based improvement of nonparametric functional time series forecasting: application to intra-day household-level load curves. *IEEE Transactions on smart grid*, 5 (1), 411-419.

Febrero-Bande, M. and Oviedo de la Fuente, M.., 2012. Statistical Computing in Functional Data Analysis: The R Package fda.usc. *Journal of Statistical Software*, 51 (4), 1–27.

Goia, A., May, C. and Fusai, Gianluca, 2010. Functional clustering and linear regression for peak load forecasting. *International Journal of forecasting*, 26, 700-711.

Guardiola, I.G., Leon, T. and Mallor, F. 2014. A functional approach to monitor and recognize patterns of daily traffic profiles. *Transportation Research Part B, 65, 119-136.*

Hitchcock, D.B., Booth, J.G. and Casella, G., 2007. The effect of pre-smoothing functional data on cluster analysis. *Journal of Statistical Computation and Simulation*, 77, 1043-1055.

Hyndman, R. J. and Ullah, M. S. 2007. Robust forecasting. *Computational Statistics & Data Analysis*, 51, 4942-4956.

INE, 2010, Household Budget Survey, Methodology, at www.ine.es/en/metodologia/t25/t2530p458_en.pdf

Liebl, D.., 2013. Modeling and forecasting electricity spot prices: a functional data perspective. *The Annals of Applied Statistics* , 7 (3), 1562-1592.

Muratori, M.; Roberts M. C.; Sioshansi, R.; Marano, V. and Rizzoni, G. (2012)A highly resolved modeling technique to simulate residential power demand. *Applied Energy* .

Paatero, J. V and Lund, P. D. 2006, *A model for generating household electricity load profiles*. *International Journal of Energy Research*;30: 273-290

Ramsay, J.O. and Silverman, B.W., 2005. *Functional Data Analysi, 2nd Edition*. New York: Springer.

Swan L.G. and Ugursal V.I. 2009. Modeling of end-use energy consumption in the residential sector: a review of modeling techniques. *Renewable and sustainable energy reviews,* 13, 1819-1835.

Weron, R., 2006. *Modelling and forecasting electricity loads and prices: a statistical approach.* Wiley.

AUTHORS BIOGRAPHY

Fermín Mallor is Professor in the Public University of Navarra. His research interests are operations research, simulation and reliability.

José A. Moler is Associate Professor in the Public University of Navarra. His research interests are stochastic processes, urn models, experimental designs, and clinical trials.

Henar Urmeneta is Associate Professor in the Public University of Navarra. Her research interests are stochastic processes, probability theory and experimental designs.

DEVS-BASED INTERACTIVE GEOSIMULATION FRAMEWORK FOR PUBLIC TRANSPORT ANALYSIS AND PLANNING

Arnis Lektauers[(a)], Yuri Merkuryev[(b)]

[(a) (b)] Department of Modelling and Simulation, Riga Technical University, Latvia

[(a)]arnis.lektauers@rtu.lv, [(b)]jurijs.merkurjevs@rtu.lv

ABSTRACT

The paper presents a new DEVS-based simulation framework for multi-modal public transport analysis and planning based on the concept of geosimulation that integrates the capabilities of multi-agent modelling and geographical information systems.

The proposed framework provides such important simulation aspects as execution possibilities of large-scale models, the support of user interactivity during the simulation execution process, as well as an effective synchronization between simulation and visualization processes.

Underlying concepts, implementation details and evaluation results of the proposed framework are discussed. The practical importance and application possibilities of the research results are demonstrated by analysing public transport simulation scenarios for the Vidzeme planning region of Latvia.

Keywords: DEVS, geosimulation, public transport

1. INTRODUCTION

In recent years, new forms of simulation have come into popular use in urban, environmental and transportation research, supported by an array of interdisciplinary advances in many scientific areas, especially in the geographical and computer sciences. These models are most commonly based on *Cellular Automata* (CA) or *Multi-Agent Systems* (MAS) formalisms and are often applied to the simulation of spatial systems in dynamic and high-resolution contexts (Ferber and Müller 1996). Modelling systems behaviour with explicit dependency of the geographic space requires a geographic information support that is usually accomplished with *Geographic Information Systems* (GIS).

A relatively new alternative for the research of spatially linked dynamic systems is geosimulation (Benenson and Torrens 2004) that is based on the concept of *Geographic Automata Systems* (GAS), which tightly couples spatial data and process models within a single integrated framework.

Although CA, MAS or GAS are intuitive and relatively straightforward for verification, they have an evident disadvantage – they do not provide any common formalism for model representation.

In the area of passenger transportation, there has been a tendency in recent years to increase investments in public transit projects and to reduce them in road construction (Laporte et al. 2011). Public transit systems or public transportation systems are increasingly complex incorporating diverse travel modes and services. The need to integrate and efficiently operate these systems poses a challenge to planners and operators (Toledo et al. 2010). By using new technologies and applications, as well as development assisting and evaluation tools prior to field implementation in public transportation systems, it is possible to find a solution for this complex problem area.

Simulation models have been established as a primary tool for transportation systems evaluation at the local operational level (Cortés, Burgos, and Fernández 2010). However, traditionally, simulation methods have not played a major role at the regional planning level, but several tools and models developed in recent years (Toledo et al. 2010; MATSim 2014; Behrisch et al. 2011) can assist the decision process and help produce transportation infrastructure designs that can be used by the transportation planners for further evaluation.

The domain of traffic and transportation systems is well suited to an agent-based approach because of its geographically distributed nature and its alternating busy-idle operating characteristics (Chen 2010). Usually, traffic simulation models are macroscopic, mesoscopic or microscopic. In response to the need for models that can capture both local traffic phenomena in detail, and effects on a larger surrounding network, hybrid models have recently appeared integrating macroscopic, mesoscopic and microscopic simulation approaches in different combinations (Burghout, Koutsopoulos, and Andreasson 2006).

The objective of this paper is to present a new DEVS-based simulation framework for multi-modal public transport analysis and planning based on the concept of geosimulation that integrates the capabilities of multi-agent modelling and geographical information systems. The application of the proposed public transport simulation framework is demonstrated by applying it to a public transport system in a territorial-administrative unit of Latvia called Vidzeme Planning Region.

2. GEOSIMULATION FRAMEWORK

The proposed geosimulation framework implements the concept of geosimulation simulation, allowing explicit modelling of each transport participant, such as vehicle or passenger, at a microscopic or mesoscopic level. The mesoscopic simulation considers particular vehicles in some form, but represents their interactions at relatively low detail (Burghout 2004). The microscopic simulation models every single vehicle as an object with its own position, direction, speed, and acceleration.

2.1. DEVS-Based Framework

The *Discrete Event System Specification* (DEVS) (Zeigler 1976, Zeigler, Praehofer, and Kim 2000) is a generic system-theoretical formalism that is provided for the description and definition of discrete-event systems dynamics allowing one to map systems specifications into most classes of simulation models (differential equations, cellular automata, etc.). For each class of model, one DEVS sub-formalism enables specification of one correspondent simulation model. As the specification of complex systems often needs to grasp different kinds of simulation models, connections between the models can be performed using DEVS multi-formalism concepts.

2.1.1. V-DEVS Specification

This paper proposes a new extension to the DEVS formalism called V-DEVS allowing the integration of the geosimulation concept (including CA, MAS and GAS) into a common DEVS-based framework for modelling and simulation of spatially linked dynamic systems at the mesoscopic and microscopic levels. This approach provides the following main advantages:

- Common formalism for model definition and representation of geographical automata systems;
- Unified basis for the integration of systems modelling and computer visualization;
- Seamless component-oriented coupling and synchronization of simulation processes, visualization and user interaction.

An atomic V-DEVS model is defined as the following cortège:

$$AM_{V-DEVS} = \langle X, Y, S, \{RM_r\} \rangle, \quad (1)$$

where

$RM_{r\in\{meso,micro\}} = \{RM_{meso}, RM_{micro}\}$ is a resolution object model set containing DEVS sub-models of mesoscopic and microscopic levels;

$X = X^{meso} \bigcup X^{micro}$ is an input event set;

$Y = Y^{meso} \bigcup Y^{micro}$ is an output event set;

$S = RM_{meso}(S) \times RM_{micro}(S)$ is a set of sequential states as a Descartes multiplication of resolution object model states.

Each resolution object model RM_r is based on the classic atomic DEVS model structure (Zeigler 1976):

$$RM_r = \langle X, Y, S, \delta_{ext}, \delta_{int}, \lambda, ta \rangle, \quad (2)$$

where

$X = \{(p, v) \mid p \in InPorts, v \in X_p\}$ is a set of input ports and values;

$Y = \{(p, v) \mid p \in OutPorts, v \in Y_p\}$ is a set of output ports and values;

S is a set of sequential states;

$\delta_{ext} : Q \times X \to S$ is the external state transition function;

$\delta_{\text{int}} : S \to S$ is the internal state transition function;

$\lambda : S \to Y$ is the output function;

$ta : S \to R^{+}_{0,\infty}$ is the time advance function;

$Q = \{(s, e) \mid s \in S, 0 \le e \le ta(s)\}$ is the set of total states;

e is the elapsed time since the last transition.

Equations 1 and 2 provide a formal basis for event-based simulation at the mesoscopic and microscopic levels.

In Figure 1, a general dynamics of V-DEVS atomic model activity is depicted.

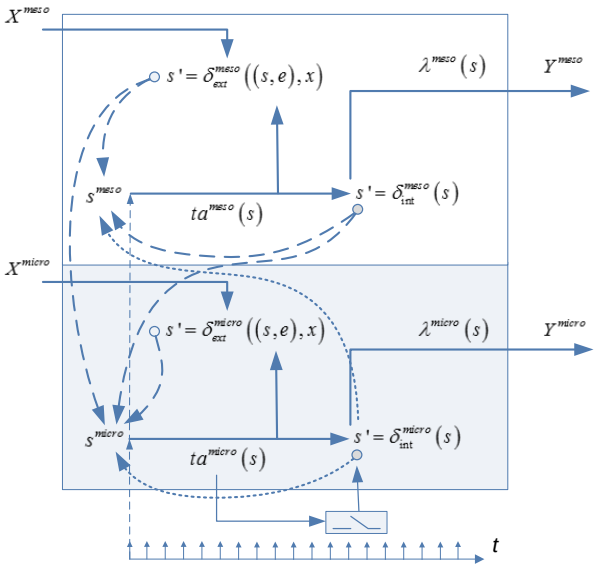

Figure 1: The Dynamics of V-DEVS Atomic Model

An important condition is time synchronization between the mesoscopic and microscopic V-DEVS parts and, therefore, the following inequality should be taken into account:

$$ta^{micro}(s^{micro}) \le ta^{meso}(s^{meso}), \quad (3)$$

if $ta^{meso}(s) \neq +\infty \wedge \delta_{ext}^{meso}(s, x^{meso}, e) \neq \varnothing$.

In the V-DEVS formalism, there isn't directly a confluent transition function defined, as is the case in the parallel DEVS formalism. If the model receives external

events together with its internal state transition at the time moment $ta(s)$, then in the V-DEVS formalism a default confluent transition function is used in the same way as in the classical DEVS formalism (Zeigler 1984):

$$\delta_{conf}(s,x) = \delta_{ext}(\delta_{\text{int}}(s),0,x). \quad (4)$$

2.1.2. V-DEVS-Based Formalization of Geosimulation

To interpret geosimulation paradigm with the means of V-DEVS formalism, it is necessary to translate the corresponding geographic automata objects, relationships between them, and the rules of automata behaviour into V-DEVS elements (Equations 1, 2).

Each geographic automata is spatially positioned object, embedded in a GIS layer having a vectorial representation. Each such object can be specified as the following V-DEVS model:

$$AM_A = \langle X_A, Y_A, S_A, \{RM_{r_A}\} \rangle, \quad (5)$$

where

$S_A = \langle (x,y), VD_A, phase \rangle$ is a set of sequential states;

$(x,y) \in \mathbb{R}^2$ is object position;

VD_A is object dynamic state sub-set including direction, speed, acceleration;

$phase = \{'active', 'passive', 'moving', ...\}$ is the current phase of object dynamic behaviour.

3. FRAMEWORK IMPLEMENTATION

For a simulation to be useful for transportation analysis and planning, it must not only support a wide variety of features, but it must also be applicable to large-scale, real-world applications.

Public transport models developed with the implemented software prototype can be interactively explored in a multi-scenario mode within different simulation time intervals. Currently, the simulator supports two configurable simulation time modes regarding transit routes and trips used by transit operators during summer school holidays or school time.

The following list gives an overview of the main features of the developed transit simulation system prototype:

- Multi-modal simulation of regional and intercity bus and train traffic;
- GIS based infrastructure for spatial data processing;
- Graphical user interface for simulation data preparation, visualization and analysis;
- Interactive real-time simulation and visualization with possibilities of speeding-up the simulation runs by different time scales.

The simulation data preparation, network data visualization, simulation execution, vehicle movement animation and results analysis is managed through the graphical user interface (GUI) (Figure 2).

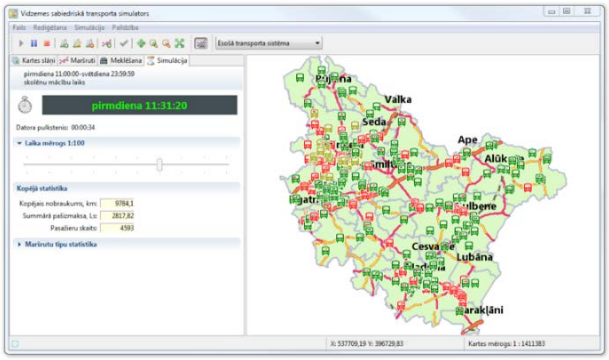

Figure 2: User Interface of Public Transport Simulator

3.1. System Architecture

In Figure 3, a general architecture of the developed public transport simulation system prototype is shown. The geosimulation system uses open source software components based on Java programming tools providing a unified development environment for different operating systems.

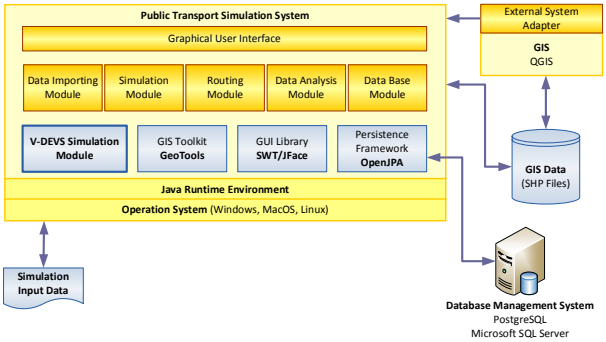

Figure 3: General Architecture of Public Transport Simulation System

For geospatial data processing, visualization and analysis the GIS toolkit called GeoTools (OGC 2014) is used. GeoTools is an open source Java GIS toolkit implementing many Open Geospatial Consortium (OGC) specifications including features for vector and raster data access available in different file formats and coordinate reference systems.

The system includes several integrated interactive analysis features:

- Assessment of route network traffic intensity;
- Assessment of public transport stops availability;
- Assessment of settlements accessibility.

3.2. Simulation Data

Each simulation run needs some initial data, which in the case of transportation simulation usually means a transportation network and the so-called “initial demand”. The initial demand describes the initial day plans of all simulated transportation system participants.

The model database contains both spatial and non-spatial data of different bus and railway routes. The route data are stored and processed in a combination with transit schedules, fares and vehicle types.

The transportation network is represented by nodes and links. The data that describe the simulated network is read from the spatial network database, which includes spatial definitions and related attributes of all the network objects. Nodes are either intersections of several roadways or points of road type change or public transport stops. Each node is represented by its type (intersection, public transport stop, etc.), and a unique identification number. Links are directional roadways that connect nodes. Each link is characterized by its type (freeway, urban street, railroad, etc.), an identification number, and starting and end nodes.

The non-spatial relational database contains 19 tables that store all the necessary information about public transit routes, trip schedules, transit agencies, vehicles, stop facilities, fares, planned passenger counts and transit time modes. For an universal object-relational access to different possible database management systems, the OpenJPA (The Apache Software Foundation 2014) data persistence framework is used.

3.3. Simulation Flow

The simulation flow starts with building of road network (Figure 4). The simulation environment contains a dedicated module that on the basis of the available GIS data automatically generates the network data in a file format necessary for the V-DEVS simulation engine.

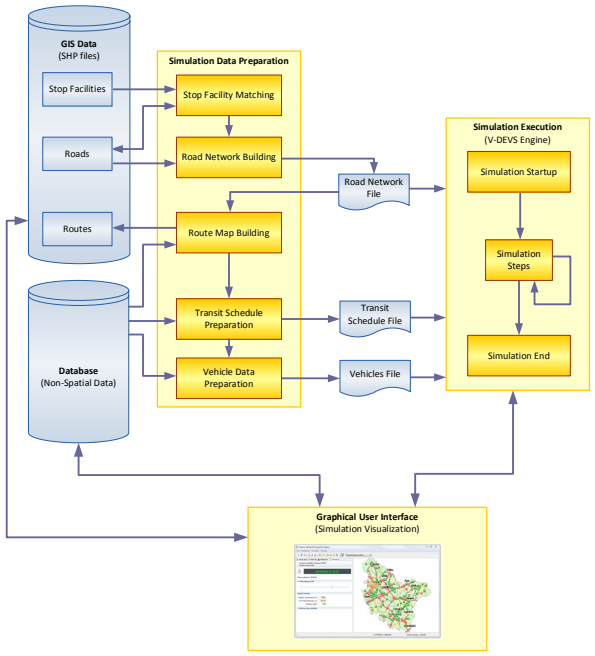

Figure 4: Data Preparation and Simulation Execution Steps

For public transit simulation purposes, the V-DEVS simulation engine requires three specific input files – road network file, transit schedule file and vehicles file. These files are automatically generated by the simulation system in the case when the spatial or non-spatial data that is stored in the database or in shape files is changed. This is the simulation data preparation process.

As previously stated, the road network is a graph consisting of links representing road segments and nodes representing road crossing or road type change point. Only a limited number of vehicles can leave a link per time step corresponding the flow capacity of a link. Nodes do not have a lot of internal logic – in each time step, the foremost vehicles of each incoming link are moved over the node to the next link in their route.

Also the public transport stop facilities are represented by nodes in the road network. Therefore a special module for the conversion of stop facility location data into network nodes is implemented.

3.4. V-DEVS Simulator

Within the proposed framework, a priority queue based V-DEVS simulator algorithm is implemented. The algorithm implements the processing of simulation cycles consisting of event simulation procedures at the mesoscopic and microscopic levels.

The implementation of the priority queue V-DEVS algorithm is based on the principles proposed by (Muzy and Nutaro 2005) and is built in such a way that the simulation efficiency in comparison to the hierarchical simulator algorithm can be improved with respect to the following aspects:

- Abandonment of unnecessary use of simulator and coordinator objects;
- Speed up of event scheduling by processing only active models;
- Abandonment of unnecessary use of internal synchronization messages;
- Abandonment of unnecessary use of event routing messages.

A Root Coordinator is used which executes the main simulation loop until the final simulation time is reached (Figure 5). The priority queue simulator algorithm uses only two simulators for all coupled and atomic simulation models (Figure 6). The processing of mesoscopic events implements the mesoscopic simulator, but the processing of microscopic level events implements the microscopic simulator. Both simulators use priority queue to store future events and are identical in structure. Such an implementation allows one to reduce substantially the overhead of message processing for simulation execution because instead of many coordinator and simulator objects, only two simulator objects are used for all atomic and coupled V-DEVS models.

4. PUBLIC TRANSPORT MODELLING APPROACH

The public transport model is hierarchically composed as a coupled V-DEVS model consisting of statically linked traffic dispatcher, vehicle, traffic monitor and traffic visualizer sub-models (Figure 7). The V-DEVS

simulator models vehicles individually but does not represent lanes explicitly. The microscopic simulation level is used for modelling coordinate-based continuous movement of public transport vehicles.

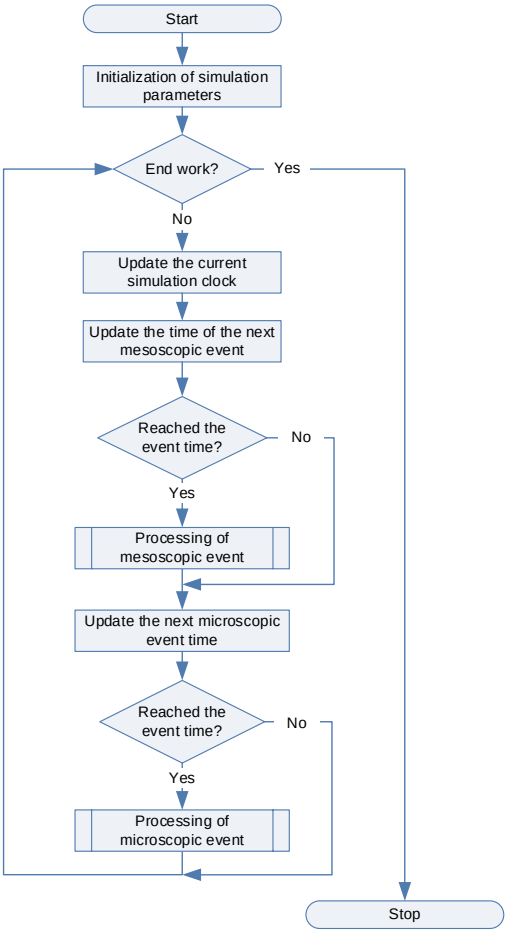

Figure 5: Base Algorithm of V-DEVS Simulator

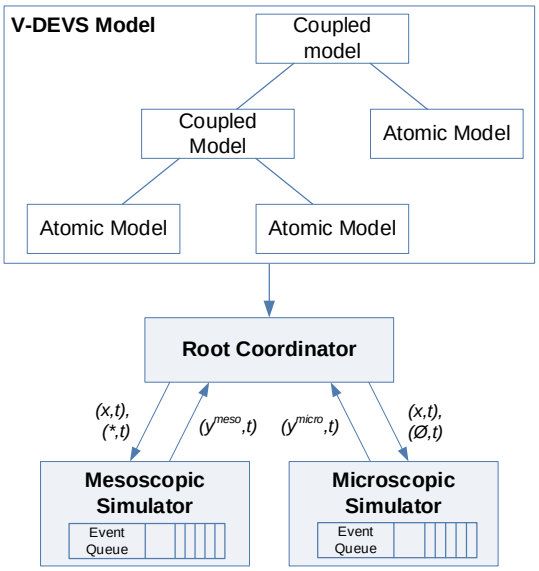

Figure 6: An Overall Architecture of Priority Queue V-DEVS Simulator

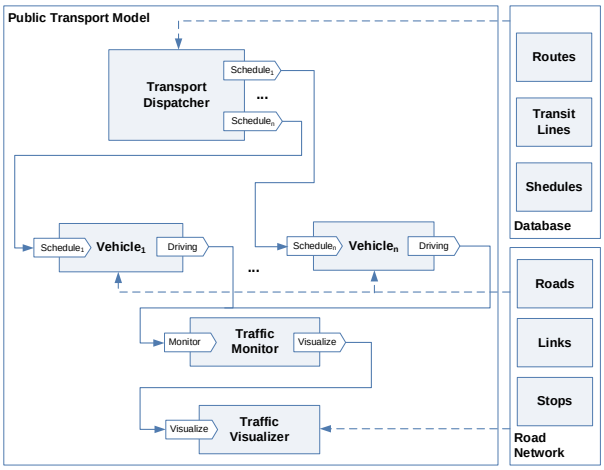

Figure 7: Public Transport Model

4.1. Transport Dispatcher Model

Transport Dispatcher is an atomic model that implements the mesoscopic part of V-DEVS formalism. Transport Dispatcher generates the initial transport demand describing the initial day plans of all simulated transportation system vehicles.

The Transport Dispatcher manages a list of scheduled trips, which allows explicit modelling of trip chaining. The vehicle arrival times are obtained according to the corresponding transit schedules, defined and stored in the trip schedule database table.

4.2. Vehicle Model

Vehicle is defined as an atomic V-DEVS model (Equation 5) that implements both mesoscopic and microscopic levels.

Public transport vehicles follow fixed routes according to a pre-defined timetable provided by the Transport Dispatcher Model.

At the start of the simulation, a list of the transit lines, transit schedules and public transport vehicles that are modelled is read and corresponding vehicle models are created and initialized. To each trip schedule is assigned a corresponding vehicle.

4.2.1. Vehicle Movement Modes

Public transport vehicles follow a fixed route through the network. In order to make the model more realistic, the vehicle moving state between bus stops is divided into three phases: accelerating, constant-speed traveling and decelerating (Figure 8). Three sequential mesoscopic events will be scheduled to model the traveling process, which includes ending acceleration, starting deceleration and stopping at a bus stop.

A vehicle that enters a link on its route checks whether there are stops to be serviced on this link. If there are no stops on the link, the link exit time is calculated at the mesoscopic level, and an event to enter the link is added to the mesoscopic event list. Link travel times are calculated on the basis of planned traveling time between nearest stops and link throughput (road surface type, speed constraints).

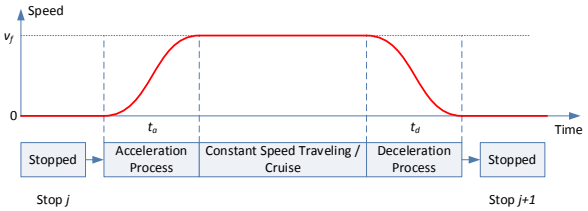

Figure 8: Vehicle Moving between Stops

Acceleration time t_a (in seconds) from a public transport stop implemented in the model is based on the one adopted in the (Akçelik and Besley 2001):

$$t_a = \frac{v_f}{a_{aa}}, \quad a_{aa} > 0 \tag{6}$$

where

v_f final speed in acceleration (km/h);

a_{aa} is average acceleration rate (m/s^2) calculated as follows:

$$a_{aa} = f_{aHV}\left[p_1 + p_2 PWR\sqrt{v_f} + \sqrt{PWR}\cdot p_3 - \right. \tag{7}$$
$$\left. -\left(p_4\sqrt{v_f} + p_5 Gr\right)/PWR\right]/3.6,$$

where

f_{aHV} is adjustment factor for heavy vehicle (bus) acceleration rates;

Gr is approach grade (%);

$p_1 \dots p_5$ is acceleration model calibration parameters;

PWR is power to weight ratio calculated from:

$$PWR = 1000 \cdot \frac{P_{\max}}{M_{HV}}, \tag{8}$$

where

$P_{\max}$ is maximum rated engine power;

M_{HV} is vehicle mass (kg).

Deceleration time t_d (in seconds) implemented in the model is based on the one adopted in the (Akçelik and Besley 2001):

$$t_d = -\frac{v_i}{a_{ad}}, \quad a_{ad} < 0, \tag{9}$$

where

v_i is initial speed in deceleration (km/h);

a_{ad} is average deceleration rate (m/s^2) calculated as follows:

$$a_{ad} = f_{dHV}\left[p_1 + p_2 PWR\sqrt{v_i} + \sqrt{PWR}\cdot p_3 - \right. \tag{10}$$
$$\left. -p_4\sqrt{M_{HV}} + p_5 v_i + p_6 Gr\right]/3.6,$$

where

f_{dHV} is adjustment factor for heavy vehicle (bus) deceleration rates;

$p_1 \dots p_6$ are deceleration model calibration parameters.

Public transport vehicles stop at fixed points along the route to pick up and set down passengers. The stop time for a particular vehicle is sampled from a normal distribution using the mean stop time and deviation.

4.2.2. Passenger Flow Modelling

During the simulation, the vehicle model maintains updated passenger loads and determines crowding level, as well as the maximum number of passengers that can board at each stop.

Passenger flow is represented by the arrival rates at stops of passengers for each transit line and the demand to get off the bus at each stop. The public transport at a regional level is a relatively low-frequency service, therefore the passenger arrivals are assumed to follow a lognormal distribution (Cats et al. 2010):

$$B_{ijk} \sim Lognormal\left(\mu_{ijt_k}, \sigma_{ijk}\right), \tag{11}$$

where

B_{ijk} is the number of passengers wishing to board line i at stop j on trip k;

μ_{ij} is expected arrival time for line i at stop j;

σ_{ijk} is headway deviation on line i at stop j between proceeding bus.

The passenger alighting process is assumed to follow a binomial distribution (Morgan 2002; Cats et al. 2010):

$$A_{ijk} \sim Binomial\left(L_{ijk}, P_{ijk}\right), \tag{12}$$

where

A_{ijk} is number of alighting passengers from line i at stop j on trip k;

L_{ijk} is vehicle load on arrival at stop j on trip k of line i;

P_{ij} is the probability that a passenger on line i will get off the bus at stop j.

4.3. Traffic Monitor and Traffic Visualizer Models

Traffic Monitor model implements the mesoscopic and microscopic parts of the V-DEVS formalism. Traffic Monitor receives input events from moving vehicles and calculates the total statistics of the public transport system including total fuel costs, total passenger count, etc.

Traffic Visualizer is an atomic V-DEVS model linked with graphical user interface that receives and aggregates input events from moving vehicles and manages and synchronizes the interactive animation process of public transport simulation.

5. CASE STUDY

This section describes how the transport simulation was applied in the Vidzeme region in Latvia, detailing the steps for data preparation as well as for configuring and running the simulation. It then analyses the computational capabilities of the large-scale application, as well as estimates the optimization possibilities and enhancement directions of the regional public transport network.

The road network of the Vidzeme Planning Region that is dynamically generated from the available GIS data contains 137521 arcs and 62183 nodes.

The public transportation system of the Vidzeme Planning Region is characterised by the following statistical data:

- 2993 bus stops;
- 2173 bus stop facilities assigned to existing public transit routes;
- 33 railway stations and stops;
- 78 regional intercity routes;
- 222 regional local routes;
- 36 city routes;
- 316 regional intercity trips per working day;
- 1230 regional local trips per working day;
- 162 city trips per working day;
- >74 school bus trips per working day.

The presented study is primarily focused on the evaluation of public transport routes at the network level basing on the transportation social aspect.

5.1. Simulation Scenarios

One of the most important public transportation network efficiency indicators is the trip count per route during a working day or the route traffic intensity. The developed software system contains a module for assessing the route traffic intensity.

Another important indicator for assessment of the public transport quality is the public transport availability. Availability means that the public transport service is within a reasonable distance from where they are and where they want to be.

The performed analysis using the functionality of public transport availability calculation implemented in the simulation system, shows that 59 % of the Vidzeme region inhabitants in average are living within a radius of 2 kilometres from public transit stop facilities. This result is smaller than the public transport stops availability in other planning regions of Latvia. In Figure 9, the map of public transport availability buffer zones located at centres of stop facilities is shown.

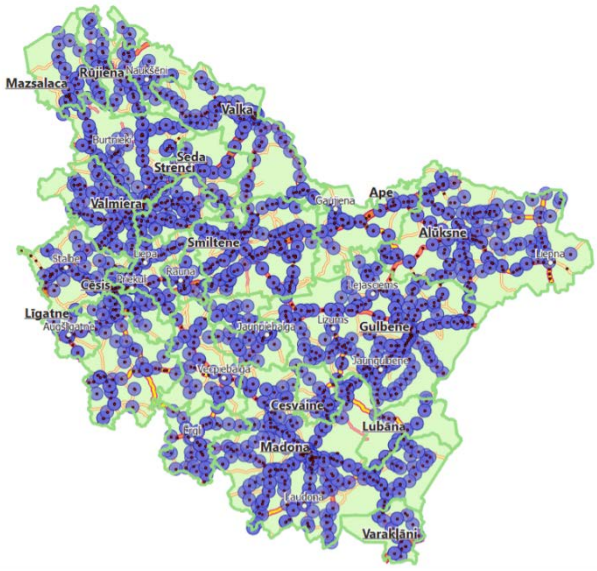

Figure 9: Map of Public Transport Availability in Vidzeme Planning Region

Accessibility is a key element to transport geography (Curtis and Jan 2008), since it is a direct expression of mobility either in terms of people, freight or information. Accessibility is defined as the measure of the capacity of a location to be reached by, or to reach different locations (Rodrigue, Comtois, and Slack 2009). Therefore, the capacity and the structure of transport infrastructure are key elements in the determination of accessibility.

The described simulation system calculates public transport accessibility in the terms of time necessary to reach a chosen destination. By combining the calculated stop facility availability data with public transport traffic intensity it is possible to estimate settlements accessibility time.

In Figure 10, the estimated average passenger count per working day in regional transit lines with largest transport intensity is shown.

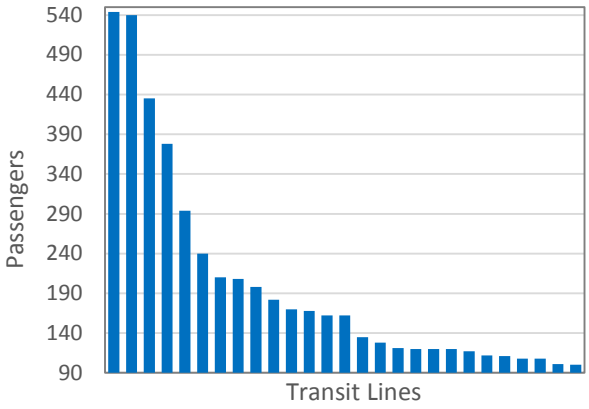

Figure 10: Estimated Average Passenger Count per Working Day in Regional Transit Lines with Largest Transport Intensity

5.2. Simulation-Based Optimization Possibilities

In the performed case study analysis, four optimization alternatives are defined. The initial alternative is to use the existing public transport infrastructure without any changes. The second alternative is related to the improvement of the roads quality and the public transit network density. The third alternative is to increase the count and diversity of public transport vehicles.

During the development of public transit geosimulation system there are performed optimization experiments and scenarios on the basis of the fourth alternative that is related to the improvement of the multimodal public transport infrastructure. This includes the coordination of the railway and bus traffic, planning of the public transport stops layout, modification of the existing routes and optimization of the vehicle trips count. The main goal of the proposed optimization scenarios is to fulfil the social aspect of public transport.

The first proposed optimization scenario is related to the adaptation of the public transport capacity to the number of passengers. The performed data analysis and simulation experiments have shown that in Vidzeme region there exist 166 regional trips of local importance exist where the expected number of passenger per a trip is less than 25. Therefore in these trips it is possible to use buses with smaller capacity and at the same time with smaller fuel consumption (Table 1).

Table 1: Estimated Fuel Consumption Costs For 7 Working Days

Scenario	Costs (EUR)	Cost Savings (%)
Initial alternative: Buses with consumption of 30 l/100 km usage	114,091	-
Buses with consumption of 25 l/100 km usage	107,005	6.2%
Buses with consumption of 20 l/100 km usage	99,908	12.4%

The second optimization scenario is to increase the trip count in routes where the existing trip count per working day is smaller than 2. In the model there are added 18 new trips on 293 bus route kilometres, thus improving the quality of public transport support in these road segments (Figure 11).

The third possible optimization scenario is to improve the accessibility of the region cities by decreasing the stops count within the existing trips. By decreasing route stop count per a trip and at the same time by increasing the distance between stops from 4 to 6 kilometres on average it is possible to improve the accessibility up to 10 %. This alternative can be practically implemented in a real life by using partly express buses.

6. CONCLUSIONS

In this paper, a new DEVS-based simulation framework for multi-modal public transport analysis and planning is presented. The implemented framework is approbated in the Vidzeme Planning Region of Latvia providing a novel solution in the context of regional transportation planning in Latvia. The developed solution is considered as a useful tool in assisting decision-makers in development planning allowing the evaluation of alternative public transit scenarios and planning options.

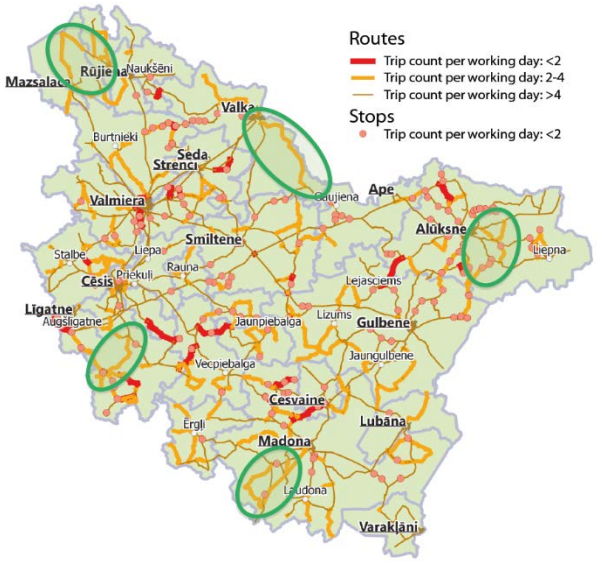

Figure 11: Map of Public Transport Availability and Optimization Possibilities in the Vidzeme Planning Region

The future of the proposed simulation system will include an increasing level of dynamics and accuracy of the modelled transportation infrastructure. The application of modern Web technologies will expand the availability of the public transport simulation to a wide area of users with different knowledge, skills and experience.

ACKNOWLEDGMENTS

Support for this work was provided by the Riga Technical University through the Scientific Research Project Competition for Young Researchers No. ZP-2014/18.

REFERENCES

Akçelik, R., and Besley, M., 2001. Acceleration and Deceleration Models. In *23rd Conference of Australian Institutes of Transport Research (CAITR 2001)*, 1–9. 2001, Melbourne, Australia: Monash University.

Behrisch, M., Bieker, L., Erdmann, J. and Krajzewicz, D., 2011. SUMO - Simulation of Urban MObility: An Overview. In *SIMUL 2011, The Third International Conference on Advances in System Simulation*, 63–68. 2011, Barcelona, Spain.

Benenson, I., and Torrens, P.M., 2004. *Geosimulation: Automata-Based Modeling of Urban Phenomena*. West Sussex: John Wiley & Sons.

Burghout, W., Koutsopoulos, H.N.,and Andreasson, I., 2006. A Discrete-Event Mesoscopic Traffic Simulation Model for Hybrid Traffic Simulation. In *Intelligent Transportation Systems Conference,*

2006. ITSC '06. IEEE, 1102–1107. 17-20 September 2006, Toronto.

Burghout, W., 2004. *Hybrid Microscopic-Mesoscopic Traffic Simulation*. Doctoral Dissertation, Swedish National Road and Transport Research Institute (VTI).

Cats, O., Burghout, W., Toledo, T., and Koutsopoulos, H.N., 2010. Mesoscopic Modeling of Bus Public Transportation. In *89th Transportation Research Board Annual Meeting*. January 10-14, 2010, Washington DC.

Chen, B., 2010. A Review of the Applications of Agent Technology in Traffic and Transportation Systems. *IEEE Transactions on Intelligent Transportation Systems* 11: 485–97.

Cortés, C.E., Burgos, V. and Fernández, R, 2010. Modelling Passengers, Buses and Stops in Traffic Microsimulation: Review and Extensions. *Journal of Advanced Transportation* 44 (2): 72–88.

Curtis, C., and Scheurer, J., 2008. Planning for Sustainable Accessibility: The Implementation Challenge. *Transport Policy* 15 (2): 104–12.

Ferber, J, and Müller, J.P., 1996. Influences and Réaction: A Model of Situated Multiagent Systems. In *Proceedings of 2nd International Conference on Multi-Agent Systems*, 72–79. Kyoto, Japan.

Laporte, G., Mesa, J.A., Ortega, F.A., and Perea, F., 2011. Planning Rapid Transit Networks. *Socio-Economic Planning Sciences* 45 (3): 95–104.

MATSim, 2014. *MATSim: Multi-Agent Transport Simulation Toolkit*. Available from: www.matsim.org [Accessed May 14, 2014]

Morgan, D.J., 2002. *A Microscopic Simulation Laboratory for Advanced Public Transportation System Evaluation*. Master Thesis. Massachusetts Institute of Technology.

Muzy, A., and Nutaro, J., 2005. Algorithms for Efficient Implementations of the DEVS&DSDEVS Abstract Simulators. In *Proceedings of the 1st Open International Conference on Modeling & Simulation*, 401–407. June 2005, France, ISIMA/Blaise Pascal University.

OGC, 2014. *GeoTools The Open Source Java GIS Toolkit*. Available from: http://geotools.org [Accessed July 10, 2014]

Rodrigue, J.P., Comtois, C., and Slack, B., 2009. *The Geography of Transport Systems*. 2nd ed. Abingdon, Oxon, New York: Routledge.

The Apache Software Foundation, 2014. *Apache OpenJPA Project*. Available from: http://openjpa.apache.org [Accessed July 10, 2014]

Toledo, T., Cats, O., Burghout, W., and Koutsopoulos, H.N., 2010. Mesoscopic Simulation for Transit Operations. *Transportation Research Part C: Emerging Technologies* 18 (6): 896–908.

Zeigler, B.P, 1976. *Theory of Modelling and Simulation*. New York: John Wiley & Sons.

Zeigler, B.P., 1984. *Multifacetted Modelling and Discrete Event Simulation*. San Diego, CA, USA: Academic Press Professional, Inc.

Zeigler, B.P., Praehofer, H., and Kim, T.G., 2000. *Theory of Modeling and Simulation: Integrating Discrete Event and Continuous Complex Dynamic Systems*. 2nd ed. Academic Press.

AUTHORS BIOGRAPHY

Arnis Lektauers, Dr.sc.ing., is an Associate Professor at the Department of Modelling and Simulation of Riga Technical University (RTU). His main professional interests include the research and development of interactive hybrid modelling and simulation algorithms with an application to complex systems analysis. A. Lektauers is a member of Latvian Simulation Society, member of Latvia Section of the Institute of Electrical and Electronics Engineers (IEEE), member of the Council of RTU Faculty of Computer Science and Information Technology, member of System Dynamics Society. He is the author of 1 textbook and more than 30 papers in scientific journals and conference proceedings in the field of information technology.

Yuri A. Merkuryev is Corresponding Member of the Latvian Academy of Sciences, Habilitated Doctor of Engineering, Professor and Head of the Department of Modeling and Simulation of Riga Technical University. His professional interests include methodology of discrete-event simulation, supply chain simulation and management, as well as education in the areas of simulation and logistics management. He is the President of the Latvian Simulation Society, board member of the Federation of European Simulation Societies (EUROSIM), senior member of the Society for Modeling and Simulation International (SCS), IEEE Senior Member and Chartered Fellow of British Computer Society. He is the author of more than 300 publications.

A DECISION MODEL TO INCREASE SECURITY IN A UTILITY NETWORK

Jochen Janssens[(a)], Luca Talarico[(b)], and Kenneth Sörensen[(c)]

[(a)(b)(c)]University of Antwerp, Faculty of Applied Economics, ANT/OR – University of Antwerp Operations Research group, Prinsstraat 13, 2000 Antwerp, Belgium

[(a)]jochen.janssens@uantwerpen.be, [(b)]luca.talarico@uantwerpen.be, [(c)]kenneth.sorensen@uantwerpen.be

ABSTRACT

In this paper we propose a decision model aimed at increasing security in a utility network (e.g., smart grid, water network). This model assumes that all edges (e.g., pipes, cables) have a certain, not necessary equal, probability of failure, which can de reduced by taking appropriate arc-specific security measures. These are combined in security strategies that should be applied to minimize the risk of disconnecting an origin node from a destination node. We develop a simple but effective metaheuristic approach to solve this problem. Detailed experiments on realistic instances are conducted and the relationships between solutions and problem parameters are tested by simulating different scenarios.

Keywords: network security, metaheuristics, knapsack problem.

1. INTRODUCTION

In modern day society, utility networks such as electricity, water, gas, and communication networks are taken for granted. People expect that they function at all times, and are capable of handling all demand placed on them. However, there is a real risk of failures in all types of networks. Those failures might make the network unavailable with a resulting interruption of the service/connection between two network points which are represented by a origin node (i.e., the point from which the service or the product is send to the customer through the network) and a destination node (i.e., the customer or the point to which the product, service is delivered through the network).

Network breakdowns can have *safety*-related causes such as natural phenomena (e.g., earthquakes, storms), human errors, or mechanical defects such as in pumps and valves, caused by the regular wear and tear. In addition, network breakdowns can be due to *security*-related causes such as intentional terrorist attacks and/or malicious sabotages.

After 9/11, the protection of utility networks against intentional attacks has received great attention among network providers. In fact terrorist attacks on utility network are not rare and might cause huge losses in a nation's economy. For these reasons in the remainder of the paper our focus is on network security rather than safety.

Network providers and managers can reduce the risk of a network breakdown after a terrorist attack addressed at one or several network arcs by applying preventive security measures in order to reduce network vulnerabilities.

The security budget that can be spent on these security measures, however, is generally limited. The current economic situation has increased the pressure on limiting even further many budgets and investments in security. In this work, a combination of security measures for one arc is called a security strategy for that arc.

The problem defined in this paper is to reduce the risk of a utility network being (partially) out of service, which is measured as the risk to break the connection between an origin and a destination node, by reducing the risk or the effects of an intentional attack on the network by selecting security strategies from a list of available ones.

Since the budget is limited and the security strategies can only be applied locally, i.e., on a specific link in the network, the security strategies should be chosen in such a way that the reduction of the risk of the network service being down is as large as possible while keeping the total cost of the security strategies within the budget.

Once we consider realistic cases, in which hundreds of links (in our case from 100 up to 500) might compose the network and dozens different security strategies (in this paper from 5 up to 20) might be available for each network arc, the problem can turn out to be so large that it will become computationally infeasible to solve it in a reasonable amount of time with exact algorithms. Therefore we will explore the use of metaheuristics to support this decision problem.

The paper is organized as follows. In Section 2 we give a brief overview of the state of the art. Section 3 clarifies the problem of selecting the best strategies to increase the security of the whole network is described and modelled as an optimisation problem. In Section 4, we present a metaheuristic to solve the network security problem. Section 5 presents some preliminary results about the computational experiments of the metaheuristic presented in this paper. Section 6 concludes the paper and presents some idea of further developments. During the conference more details about the scenarios that have been designed to investigate the relationships between the problem/heuristic parameters and the solutions quality will be presented.

2. LITERATURE REVIEW

Following the 9/11 attacks, network security has received growing attention within the scientific community. Although significant research has been done to improve best practices in the field of security, few papers have addressed the relationship between risk-related variables and an objective related to cost-effective network security decisions. Nevertheless, security measure selection problems have received some attention in more recent literature.

The problem of selecting the right security measures given a limited budget is clearly not an easy task. Most security planning models in the literature are qualitative, and only few of them rely on quantitative approaches. In case of a pipeline network, the security risk assessment procedure elaborated by Reniers and Dullaert (2012) may be used. After a careful pipeline security risk assessment, the user is in possession of pipeline segment risk data as well as pipeline route risk data. Assuming that the security risk analyst determines a set of available security measures and defence strategies for application to the different pipeline segments and/or for the pipeline routes, a selection of the most effective security measures with respect to the available budget (either for a single pipeline segment or for a pipeline route) can be calculated. If the cost of the security measures is known in advance a mathematical approach can be used to solve the problem of optimal allocation of security resources by solving a knapsack problem. Reniers et al. (2012) explain how this well-known technique in the field of Operations Research is easy to use in case of security optimisation problems. A practical application to secure an illustrative pipeline infrastructure used to transport oil is described in Talarico et al. (in press 2014).

In Bistarelli et al. (2007) a method for the identification of the assets, the threats and the vulnerabilities of ICT systems is introduced. Furthermore, a qualitative approach for the selection of security measures to protect an IT infrastructure from external attacks is discussed. In particular, two security models based on defence trees (an extension of attack trees) and preferences over security measures are proposed.

In Viduto et al. (2012) the security of a telecommunication network is analysed from a quantitative point of view. Knowledge of potential risks enables organisations to take decisions on which security measures should be implemented before any potential threat can successfully exploit system vulnerabilities. A security measure selection problem is presented in which both cost and effectiveness of an implemented set of security measures are addressed. A Multi-Objective Tabu Search (MOTS) algorithm is developed to construct a set of non-dominated solutions, which can satisfy organisational security needs in a cost-effective manner.

In Sawik (2013) a similar security measure selection problem for an IT infrastructure is formulated as a single- or bi-objective mixed integer programming problem. Given a set of potential threats and a set of available security measures, the decision maker needs to determine which security measure to implement, under a limited budget, to minimize potential losses from successful cyber-attacks and mitigate the impact of disruptions caused by IT security incidents.

The prevention of heavy losses due to cyber-attacks and other information system failures in an IT network is usually associated with continuous investment in different security measures. In Bojanc and Jerman-Blažič (2008) several approaches enabling the assessment of the necessary investments in security technology are addressed from an economical point of view. The paper introduces methods for the identification of risks in ICT systems and proposes a procedure that enables the selection of the optimal level of investments in security measures.

Once security risks have been identified, the potential loss associated with their occurrence, as well as their probability of occurrence must be determined. Determining both probability of occurrence and potential impact of each risk is done in a process called *risk assessment*. Performing a risk assessment phase allows to take decisions regarding the necessary investment in security controls and systems. In our paper we assume that a preliminary risk assessment phase has been conducted by experts, in order to determine the probability of attacks associated with each network arc together with the costs and benefits of each available security measure.

Our approach extends the works of Reniers and Dullaert (2012) and Reniers et al. (2012) by defining a single-objective problem and proposing a quantitative method to select appropriate security measures. A different objective function is used, which relies on the minimization of the risk of the network to be not accessible between a couple of network nodes instead of the maximization of the effectiveness of the security measures used. Moreover, in our work, since a list of security measures is defined for each arc of the network, the model incorporates not only decisions taken at the level of the network, as done in Reniers and Dullaert (2012), Reniers et al. (2012) and Sawik (2013), but it depends on the choices made at the level of single network arcs.

3. PROBLEM DESCRIPTION

The utility network can be represented by using a graph $\mathscr{G} = \{\mathscr{N}, \mathscr{A}\}$, where $\mathscr{N}$ represents a set of nodes and $\mathscr{A}$ a set of arcs, connecting the nodes. All arcs $a_i \in \mathscr{A}$ have a probability of being attacked and failing, denoted as p_i. A set of security strategies $\mathscr{S}_i$, is defined for each arc $a_i \in \mathscr{A}$ and it comprises all security strategies s_{ij} that are available for this arc.

For each security strategy s_{ij} of arc a_i there are a cost c_{ij} and a value p_{ij}, which represents the probability of failure of this arc when s_{ij} is applied. Only one security strategy per arc can be applied. A security strategy can be a combination of single security measures (see e.g., Table 1). A combination of security measures can have a different effectiveness than the sum of the impact of

Table 1: Set of security strategies $\mathscr{S}_i$ for arc a_i

Strategy	Security measures	Cost	Probability
0	-	0	0.6
1	A	100	0.5
2	B	150	0.45
3	C	200	0.4
4	A&B	250	0.32
5	B&C	300	0.25

the individual security measures due to some interaction effects. In some cases, combinations of single security measures might not be available due to their incompatibility.

The default security strategy s_{i0}, that has a cost $c_{i0} = 0$, is a default state that indicates that no security measures are applied. Its related probability p_{i0} represents the risk of arc a_i failure in case no security measure is selected. It represents the probability of failure of that arc given that an attacker is rational. The probabilities are unique for each arc, and are based on several information such as geographical location, length, criticality of that arc in the network. We assume that these probabilities are predefined in the risk assessment done by a security professional.

The model proposed in this paper makes the assumption that only arcs can be attacked and that nodes are well protected and no viable target for an attack. In future research the model will be extended to a more general case where nodes are targets as well.

Given an origin node o and a destination node d in the network, the quality of a solution (i.e., a selection of a security strategy for each arc) is defined as the probability that no path exists between node o and node d. This would make it impossible for a service or good from node o to reach node d (e.g., it would be impossible to make a phone call from node o to node d, if all connections to node d were unavailable).

In a communication network it is necessary that the whole network remains connected after an attack in order to guarantee a proper transfer of data between an origin node and a destination node. While extending the analysis to water/gas/electricity networks it is possible that after an attack a sub-network could still operate, but the transfer of a service/product between a supplier (our origin node) and a final user (our destination node) is not possible due to the lack of connections after an attack. In fact some arcs that are not available due to an attack might disconnect the end user from the global utility network.

In this paper, since the decision problem is introduced for the first time, the problem is simplified by making the assumption that only one supplier and one customer exist in the network. However, several intermediate network nodes through which the service/goods pass along the network to reach the customer are considered. In future work, this model will be extended as to evaluate several utility suppliers and several customer in the network, minimizing the risk that any customer is separated from any of the suppliers. In addition supplier capacity, customer demand and importance of either of them might be considered.

Given the fact that we have a single source node and a single destination node, in order to calculate the risk of the network being out of service, we make use of probability theory. Probability theory is used extensively in reliability theory and in reliability studies of systems. For an overview, we refer to Bazovsky (2004); Ministery of Defence (UK) (2011); Romeu (2004).

In order to mathematically state the decision problem associated to the selection of the best set of security strategies to increase the overall network security, we first have to define the risk for the network $\mathscr{G}$ being not available between source node o and destination d. For this reason we define a set $\mathscr{C}$. This set contains the combinations of arcs that will disconnect all paths in the network between nodes o and d. In other words each element l of set $\mathscr{C}$ represents a combination of arcs, contained in set $\mathscr{A}_l^E$, for which failure happens, and arcs contained in set $\mathscr{A}_l^N$, which do not fail. It should be noted that $\mathscr{A}_l^E \cup \mathscr{A}_l^N = \mathscr{A}$, $\forall l \in \mathscr{C}$. In addition, an element l in set $\mathscr{C}$ contains a critical combination of arc failures (from now on called scenarios) since if the arcs in $\mathscr{A}_l^E$ are out of service, a network breakdown between o and d is generated. The cardinality of set $\mathscr{C}$ depends on the topology of the network $\mathscr{G}$ and the position of nodes o and d within the network. Let B represents the available security budget and x_{ij} a binary variable, that takes values 1 when the security strategy j on arc i is applied, and 0 otherwise.

$$\min \quad \sum_{l \in \mathscr{C}} R_l \tag{1}$$

s.t.

$$\sum_{i \in \mathscr{A}} \sum_{j \in \mathscr{S}_i} c_{ij} \cdot x_{ij} \leq B \tag{2}$$

$$p_i = \sum_{j \in \mathscr{S}_i} p_{ij} \cdot x_{ij} \qquad \forall i \in \mathscr{A} \tag{3}$$

$$R_l = \prod_{i \in \mathscr{A}_l^E} p_i \cdot \prod_{k \in \mathscr{A}_l^N} (1 - p_k) \qquad \forall l \in \mathscr{C} \tag{4}$$

$$\sum_{j \in \mathscr{S}_i} x_{ij} = 1 \qquad \forall i \in \mathscr{A} \tag{5}$$

$$x_{ij} \in \{0,1\} \qquad \forall i \in \mathscr{A}, \forall j \in \mathscr{S}_i \tag{6}$$

The objective function (1) minimizes the total risk for the network being out of service between nodes o and d. The total network risk is given by the sum of risks associated to single scenarios happening. Constraint 2 ensures that the total cost associated to the selected security strategies does not exceed the predefined security budget B. Equation 3 is used to define the probability p_i associated to a failure of arc a_i. Equation 4 gives us the risk for a scenario happening, which disconnects the paths in the network between nodes o and d. Equation 5 forces the decision process to select at maximum one security

strategy to protect arc a_i. It should be noted that $x_{i0} = 1$ means that for arc a_i no security measures have been applied. Finally, constraint 6 represents the domain of the decision variable, which ensures that no partial security strategies are allowed.

4. SOLUTION APPROACH

The decision problem of selecting appropriate security strategies given a budget constraint, in order to reduce the risk for the utility network being down, belongs to the more general category of knapsack problems.

The single objective knapsack problem is one of the best known combinatorial optimisation problems. This problem can be described as follows: given a set of n items, each with a certain weight w_i and a certain profit p_i with $i \in [1,n]$, the objective is to select the subset of items of which the total profit is maximal, and the total weight does not exceed the knapsack capacity C.

Applications of the knapsack problem are frequently encountered in several real-world decision-making processes in different fields such as portfolio management, menu planning, design of experiments. For a detailed review of the knapsack problem, the reader is referred to Wilbaut et al. (2008).

Our problem, since the objective function is not linear, belongs to the class of non-linear knapsack problems, also known as the non-linear resource allocation problem. This problem also belongs to the category of combinatorial optimisation problems (see Bretthauer and Shetty (2002)). As the problem instances grow larger, an exact algorithm will require an exponential amount of time. Therefore, we decided to sacrifice the optimality for near optimal solutions that can be calculated in a very short amount of time. To achieve this goal we will make use of metaheuristics.

The metaheuristic that has been developed in this paper is shown in Algorithm 1. It belongs to the category of iterated local search algorithms (ILS). The reader is referred to Lourenço et al. (2010) for a recent survey on ILS. More specifically, a greedy random adaptive search procedure (GRASP) is combined with a variable neighbourhood descent (VND) to improve the current solution and finally two perturbation heuristics are used to escape from local optima. In addition a tabu list is used during the whole execution of the heuristic to avoid an exploration of solutions that have been analysed in previous iterations.

The first step of this iterative solution approach consists of running a GRASP constructive heuristic that selects promising arcs, and selects from that set of promising arcs the best security strategy. This selection is repeated until the security budget does not allow any further security strategies.

After the GRASP procedure is finished, we use local search to improve the current solution by using a VND block. This local search is executed until the algorithm finds no more improvement. Once this is the case, a perturbation is applied to escape the local optimum, and the algorithm continues with a local search from this perturbed solution. If after a predefined number of perturbations no better solution can be found, the algorithm is restarted from a new solution generated by the GRASP constructive heuristic.

Algorithm 1 Metaheuristic structure

```
Initialize both Problem and Heuristic parameters
let x be the current solution and f(x) its cost
let x* be the best solution found so far and f(x*) its cost
x ← GRASP Heuristic()
x* ← ∅, f(x*) ← ∞
while (max number of iterations not reached) do
   x ← Improvement(x)
   if (f(x) < f(x*)) then
      x* ← x, f(x*) ← f(x)
      update number of iterations without improvement
   end if
   if (max number of iterations without improvement not
   reached) then
      x ← Perturbation(x)
   else
      x ← GRASP heuristic()
   end if
   update number of iterations
end while
return x*
```

5. COMPUTATIONAL RESULTS

In this sections we provide some preliminary results of the computational experiments by using the solution approach described before on some realistic instances.

In a first step, the parameters for the solution approach are tuned in order to achieve the best results on average. This step is executed by doing a full factorial experiment on small but realistic instances.

Then, using the best parameter settings for the solution approach, we analyse the influence of each metaheuristic components on both the quality of the solutions and the running time. In particular the VND heuristic on average can improve the initial solutions generated by the GRASP constructive heuristic by 1%. Moreover the perturbation is quite effective since it can efficiently help the solution approach by escaping from local optima and improve the quality of solutions on average by 0.14%.

In Figure 1 we report the evolution of the objective function associated with both the best and the current solutions over time. It can be noticed that our solution approach is able to converge towards good results in a short CPU time also in case of large instances. It should be noted that the marginal improvement of the best solution found so far significantly decreases when the running time is increased.

Analysing the plot associated with the current solution in Figure 1 the behaviour of the solution approach on the quality of the solution should become clear. After the perturbation, that destroys the quality of the solution, small improvements obtained during the VND

heuristic can lead to better solutions. One can clearly distinguish the perturbation strategy that allows the algorithm to efficiently escape from local optima. Starting from the perturbed solution, presented by a higher objective value (thus denoted with a pick), the VND heuristic guides the current solution trough small improvements towards a new local optimum and a hopefully a new and better solution becomes available. The fact that the VND heuristic is able to decrease the value of the perturbed solution and detects new local optima prove the efficiency of the VND.

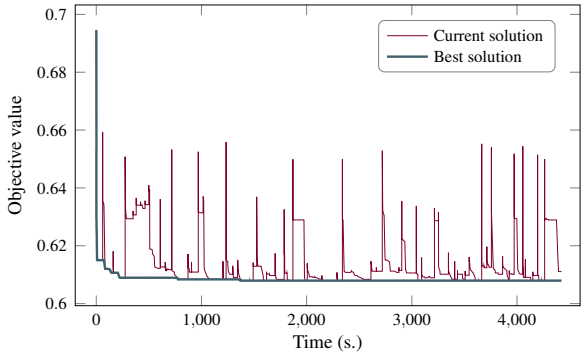

Figure 1: Plot of the objective value over time.

6. CONCLUSION & DISCUSSION

In this paper we describe a model for the selection of the appropriate security strategies given a limited budget to increase the security of an infrastructure such as pipelines transportation systems, telecommunication networks, smart grids.

By selecting an origin node and a destination node it is possible to define the risk associated to the interruption of service (or material flow) due to external, malicious attacks (e.g., terrorism, vandalism) directed at the destruction of one or several arcs.

Redundancies in the network might be used by the service provider or network owner in order to keep the service available in case of problems affecting a single arc of the network. However, attacks directed at critical arcs might disrupt the complete infrastructure and service.

An exact evaluation of the risk for the whole network to be down might be a difficult task, especially when several loops are present inside the network. Loops might be added to increase the networks reliability. In order to reduce the complexity of computations, we defined an approach to have an accurate estimate of the risk for the network being down.

This method considers the global impact of a limited number of arcs that are unavailable at the same time and therefore might disconnect the origin node from the destination node. In order to prevent such episodes that could induce significant economic loss, security strategies can be implemented to increase the reliability of each network arc.

We assume that each arc presents different characteristics in terms of vulnerability to external attacks due to internal and external factors such as geographical location, length, materials used, operating conditions. In addition, we assume to have available for each arc a list of security strategies each one with different characteristics in terms of cost and effectiveness. The decision support model presented in this paper attempts to define a ideal mix of such strategies in order to increase the security of the overall network respecting the budget. This budget might restrict the choice between security strategies.

The decision model considered in this paper addresses multilevel decisions, since a decision made at the level of a single arc might affect the security of the whole network. We proposed a heuristic algorithm, which exploits the benefits offered by tabu search combined with a GRASP and an iterated local search solution approach, to solve this combinatorial optimisation problem.

We tested our solution approach on a set of instances that mimic possible realistic scenarios. During the conference we will report the relationship between risk reduction offered by the solutions and the instance parameters such as: vulnerability of the network arcs, cost and effectiveness of the available security strategies, criticality of the segments and security budget allocations.

ACKNOWLEDGEMENTS

This research was partially supported by the Interuniversity Attraction Poles (IAP) Programme initiated by the Belgian Science Policy Office (COMEX project).

References

Bazovsky, I., 2004. *Reliability Theory and Practice*. Dover Civil and Mechanical Engineering Series. Dover Publications. ISBN 9780486438672.

Bistarelli, S., Fioravanti, F., and Peretti, P., 2007. Using CP-nets as a guide for countermeasure selection. In *Proceedings of the 2007 ACM symposium on Applied computing*, pages 300–304. March 11 - 15, Seoul, Republic of Korea.

Bojanc, R. and Jerman-Blažič, B., 2008. An economic modelling approach to information security risk management. *International Journal of Information Management*, 28 (5), 413 – 422.

Bretthauer, K. M. and Shetty, B., 2002. The nonlinear knapsack problem – algorithms and applications. *European Journal of Operational Research*, 138 (3), 459 – 472.

Lourenço, H., Martin, O., and Stützle, T., 2010. *Iterated Local Search: Framework and Applications*. Springer New York.

Ministery of Defence (UK), 2011. Chapter 6: Probabilistic R&M Parameters and redundancy calculations. In *Applied R&M Manual for Defence Systems (GR-77), Part D - Supporting Theory*. Abbey Wood, Bristol, UK Ministery of Defence.

Reniers, G. and Dullaert, W., 2012. TePiTri: A screening

method for assessing terrorist-related pipeline transport risks. *Security Journal*, 25 (2), 173–186.

Reniers, G. L., Sörensen, K., and Dullaert, W., 2012. A multi-attribute systemic risk index for comparing and prioritizing chemical industrial areas. *Reliability Engineering & System Safety*, 98 (1), 35–42.

Romeu, J. L., 2004. Understanding series and parallel systems reliability. *Selected Topics in Assurance Related Technologies (START)*, 1 (5), 1 – 8.

Sawik, T., 2013. Selection of optimal countermeasure portfolio in IT security planning. *Decision Support Systems*, 55 (1), 156–164.

Talarico, L., Sörensen, K., Reniers, G., and Springael, J., in press 2014. Pipeline security. In Hakim, S. and Shiftan, D. C. Y., editors, *Securing Transportation Systems*. New York, Springer Science and Business Media, LLC.

Viduto, V., Maple, C., and Huang, W.and López-Peréz, D., 2012. A novel risk assessment and optimisation model for a multi-objective network security countermeasure selection problem. *Decision Support Systems*, 53 (3), 599–610.

Wilbaut, C., Hanafi, S., and Salhi, S., 2008. A survey of effective heuristics and their application to a variety of knapsack problems. *IMA Journal of Management Mathematics*, 19 (3), 227–244.

AUTHORS BIOGRAPHY

Jochen Janssens received his Master in Information Management, from the KU Leuven in 2011. Following his graduation, he joined ANT/OR, the University of Antwerp Operations Research Group. To date, he is working there as a doctoral student in the field of metaheuristics and complex optimisation problems. His main interests lie in logistics, Smart Grid optimisation and other network problems.

Luca Talarico graduated as an industrial engineer in utility management at the University of Calabria (Italy) in 2005. In 2007 he obtained his master degree in management engineering with a focus on integrated logistics at the University of Calabria. In 2011 he achieved a post graduate degree in business administration (MBA) at the Alma Graduate School of Bologna. He is in the course of getting his PhD in risk management for routing problems. In his former professional career, he worked as a project manager and logistics expert at Ceva logistics and Auchan group.

Kenneth Sörensen, PhD obtained his Doctoral degree in Applied Economics at the University of Antwerp in 2003. He is founder of ANT/OR, the University of Antwerp Operations Research Group (http://antor.ua.ac.be) and EU/ME, the metaheuristics community, the largest international forum for researchers in the field of optimization using metaheuristics. He is currently full research professor at the Department of Engineering Management of the Faculty of Applied Economics at the University of Antwerp. His research focuses on (applications of) operations research, mainly optimization.

A RIGOROUS APPROACH FOR SMART GRID SYSTEMS ENGINEERING USING CO-SIMULATION

Brett Bicknell[(a)], Karim Kanso[(b)], José Reis[(c)] , Neil Rampton[(d)], Daniel McLeod[(e)]

[(a,b,c)] Critical Software Technologies, UK
[(d,e)] Selex ES, UK

{[(a)]BBicknell, [(b)]KKanso, [(c)]JReis}@criticalsoftware.co.uk
{[(d)]Neil.Rampton, [(e)]Daniel.Mcleod}@selex-es.com

ABSTRACT
This paper reports on the progress of a case study exploring the application of simulation and formal methods to the development of a cyber-physical smart grid voltage control system. The control system is required to monitor voltage across the low-voltage network and adjust it accordingly to ensure it is within required bounds. Formal methods are used to ensure that the control system fulfils its requirements, and simulation is used to validate the system and its requirements. It is demonstrated that using both formal verification and validation within a single toolset provides both an increased level of assurance that the system is correct and reduced development costs due to early identification of errors. In essence the methodology described in this paper, when correctly applied, improves system level design at the initial phase of systems engineering.

Keywords: continuous models, formal methods, Modelica, Event-B

1. INTRODUCTION

The modern power distribution network requires more intricate control methods compared to the traditional top-down approach, due to the increased uptake of micro-generation and the requirement to reduce energy waste alongside growing demand. Traditional SCADA control methods using operator driven controls are not likely to be practical, and hence automation must be applied in the distribution network. Providing assurance on these automatic closed-loop control techniques is extremely challenging, due to the overwhelming number of scenarios and potential inputs that have to be considered. Empirical testing may be impracticable due to the durations required to achieve suitable results, and even then it provides no guarantee that a representative range of conditions have been uncovered. Solutions that are designed to react dynamically to such a wide array of inputs are also difficult to test on anything but a full deployment on a real network.

1.1. ADVANCE

Through the FP7 ADVANCE project (Advanced Design and Verification Environment for Cyber-physical System Engineering) Critical Software Technologies and Selex ES are investigating an alternative approach to better support the verification and validation of cyber-physical systems (Edmunds, Colley, and Butler 2012; Colley and Butler 2014). Cyber-physical systems are characterized as computing systems that control physical systems.

Within the ADVANCE toolset, discrete models of the control system and supporting elements are developed and verified, and then co-simulated with continuous models of the environment to validate the requirements. The advantage is twofold; first, the control system is verified using mathematical proof, to ensure the logic is sound and the requirements of the system are complete and consistent. The properties that the control system is expected to uphold – for example, maintaining voltage levels within given thresholds – are specified formally as invariants. Secondly, the control system is validated through simulation against realistic environmental inputs, during which any violation of the formal invariants is highlighted. To support the simulation activities, test cases are automatically generated which are used to check that suitable test coverage has been achieved. In all, this provides a higher level of assurance and confidence on the system before it is deployed or even physically tested. It has the potential to reduce engineering costs by identifying issues early in the system's lifecycle.

1.1.1. Discrete Models

The discrete models are specified using the Event-B modelling language (Abrial 2010). Event-B is developed over set theory, and is used to define abstract state machines consisting of events (transitions) and variables, where the events can change the state of the variables. This means that once a system is modelled in Event-B, it can be analysed formally, and unambiguously.

Within the ADVANCE project, the Rodin toolset is being actively developed. Rodin is an Event-B plugin for the Eclipse framework that allows for the development and analysis of Event-B models (Abrial et al. 2010). Moreover, Rodin provides the capability for formal proofs to be carried out within classical first order logic, which allows for the developer to mathematically determine whether certain properties of the system – i.e. invariants – hold under all circumstances.

It is also possible to explore the validity of the invariants through simulation and model-checking of Event-B models within Rodin. This is advantageous as it allows for not only determining whether the system violates a property, but also how it violated the property by providing an execution trace of the system.

1.1.2. Continuous Models

The continuous models are specified using Modelica, an open, object-oriented, multi-domain, modelling language (Fritzson 2010). Conceptually, Modelica is similar to the Simscape package of Simulink, in that it allows for physical systems to be specified by connecting various blocks together. For example, these blocks could represent a resistive electrical load, or rotational mechanics. Importantly, each block contains variables (discrete and continuous) and their defining equations, which are either simple equalities or differential equations. Modelica was chosen due to its open nature; however it is possible to use other tools to create the continuous models.

Using a Modelica simulation tool, such as OpenModelica, it is possible to simulate the physical model to determine how it behaves. The simulated model is inspected to investigate its behaviour over time, typically by plotting the time-evolution of different variables in the model. This provides feedback as to the correctness of the physical model; i.e. it is established whether the model exhibits the correct behaviour before co-simulation with the discrete models.

In this work, it is required that the Modelica models are converted into a binary format (that includes the differential equation solver), so that it is possible for Rodin to import and use them.

1.2. Overview

The paper is structured as follows: Section 2 introduces the case study around the low-voltage network control, Section 3 overviews related works, Section 4 discusses the modelling techniques required for the case study, and Section 5 gives an overview of the simulations undertaken and the results obtained so far. Section 6 provides concluding remarks.

2. CASE STUDY OVERVIEW

One of the case studies used to evaluate the ADVANCE methodology during the project concerns the development of an algorithm which provides automated control of the power distribution in a low-voltage network. The high level architecture of the case study is depicted in Figure 1.

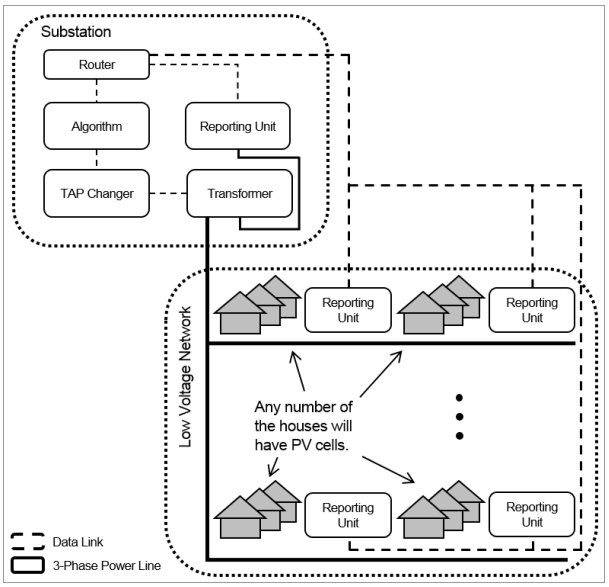

Figure 1: Case Study Architecture

A transformer with an On-Load Tap Changer (OLTC) is installed at a secondary substation, along with reporting units which are installed approximately half way and at the end of each feeder. The OLTC is capable of changing the transformer ratio through a number of discrete steps, providing stepped regulation of the output voltage. Reporting units measure the L-N (Live-to-Neutral) voltage for each phase of the feeder they are connected to and report their measurements to the substation.

The goal is for the algorithm to control the voltage on the low-voltage network efficiently, and ensure it remains within statutory limits. This is achieved by giving the algorithm the capability to set the target voltage setting for the OLTC, which in turn will select the most appropriate tap position to fulfil the target. The algorithm determines the target voltage for the OLTC by monitoring the voltage values provided by the reporting units.

Historically, there has not been a substantial issue with maintaining voltage levels across the network; transformer settings were determined during substation installation and rarely changed. However, with the increasing adoption of consumer micro-generation, typically in the form of photovoltaic cells, energy flow is now exhibited both towards and away from the substation. Additionally, increasing use of low carbon technologies, including electric vehicles and heat pumps, are increasing the demand on the network. The effect is a more dynamically changing voltage on the network, which increases the risk of the voltage in parts of the network going outside of the statutory limits. As the penetration of low carbon technologies increases over the coming decade, the need for more sophisticated

voltage management solutions will become ever more prevalent.

The algorithm considered in the case study is structured as described in Figure 2, where the busbar variable represents the voltage on the low-voltage side of the transformer. The intention is that the algorithm periodically reads the inputs, using reports which are sent by the reporting units monitoring different points of the network, and then every *k* time steps executes a number of rules that calculates the new target voltage for the OLTC.

```
Initialise()
do {
  ReadInputs()
  if (time mod k == 0) {
    ComputeMinMaxValues()
    if (max > A) {
      if (min < B) {
        target := busbar - X
      } else { if … }
    } else { if … }
    OutputTarget()
  }
 } while(sleep(1minute))
```

Figure 2: Algorithm Pseudo-Code

The properties of the system that need to be checked – which are specified in the models as Event-B invariants – are derived from the stakeholder requirement on the system to keep the voltage within required bounds at all points on the network. The challenge is in verifying the behaviour of the algorithm against these invariants, taking into account realistic power throughput as well as the effect of late or missing reports from the reporting units, and electrical faults on the network.

It is clear that scenarios such as this are archetypal of modern cyber-physical systems; where there are numerous computing systems all cooperating over potentially unreliable communications channels to achieve a common goal. Further, the unreliable nature of the communications mechanism means that it is challenging for formal methods alone to verify this system – typically a formal approach would assume that the communications mechanisms are reliable. In fact, this is where simulation plays a critical role to further assist in verifying the system.

In the following sections, it is considered what the discrete and continuous models in this scenario are, and how they are first verified formally and then simulated together to verify the system as a whole. But first, related works are considered.

3. RELATED WORK

It is well known that formal methods have been successfully applied to large industrial software systems, a recent survey of these has been compiled by Jim Woodcock (Woodcock et al. 2009). In an attempt to allow for formal methods to be applied to systems that are dependent on the physical wold (i.e. cyber-physical systems), formal hybrid methods were developed (Henzinger 2000). These are methods that combine discrete and continuous constructs. However, due to the complexity of these models and the resulting infinite nature, their application was mainly limited to academia with the notable exception of KeYmaera (Platzer and Quesel 2008).

In parallel, a simulation methodology evolved for developing systems that are tightly coupled with the physical world. Coming out of these simulation based methods was the need for combining heterogeneous models and reusing models (potentially between different tools). The solution to these needs became known as co-simulation. Ptolemy was one of the first tools to use co-simulated heterogeneous models, connected in an arbitrarily hierarchical fashion (Buck 1994; Chang, Kalavade, and Lee 1996). In recent years, two non-proprietary standards for co-simulation have emerged: FMI and DESTECS (Blochwitz et al. 2011; Pierce et al. 2012). These standards necessitate that the model to be simulated contains all the solvers that it requires, so it can be treated as a black box, and thus is portable between tools.

It was inevitable that co-simulation would be used as a mechanism to combine formal discrete models and continuous models (Živojnovic and Heinrich 1996; Fitzgerald et al. 2010). One directly relevant integration of these two approaches was by George Hackenberg, where formal modelling techniques were applied to the smart grid domain (Hackenberg et al. 2012). A bespoke environment based on the FOCUS approach (Broy and Stølen 2001) was used. This allowed for the creation of discrete models representing the control systems of the appliances in a number of houses. Models of the low and medium voltage power distribution network were also created, and simulated with the discrete models. The fundamental approach is similar to that applied in this work, however, it demonstrated a proof of concept and did not apply the tool to an industrial problem. In contrast, this work is assisting in the development of an industrial system.

Vitaly Savicks and Jens Bendisposto developed the plugin to the Rodin toolset that has allowed for the co-simulation of Event-B and Modelica models described in this paper (Savicks et al. 2013).

4. MODELLING

Elements of the system were modelled using both the Event-B and Modelica modelling languages. Event-B was used to model the algorithm, the reporting units, and an abstract communication network between these components. This created an encompassing discrete model of the cyber portion of the system. The physical models were modelled using Modelica, and consist of the low-voltage power network – including domestic customer demand models and inputs from photovoltaic sources – and the OLTC, complemented with a stochastic model specifying the occurrence of communication outages. The interaction between these

models is depicted in Figure 3, which also forms the basis of the simulation setup described in Section 5.

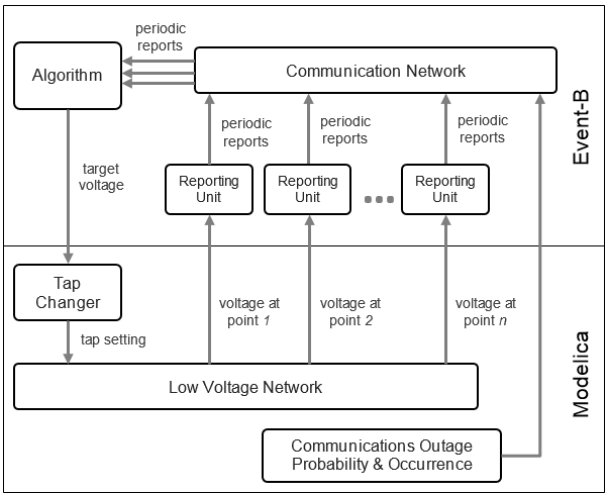

Figure 3: Modelling Strategy

From Figure 3, it can be observed that the discrete Event-B models represent the elements to be tested, whereas the continuous models represent the environment against which the system must be verified.

4.1. Event-B Models

Different strategies were required for modelling the Event-B models, each of which are detailed in this section.

4.1.1. Control Algorithm

The control algorithm was modelled using a state machine plugin for the Rodin framework, which allowed for a UML-style hierarchical approach to modelling the algorithm (Snook and Butler 2006). First, the high level state was considered, in which the algorithm can enter or leave a 'safe' mode. This safe mode is entered if the information the algorithm has about the network is not sufficiently up-to-date to make a decision; for instance, in the case that communication from a large number of reporting units is lost. A simplified example of a state machine representing this top-level view, generated in Rodin, is shown in Figure 4.

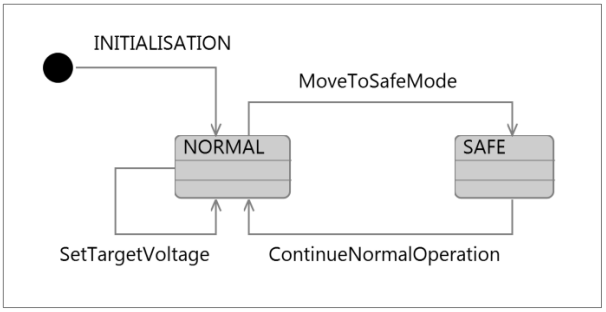

Figure 4: Event-B State Machine

These state machines can be translated to Event-B within Rodin, and further detail added to the transitions and states. A subset of the Event-B code corresponding to the state machine in Figure 4 is represented below in Figure 5.

```
variables
    state target comms_status

invariants
    @inv1 card(comms_status ▷ {FAILED}) ≥ 10
                                ⇒ state = SAFE

events
    event SetTargetVoltage
      any new_target
      where
        @grd1 state = NORMAL
      then
        @act1 target ≔ new_target
    end

    event ContinueNormalOperation
      where
        @grd1 state = SAFE
        @grd2 card(comms_status ▷ {FAILED}) < 10
      then
        @act1 state ≔ NORMAL
    end
```

Figure 5: Event-B code

The transitions in Figure 4 are translated into events, each of which has a number of guards and actions. The actions update the variables in the model, and the guards dictate when the events can occur. For example, the guard *@grd1* in the event *SetTargetVoltage* in Figure 5 ensures that the target voltage can only be changed when the algorithm is in normal mode. The action *@act1* in the same event assigns a new value to the variable that represents the target voltage.

Invariants are specified in each Event-B model, which represent the conditions, or requirements, that the model is expected to uphold. Proof obligations are generated to unambiguously determine whether each event maintains the invariants. For example, the invariant *@inv1* in Figure 5 represents the requirement that the algorithm has to enter the safe mode if the number of failed communication links exceeds a particular threshold. In order to prove that the event *ContinueNormalOperation* maintains this invariant, a guard has to be added to the event – *@grd2* – which only allows the model to exit the safe mode if the communication falls back below this threshold.

Further detail to the algorithm model was added through a number of additional modelling levels (refinements). This approach of defining a chain of models, each adding more detail, is archetypal of modelling in Event-B. It allows for the key elements of the system to be captured, whilst omitting any details which are not relevant to the properties being tested. An

example of a refinement of the *ContinueNormalOperation* event in Figure 5 is shown in Figure 6. Additional events, guards, actions, variables and invariants can be added at each refinement step.

```
event ContinueNormalOperation
  where
    @grd1 state = SAFE
    @grd3 card(mid_status ▷ {FAILED}) < 4
    @grd4 card(end_status ▷ {FAILED}) ≤ 6
    @grd5 timeout_exceeded = TRUE
  then
    @act1 state ≔ NORMAL
    @act2 counter ≔ 0
end
```

Figure 6: Refined Event

Further guards and actions have been added to the event in Figure 6 as part of the refinement. In addition, guard *@grd2* of the abstract event in Figure 5 has been replaced by the more concrete guards *@grd3* and *@grd4*, which represent the communication status of the mid and end points of the network separately. Further proof obligations are generated in the model in order to determine the consistency between the refinement levels. These proof obligations (once discharged) ensure that it is not possible to violate the invariants of more abstract levels of the model. This allows for the models to be produced in an iterative fashion alongside design or requirements generation; additional features or requirements can be added to the model as a refinement, and insurance can be generated that they are consistent with the requirements already in place.

4.1.2. Communications Network

The communications network was modelled directly in the Event-B language. Different network topologies were considered for comparison and evaluation, including a centralised and mesh network. Modelling the communications network followed a similar top-down approach, in which the first model is a generic communications model of abstract send and receive events, to which details of the particular network topology were added in subsequent refinements. Moreover, adding details into subsequent models in this manner has allowed for model reuse. Different communication networks – which use different protocols – can be (and have been) branched off the main development.

4.1.3. Reporting Units

The reporting units used a slightly different strategy, namely, decomposition. This followed an approach where the wider system (including data centres) was first abstractly formalised, then decomposed into sub-systems. Only one of these sub-systems was further developed into a model of the reporting unit. This approach of first defining the system, and then extracting the portion of the system that is to be realised ensured that the reporting units fulfilled the requirements of the wider system. The decomposition is facilitated by a Rodin plugin, developed during the ADVANCE project.

4.1.4. Formal Proof

As mentioned in the previous sections, formal proof was used to verify the correctness of the Event-B models. This not only ensured that properties internal to each element (algorithm, reporting units and communication network) were preserved correctly, but also highlighted several issues with the system – some of which were previously unknown – as a result. These issues were highlighted due to the inability to discharge the relevant proofs.

4.2. Modelica Models

The three Modelica models – the low voltage network, OLTC and specification of communication outages – were developed using different techniques: equations, state machines, and stochastic specification.

The low voltage network model encapsulates the topology of the power network – i.e. 11kV power source, transformer, feeders, houses and voltmeters – along with the standard electrical equations of power networks. A block representation of the top level model of the low voltage network is depicted in Figure 7. In addition to Figure 7, the models also contain data that represents consumption and production of power for each consumer. This data is generated by incorporating the probabilistic outputs of the CREST project into the model (Richardson 2011). The CREST models are very detailed and consider the number of occupants, when and which domestic appliances are used, when lights are used, and PV contributions.

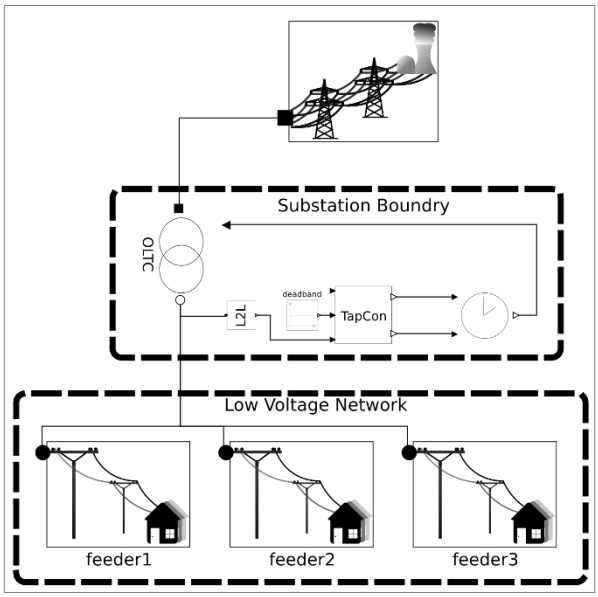

Figure 7: Low Voltage Top Level Model

The OLTC model (represented by the TapCon block in Figure 7 and elaborated in Figure 8) monitors the voltage at the transformer and changes the tap position when the voltage deviates from the target by more than a specified amount, mimicking the automated behaviour of the actual OLTC. Although the OLTC contains both discrete and continuous behaviour, it was modelled in Modelica as it is an off-the-shelf device representing part of the environment for the Event-B models. The OLTC was modelled using the Modelica state machine library, and is depicted in Figure 8, where the boxes represent states and the black bars represent transitions.

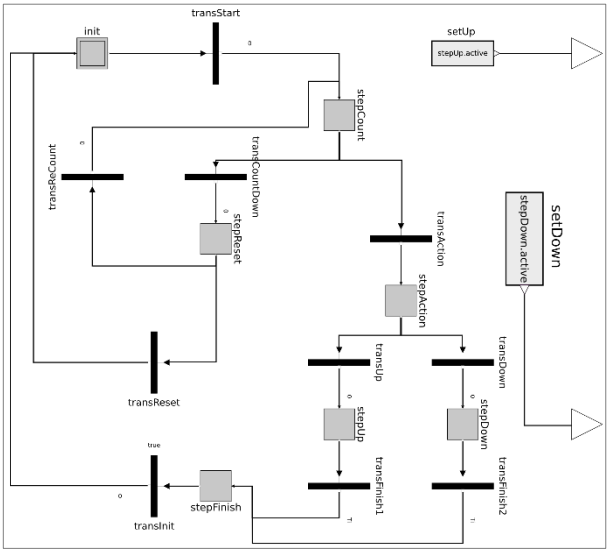

Figure 8: OLTC State Machine

The communication outage model is a stochastic model in Modelica. Based on industrial statistics it determines at what time, and for how long, a given communication link fails. The implementation of the stochastic models within Modelica is canonical, and represented by a sequence of probabilities (and associated actions) that partition the interval [0,1], then at discrete time steps, using the Peter Fritzson pseudo random number generator, generate a number in [0,1] and select the corresponding action from the sequence. In this case the action determines how long a communication link fails for.

Using industrial stochastic based simulation of the communication link failures provides a fast and efficient means to analyse the system for robustness under realistic operating conditions.

5. SIMULATION

Within the ADVANCE framework there are two types of simulation. The first, simulates the discrete models using the ProB model-checker. The second, simulates the discrete and continuous models together and is known as co-simulation.

5.1. Discrete Model Animation

To aid in verification of the discrete Event-B models, the model-checker tool ProB is used (Leuschel and Butler 2003). This allows for the models to be executed within the Rodin environment to explore their behaviour. This provides instant feedback to the model developers as to whether the models have the intended semantics. It is possible to use the model-checker to analyse the models and determine whether they deadlock or violate requirements. In either case, when one of these scenarios is identified the model-checker outputs an execution trace from the initial state of the model to the state that violates the condition. This allows for the model developer to quickly identify cases where the model does not behave as intended, fix the problems, and reanalyse. An example of this is shown in Figure 9 below. A violated condition (invariant) has been found and is highlighted in bold. The trace of events that lead to this violation is displayed in the *History* tab. The state of the variables in the model can also be examined at each step of the trace.

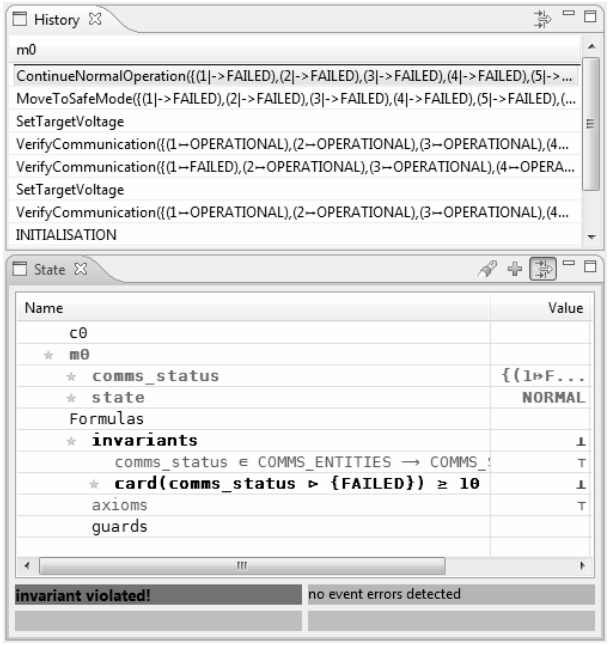

Figure 9: ProB Simulation

It is also possible to define graphical animations that depict the state of the system while it is being simulated in ProB. For example, in the case of the mesh communications network mentioned previously, an animation was developed that showed the nodes, the status of the communications links, and the volume of packets transiting each link. This is depicted in the example in Figure 10, where the boxes are nodes, the active links are represented by the solid lines, and the width of these lines represents the volume of data traffic on the link.

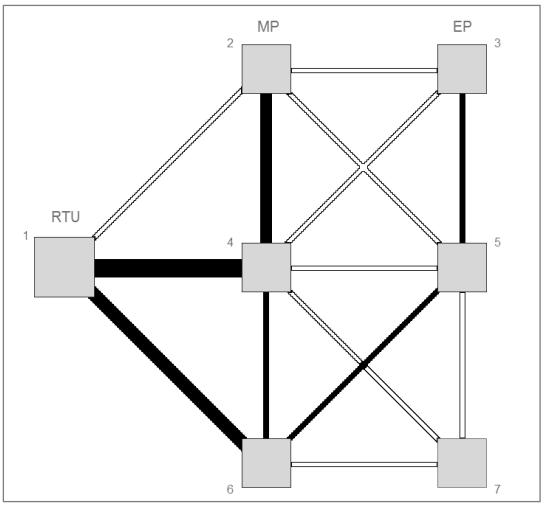

Figure 10: Mesh Network Animation

However, this type of discrete model simulation does not explore whether the models behave correctly when in situ, and the wider question of system validation is not considered – it is geared towards verifying that the models fulfil their requirements.

5.2. Co-Simulation

To validate that the system fulfils its intended purpose, the use of co-simulation is employed. The Event-B models and Modelica models are simulated in parallel, such that the outputs of one model become the inputs of another model. This is achieved through the tools developed within the ADVANCE project (Savicks 2013), and is fully integrated into the Rodin environment.

The architecture of the simulation framework is depicted in Figure 11. It is possible to integrate a number of Event-B and Modelica models into a single simulation. The configuration is used to define which inputs and outputs are linked together, and the size of the time steps of the models. Thus the simulation engine manages global temporal aspects of the simulation, it tells each model when to execute, and in the case of the Modelica models for how long. See Figure 12 for pseudo code depicting the functionality of the engine. The *performIO* step is responsible for copying values between input and output ports of the models; this is called for each model before any model starts execution, to ensure that the outputs are not overridden with new values before they are read by the other models. The current implementation of the engine does not allow for one model to interrupt the simulation, e.g. in response to an event. To mitigate this issue, the time steps of the models must be set sufficiently small enough to respond to outputs from other models.

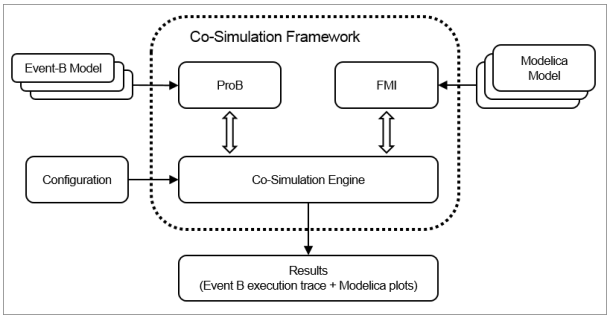

Figure 11: Conceptual View of Co-Simulation

```
int time := 0
while (time < endTime) {
  List modelsToEvaluate := empty
  int nextTime := endTime
  for m in models {
    if (time >= m.executeTime) {
      modelsToEvaluate.append(m)
      m.performIO()
    }
  }
  for m in modelsToEvaluate {
    m.execute(time,m.stepSize)
    m.executeTime += m.stepSize
    nextTime := min(nextTime,m.executeTime)
  }
  time := nextTime
}
```

Figure 12: Simulation Algorithm Pseudo Code

The configuration of the co-simulation within this case study is defined in Figure 3, where the arrows depict the linking of an output port on one model to the input port on another model. Additionally, timing configuration data is required. This details how each model perceives the progress of time with respect to the global time. For instance, the reporting units have a much higher clock cycle time than the algorithm cycle time, and the communication network needs to operate with smaller intervals to ensure packets are delivered at a realistic pace. The Modelica models are less dependent upon time, but still need to know how much time has passed and the length of the computation step required. Here, the low voltage network model operates at the same time intervals as the reporting units, to ensure that the information detected by the sensors is current.

The discrete models are simulated using the same technique as described previously, namely, with the ProB model-checker. Whereas, the continuous nature of Modelica models require the use of differential equation solvers. These solvers are embedded into the models when the model is compiled into a functional mock-up unit (FMU). An FMU is a binary representation of a model, typically produced by a Modelica toolset (Blochwitz et al. 2011).

Within Rodin, once the models have been configured, the simulation begins, which results in two

artefacts: time series for chosen variables and execution traces of the discrete models.

Within the domain of simulation, time series are common place, but taking advantage of the underlying framework of Rodin it is also possible to drill down into the execution traces of the discrete components. Thus, it is possible to understand exactly why a model makes a decision. The inputs to the model are plotted, the internal state of the model is examinable and the commands it executed are recorded. This provides a high-fidelity view of the simulation, which other toolsets often lack.

5.2.1. Results

The initial simulations pinpointed serious issues with the discrete model of the algorithm entering and leaving the designated safe mode at the wrong times. This is interesting as the models were formally developed; it in fact underlines the issue that the requirements did not fully define the safe mode behaviour. This was identified by noticing that the target was not set correctly in the simulations, then further investigation into the execution traces showed that the algorithm was entering safe mode unnecessarily. After modifying the conditions for entering safe mode, this issue was fixed.

Subsequent simulations indicated under which conditions the solution could maintain the voltage bounds. Under ideal circumstances the algorithm was able to maintain the voltage; however, when the feeders were unbalanced the voltage on some feeders could not be maintained within the UK regulated +10%/-6% bounds. This is depicted in Figure 13, where the thick line denotes the lower bound at 216. In this example the upper bound, at 253, was not breached.

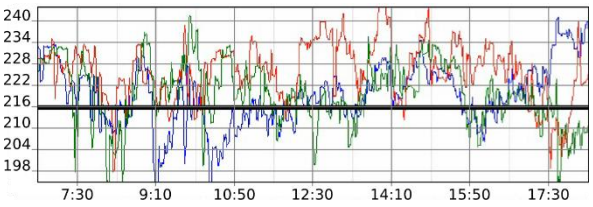

Figure 13: Feeder Violations (V)

Further observations relating to the general behaviour of the system were also raised. The system is heavily dependent on the medium voltage input. A simulated medium voltage variation (from a nominal 6.7 L-N KV or 11 L-L KV) is depicted in Figure 14, and is seen to be mirrored in the low voltage transformer output in Figure 15. Figure 15 also shows the relationship between the target set by the algorithm (dotted blue line) and the busbar voltage (on the low-voltage side of the transformer), which is as expected; notably not every target change corresponds to a tap change. The correlating changes in tap position for this example are shown in Figure 16; each discrete increment changes the busbar L-L (Line-to-Line) voltage by 8V.

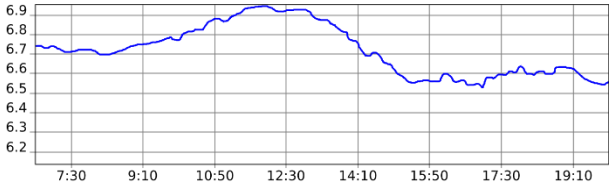

Figure 14: MV Input (KV)

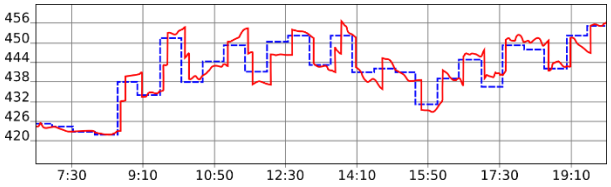

Figure 15: Busbar and Target (L-L Voltage (V))

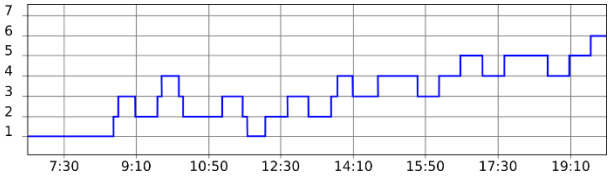

Figure 16: Tap Position

6. CONCLUSION

In this paper, the low-voltage smart energy case study of the ADVANCE project has been described and the initial results presented. The paper also overviewed the ADVANCE methodologies, with special emphasis on cyber-physical systems engineering.

The advantages of the ADVANCE framework are twofold:

- Formal development and verification of control systems, and
- Validation of the developed system against plant models.

Further, a single development environment is used for the formal development and analysis, with the freedom to integrate with any FMU plant model. In this paper, all plant models were developed using Modelica.

Changes are made to the formal models if issues are found through the verification or validation, and retested against the environment until a satisfactory solution is found.

This allows for the system to be formally analysed, simulated and improved at an early phase of the system life cycle, hence reducing time to market of complex systems.

ACKNOWLEDGMENTS

We would like to thank members of the ADVANCE consortium for their continued support throughout this work, especially the University of Southampton and Heinrich Heine University Düsseldorf for their continued support with the modelling and co-simulation.

We would also like to thank the anonymous reviewers of this paper for their time and helpful comments.

REFERENCES

Abrial, J.-R., 2010. *Modeling in Event-B: system and software engineering*. UK:Cambridge University Press.

Abrial, J.-R., et al., 2010. Rodin: an open toolset for modelling and reasoning in Event-B. *International Journal on Software Tools for Technology Transfer*. volume 12:447-466.

Blochwitz, T., et al., 2011. The functional mockup interface for tool independent exchange of simulation models. *Proceedings of 8th Modelica Conference*, pp. 105-114. March 20-22, Dresden, Germany.

Broy, M. and Stølen, K., 2001. *Specification and development of interactive systems: focus on streams, interfaces and refinement*. USA:Springer-Verlag New York.

Buck, J., Lee, E. and Messerschmitt, D., 1994. Ptolemy: A Framework for Simulating and Prototyping Heterogeneous Systems. *Int. Journal of Computer Simulation, special issue on "Simulation Software Development"* volume 4:155-182.

Chang, W.-T., Kalavade, A. and Lee, E., 1996. Effective Heterogenous Design and Co-Simulation. *NATO ASI Series: Hardware/Software Co-Design* volume 310:187-212.

Colley, J. and Butler, M., 2014. *Advanced Design and Verification Environment for Cyber-physical System Engineering*. Web. Available from: http://www.advance-ict.eu/ [May 2014].

Edmunds, A., Colley, J. and Butler, M., 2012. Building on the DEPLOY legacy: code generation and simulation. *DS-Event-B-2012: Workshop on the experience of and advances in developing dependable systems in Event-B.*

Fitzgerald, J., Larsen, P., Pierce, K., Verhoef, M. and Wolff, S., 2010. Collaborative Modelling and Co-simulation in the Development of Dependable Embedded Systems. *Lecture Notes in Computer Science*. volume 6396:12-26.

Fritzson, P., 2010. *Principles of object-oriented modeling and simulation with Modelica 2.1*. John Wiley & Sons.

Hackenberg, G., Irlbeck, M., Koutsoumpas, V. and Bytschkow, D., 2012. Applying formal software engineering techniques to smart grids. *Proceedings of 1st International Workshop on Software Engineering for the Smart Grid (SE4SG)*, pp. 50-56. June, Zurich, Switzerland.

Henzinger, T., 2000. The Theory of Hybrid Automata. *NATO ASI Series: Verification of Digital and Hybrid Systems* volume 170:265-292.

Leuschel, M. and Butler, M., 2003. ProB: A Model Checker for B. *Lecture Notes in Computer Science*. volume 2805:855-874.

Pierce, K., et al., 2012. Collaborative Modelling and Co-simulation with DESTECS: A Pilot Study. *Proceedings of 21st International Workshop on Enabling Technologies: Infrastructure for Collaborative Enterprises (WETICE)*, pp. 280-285. June, Toulouse, France.

Platzer, A. and Quesel, J.-D., 2008. KeYmaera: A Hybrid Theorem Prover for Hybrid Systems (System Description). *Lecture Notes in Computer Science: Automated Reasoning* volume 5195:171-178.

Richardson, I., 2011. *Integrated high-resolution modelling of domestic electricity demand and low voltage electricity distribution networks*. PhD Thesis. Loughborough University.

Savicks, V., Butler, M., Bendisposto, J., and Colley, J., 2013. Co-simulation of Event-B and Continuous Models in Rodin. *Proceedings of 4th Rodin User and Developer Workshop*. June, Turku, Finland.

Snook, C., Butler, M., 2006. UML-B: Formal modeling and design aided by UML. *ACM Transactions on Software Engineering and Methodology* volume 15 issue 1:92-122.

Woodcock, J., et al., 2009. Formal Methods: Practice and Experience. *ACM Computing Surveys* volume 41 issue 4:1-40.

Živojnovic, V. and Heinrich, M., 1996. Compiled HW/SW co-simulation. *Proceedings of the 33rd annual Design Automation Conference*, pp. 690-695. June, Las Vegas, USA.

AUTHORS BIOGRAPHY

Brett Bicknell holds a BSc Physics degree and has played a key role in a number of formal methods initiatives, including the FP7 ADVANCE project. His software engineering experience encompasses varying levels of criticality, including embedded systems and data solutions.

Karim Kanso has worked within the field of formal methods and software engineering for many years, on various projects in the domains of transportation and aerospace, and received a PhD in theoretical computer science.

José Reis is a Principal Consultant Engineer at Critical Software Technologies. He plays a key role in the development of model-driven engineering and formal methods within Critical Software Technologies. He has been leading the team working on the ADVANCE FP7 project and prior to that Mr. Reis was involved with DEPLOY FP7. In parallel with this Mr. Reis has been working with various prime contractors, such as BAE Submarines, EADS Astrium and AgustaWestland, with a focus on requirements engineering and verification and validation.

Neil Rampton is a professional electronics engineer who has worked for 25+ years within Selex ES. Neil has experience in a wide variety of senior engineering roles, including within engineering management, business/solutions development, programme management and change management. His project

involvement has included a wide variety of electronics and systems, including high performance thermal imaging cameras and Generic Vehicle Architectures for military vehicles. He is currently responsible for Capability and Product Strategy for Smart Energy (Smart Grid and Buildings Energy Management) and is looking at the development of Smart City & Transportation solutions.

Daniel McLeod holds a BSc Physics degree and has worked on a variety of imaging sensor systems in the Airborne, Land and Naval domains. His previous work includes algorithm development, system design, requirements analysis and verification and project management. He is currently working within the smart energy domain on a Low Voltage monitoring system and a system for automated control of low voltage transformers in response to customer demand and distributed generation.

TECHNICAL CONCEPT OF A SOFTWARE COMPONENT FOR SOCIAL SUSTAINABILITY IN A SOFTWARE FOR SUSTAINABILITY SIMULATION OF MANUFACTURING COMPANIES

Andi H. Widok[a, b], Volker Wohlgemuth[a]

[a] HTW Berlin, Wilhelminenhof Str. 75A, D-12549 Berlin, Germany
[b] University of Hamburg, Dept. of Informatics, Modeling and Simulation, Vogt-Kölln Str. 30, D-22527 Hamburg

[a]a.widok@htw-berlin.de, volker.wohlgemuth@htw-berlin.de

ABSTRACT
This paper presents the technical concept and prototype implementation of a component developed for the modeling of social sustainability criteria, as well as the description of a software suite for the simulation of sustainability criteria in producing companies. The simulation software (MILAN) already integrates the classical economical perspective as well as an environmental perspective through the inherit usage of material flow analysis (MFA) and life cycle assessment (LCA) combined in one modeling approach. The newly developed component is intended to allow for a relative free definition of social influence indicators as well as influence functions, which can subsequently be integrated in the same model and thus allow for a rather holistic sustainability simulation approach. As most of the social indicators are still very disputed, as well as dependent on the structure of the entity under observation, the free definition aims to provide the modeler with the needed flexibility to create a model of his interest, while providing him with a strong structural guideline on how the integration of social criteria can be worthwhile.

Keywords: discrete event simulation (DES), material flow analysis (MFA), life cycle assessment (LCA), social LCA (SLCA), occupational health and safety (OHS)

1. INTRODUCTION

The classical usage of simulation considering the economical perspective of manufacturing systems and its rather output oriented point of view has already been widely discussed, see for example (Banks 2005) for DES examples and (Brousseau and Eldukhri 2011) for recent advances for innovative manufacturing.

Over the last decade the environmental perspective has become more prominent and resulted in different (simulation) approaches with a focus on the environmental sustainability of production systems; examples for sustainability oriented manufacturing simulation can be found in (Seliger 2012) and (Thiede 2012), including lists of software with status overviews of their features considering sustainability assessment/simulation.

While these developments show promise, firms, and particularly manufacturing company reports rarely include the social dimension, which is also reflected by the number of simulation studies and tools addressing this topic. Many companies are issuing corporate reports which stress governance aspects and environmental practices, but tend to overlook the role of the employees or workforce (OECD 2008, cf. GRI 2013). This identifies the first big challenge of the chosen approach, as even though not many deciders will argue about the importance social criteria have considering the day to day work, the impact and the management of social values remains largely hard to quantify and qualify, and thus is only rarely supported by more complicated software tools, such as simulation software. This may also be due to the fact that simulation software in general is usually used to answer specific question and is, in that regard, itself often designed for specific users, making its usability a lesser priority (Krehahn et al. 2012). With the intention of integrating the different perspectives however, the necessity arises for higher user-friendliness and hence poses an additional challenge to the already existing one of defining usable criteria that can be simulated and correlated in a meaningful way.

The concept of the simulation software was furthermore developed with particularly regard to the main idea of sustainability, as understood hereafter, as the positive or negative reinforcement of measures contributing to the preservation or destruction of capital (economic, environmental, and social), depending on predefined normative values for that capital in question. These normative values are needed in order to have a qualification of the measures once the simulation has delivered its results. This paper will therefore:

- present the software's background (section 2),
- state the current common features of the simulation software (section 3),
- illustrate the new component (section 4),
- define interfaces and specify the interaction of the different software components (4.2 & 4.3),
- elaborate on related work and conclude with an outlook (section 5 and 6).

2. METHODICAL BACKGROUND OF MILAN

MILAN is a software solution that has been developed over the last 13 years and has seen various implementations in different programming languages. The main concept behind its initial development was the integration of material flow analysis (MFA) with the already established discrete event simulation (DES) for manufacturing cases in one single modeling approach (i.e. just one model has to be created, instead of two different models (MFA, DES) in the past) (Wohlgemuth et al. 2001; Wohlgemuth 2005).

The first development with the intention to promote resource efficiency was realized around the year 2000, when the proposal was made to use simulation techniques for supporting the application of the Material Flow Network method (Wohlgemuth, Bruns and Page 2001; Wohlgemuth 2005). Material Flow Networks were developed at the University of Hamburg (Möller 2000) and are based on the Petri-Net theory. By their means, the software is able to depict and calculate unknown environmental quantities, such as the determination of the necessary load of connected input flows considering complex systems (see Joschko, Page and Wohlgemuth 2009; Widok, Wohlgemuth and Page 2011).

While on one hand, the discrete event simulation components allowed for an accurate analysis of typically economic and industry related aspects, the material flow analysis components on the other hand added an environmental perspective to the discrete event simulation model, i.e. a consideration of relevant material flows and transformations such as:

- the consumption of commodities, resources and additives,
- the energy demand,
- waste accumulation,
- emission generation.

The first presentation of the Material Flow Simulator MILAN was made in 2006 (Wohlgemuth, Page and Kreutzer 2006), its first implementation realized using the Delphi version of DESMO-J, called DESMO-D, the framework and components in high level language Delphi. The component-based architecture was realized using COM-Technology (Wohlgemuth, Page and Kreutzer 2006). This realization, however, seemed outdated and has been renewed since 2009 two times using two different approaches. Once using the EMPINIA Framework (see http://www.empinia.org/). EMPINIA, which was developed in the course of a project called EMPORER, is designed for the development of complex domain-specific applications especially in the field of environmental management information systems (EMIS) (Wohlgemuth, Schnackenbeck, Panic and Barling 2008). It is a component-orientated extensible application framework based on Microsoft's .NET (http://www.msdn.microsoft.com/de-de/netframework) technology with the purpose of supporting and simplifying the development of complex software systems (see Figure 1).

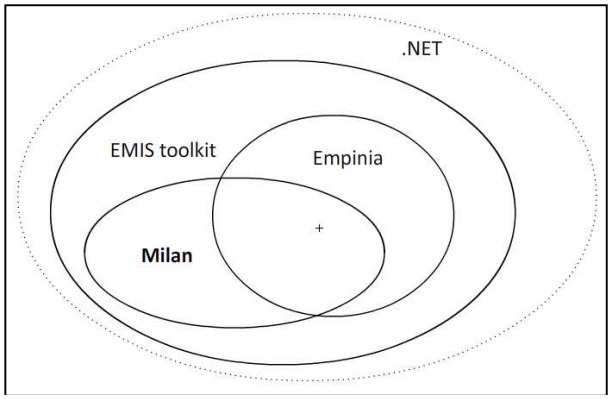

Figure 1: Environment of the 2009 implementation

In order to take advantage of newest .NET development patterns, a switch from the implemented version using model-view-controller (MVC) patterns (Jahr et al. 2009) was made to more contemporary model-view-viewmodel (MVVM) patterns within the last years. Furthermore, recent advances also facilitated the integration of LCA data in the same modelling approach (different scope) allowing for the integration of the life cycle perspective (see Reinhard, Zah and Wohlgemuth 2013).

3. FEATURES OF THE SIMULATION SOFTWARE MILAN

In order to be able to provide the described methodological functionalities different components had to be developed; their key features will be briefly outlined in the following (see also figure 1):

- a simulation core (central simulation service, interfaces and abstract base classes for models),
- a bundle for discrete event simulation (specific for DES, with scheduler, timing aspects, etc.),
- stochastic distributions (e.g. Bernoulli, Exponential, etc., to generate streams of numbers),
- a graph editor (enabling the visual representation and manipulation of models),
- property editors (facilitating the parameterization of model entities and given metadata) new editors with the same principle, were developed for the social aspects,
- a reporting suite (creating the simulation results and preparing charts depending on the scope, also facilitating export functionality),
- the material management (for the creation, management of materials, batches, bills),
- the material accounting (by its means it is possible to show, save and manage material and energy bookkeeping resulting from the simulation. The bookkeeping is realized using accounting rules, which can be added to all discrete events in combination with relevant model components),
- a LCA browser, which enables an easy, string-based search and the subsequently integration

of LCA material data, enabling life cycle inventory (LCI) and LCA in the simulation and the results.

For more information about the technical aspects of base functionalities of the simulation software, see (Jahr et al. 2009).

4. THE SOCIAL DOMAIN MODEL

4.1. Architecture overview

Figure 1 is illustrating the main components relevant for the social domain. The elements in the first two lines are building the backbone of the social component; the ones in line 3 and 4 represent elements relevant for the sustainability assessment, while those below represent simulation and technical entities facilitating the functioning of the components above.

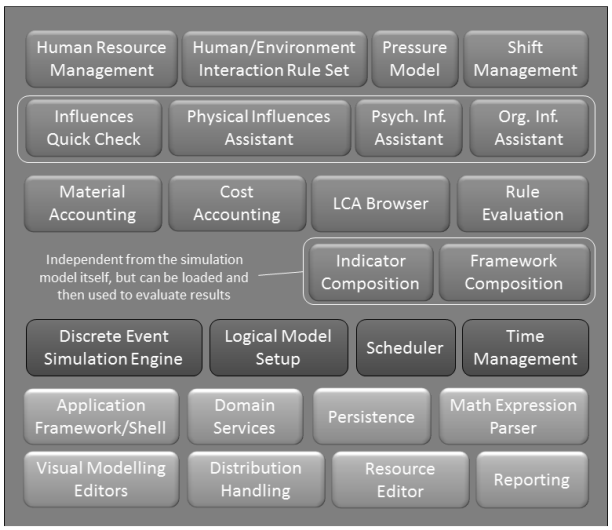

Figure 1: Relevant entities for the social domain

The concept for the social prototype was mainly oriented on two major drivers. First, the component architecture – aside from normal component-development reasons, such as high reusability and the easier understanding of the code, through clear, small packages, this also means that the usage of the social perspective is not enforced, i.e. it is possible to model social aspects through the software, but one does not have to. The software also allows to only build DES simulation models and not integrating MFA or LCA, but if the data is existing and the intention is to have a strong, holistic model, one can use the different techniques combined in one modeling approach and only a single model has to be created, incorporating the methodologies. Secondly, the free definition of influences – this is based on the conviction that social criteria, as well as their measurement, are still disputed. Based on this, it was decided that an open definition of different influences would be made possible, with different editors for the most common influences (physical, organizational, psychological), incorporating current knowledge considering the measurement of such criteria and their impact on human resources over time. These impacts however are not validated by the tool itself, i.e. the reasonableness of the defined influences and their impact lays currently with the modeler (except for logically excluding behavior).

As a result of these convictions the social criteria integration was coupled with the resource system, allowing for the integration of human resource into the model or not. Furthermore special editors were designed for the easy modelling of different influence factors which, combined with various mathematical functions, would allow for the creation of an influence on the resources over time.

The result of these influences may, once the modelling of the resources is complete, be combined with different events, such as a termination event for the simulation (for example in case of the destruction of needed resources – see also figure 3), or general state changes (considering the failure, inoperability or reduced output of workstations).

In order to allow these possibilities the resource system had to be renewed, paying tribute to different kinds of resources (human resources, usable resources (tools) and substances, hence enabling different internal handling of them and editors for their modelling. In addition the resources have a property with a list of categories, enabling for example the localization of resources. This was important in order to associate locally existing influences with human resources (noise for example). The influence would then be a logical consequence of the modelled influence factor in combination time and the chosen pressure model (see also figure 4).

4.2. Selected interfaces

The following figure shows them main interfaces for the human resource system. To note is the interface IResourceTypeAmount, which is basically a combination used to derive different quantities of different user defined types of resources and map them to the accorded resource pools. The modelling of different groups of workers, as organizational entities or in order to research age groups and other possible influence factors is in this way easily achievable.

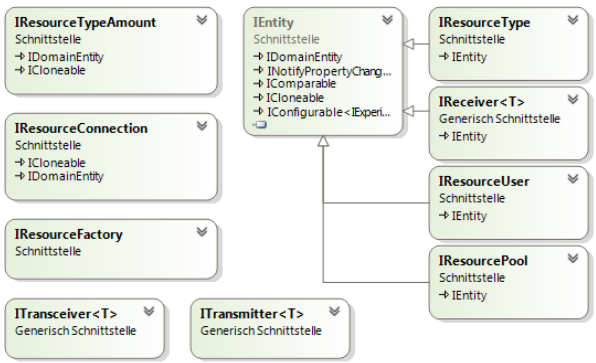

Figure 2: Interfaces of the Resource System

To note is also the observer-based functioning of the simulation routine. Figure 3 displays an example of two interfaces for the standard simulation observer and its related interface for simulation termination criteria. Through the observer-based handling of the routine feedback is easily steerable.

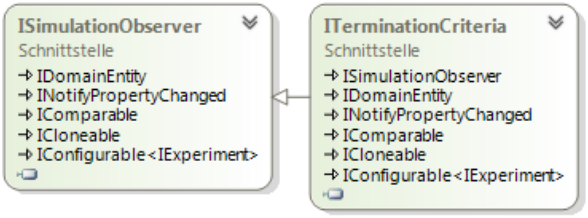

Figure 3: Simulation-flow-handling through observers

4.3. General workflow and related components

Figure 4 depicts the general workflow for integrating the social aspects into the simulation. Given that the resources were modelled in the human resource editor (where one can adjust for skill set, integration of distributions considering illness or weaknesses (also usable for the modeling of elderly workers and many others), one has different possibilities to combine the resource with the model. One way is through the workstations themselves, allowing for the modelling of necessities, i.e. an amount of a type of resource is needed for different states, or in combination with the shift management. Either way, the resource usage is giving the first answer to the question how people would be affected through their interaction, by giving the timespan of a certain influence.

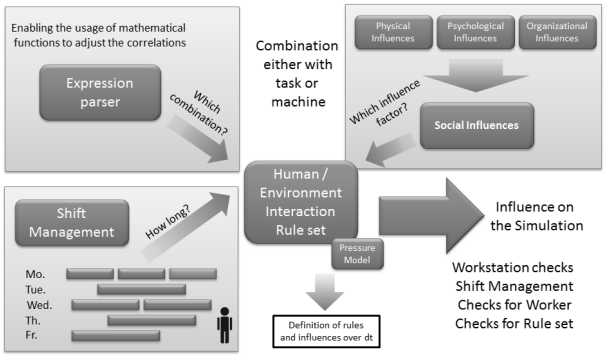

Figure 4: Relevant entities for the social domain

The shift management is basically a standard shift planning tool, which is used for both, the workstations, i.e. one can define if production processes are continuously or with breaks for a period of time. This is of course relevant for the warm up phases and different states of the workstations. Furthermore the shift management is used to attribute different human resources to their respective work-related entities. These could be different workplaces (although a workplace editor is yet to be integrated). For the moment these are the respective workstations (i.e. the rather classic DES workstations model entities). In addition the possibility is given to attribute a type of influence on the resource over time. These possible strains can be either physical, or otherwise, depending on the modeled influences through the different influence editors and the following choice of the modeler.

These editors allow for different types of influences, the main differentiation is between physical, psychological and organizational influences, where the physical editor guides the definition of a physical influence through possible input choices (strong relation to German OHS guidelines, as in strains for lifting, crouching, carrying, but also general, as in workload dependent, biological interaction, noise, etc.) all of the possible choices are backed up with known formulas for the development of the influence (such as the physical basics of noise development (and combination considering different machines) or basics for the development of particulate matter in production processes), as well as known limit values considering the strain on an average human being. The psychological editor does currently have a completely free definition of influences, while different types are suggested, no choices of formulas is, but rather the definition of a type is mandatory, which can subsequently be used in the rule set editor. The same procedure is implemented for the organizational influences. Even though many studies were incorporated in a knowledge basis for these components (a systematic review of occupational musculoskeletal and mental health studies for production systems can be found in Westgaard and Winkel 2011), the definition of the non-physical influences was implemented without structural restriction.

In order for the influences to take affect another component was needed, the human environmental influences rule set component. In this element one can choose from the previously defined social influences and by the usage of a math expression parser and the existing model of shifts and or the production system (i.e. the workstations), combine time with influences to create an impact over time. Different dose concepts were evaluated in that regard, which are also integrated in a knowledge base and selectable (note: the tool is only making a basic validation for reasonable combination choices). Once an influence is attributed to a shift or a workstation, the simulation is then calculating an impact of the indicated influence over time.

This allowed for the combination of economic, environmental and social reporting on the results of manufacturing simulations and thus combined different perspectives in a single model. Currently the reporting suite is being worked on, as the best way to visualize the different outputs has not been found yet. What can already be observed however is, that it is now possible to relate strategic question considering workload on different individuals. In this regard the planning of, for example new shifts is made easier and the planning of new production lines, which need an amount of skilled workers, can now directly be related with consequent influences on worker exposure (to different substances, workload, other influences).

5. RELATED WORK

5.1. Focus on environmental sustainability

In the course of the last decades the environmental perspective has become more and more prominent considering the simulation of manufacturing entities, examples for this focus can be found in (Thiede 2012, Seliger 2012, Reinhard et al. 2013, Andersson 2014). These references were used as orientation during the development cycles. Most other existing simulation software tools are not integrating the life cycle approach. It seems that the perception of the system borders of the simulation approach, which logically inhibits the gate to gate focus, is hindering the other. In order to change that and integrate upstream data, two strategies can be observed: on the one hand, through the integration of LCA data (for used material) at least the environmental and some social aspects of the downstream can be integrated, examples in (Kellens et al. 2011 as well as the mentioned Reinhard et al. 2013 and Andersson 2012), while on the other hand different simulation techniques (for example DES and SD and or ABS) are combined in order to model and integrate different parts of the life cycle in appropriate and possible detail/granulation. These will logically be integrated once the simulation has finished; a comparison of the output of such differently combined modelling approaches can be found in (Jain et al. 2013). The combination of these different models is however usually happening via interfaces not integrated in a single model, while the here presented approach depicts the integration of LCA and DES in one modeling approach, see also (Widok et al. 2011) and (Widok et al. 2012) for more details on the environmental sustainability perspective.

5.1. Focus on social sustainability and OHS

Social criteria remain a lesser focus of the simulation of manufacturing entities (Schneider 2008, OECD 2008). In (Heilala et al. 2008) ergonomic criteria are, as part of the social domain, integrated in one simulation approach; (Lind et al. 2009) displays the results in more detail. These references were used to validate the possibility of a broader social sustainability approach and thus helped to depict and conceptualize the ergonomic part of the influence factors. In (Makhbul et al. 2013) stress at the workplace is analyzed and ergonomic workstation factors categorized, which gave ideas for the integration of the organizational and psychological influence editors. Implications towards the work performance of following measures can be found under (Yahaya et al. 2011), while these findings were very interesting they are currently only integrated through a knowledge base, accessible during the modelling process, due to the complexity of the possible internal feedback. Detailed analysis of occupational musculoskeletal and mental health with specific focus on production systems can be found in (Westgaard and Winkel 2011), they also show an overview over relevant studies as well as highlight the significance of the findings of these studies. This paper can be used to assess what criteria are worthwhile to be modelled and how possible results should be questioned. A detailed analysis of historic occupational safety measures as well as trends can be found in (Luczak 2002), these helped to categorize the chosen integration approaches and depict the general functioning of the “work system”. Examples and guidelines for shift-management/workplace fatigue can be found in (Department of Labour New Zealand 2007). The given guidelines helped to design the interaction between the shift-management and the influence/pressure models. Furthermore, in Germany a new guideline by the association of German engineers has been published, depicting the representation and physical strains on humans in virtually modeled manufacturing halls, an analysis is described in (Zülch et al. 2013), those were used in combination with (Zaeh and Prasch 2007) where the authors are making suggestions for systematic workplace/assembly redesign for aging workforces, in order to work out the influence factor operations in the modelling process.

5.1. Focus on ELCA and SLCA integration

A literature review of social sustainability assessment methodologies can be found in (Benoît and Vickery-Niedermann 2010), this paper was also very valuable considering LCA integration and possible SLCA adaptations. Considering SLCA, one has to note author Jørgensen, who published many excellent papers (Jørgensen et al. 2007) for example on the integration of SLCA criteria in companies, summaries of his work are in (Jørgensen 2010). Most of his work has been reviewed and different methodologies tested for the SLCA integration.

Lastly the capital approach for sustainability evaluation is explained in chapter v. of (UN 2007), which was relevant for framework compositions and consequently result qualification, i.e. reporting mechanisms (see also Spangenberg et al. 2010 and GRI guidelines (GRI 2013)).

6. CONCLUSION

At the basis of the integration of social criteria stands our experiences from the past considering the integration of environmental perspective in the simulation tool MILAN. At the time environmental criteria overcame the once thought immeasurability as over the last decades their data maturity grew. It is our understanding that the high focus on environmental sustainability aspects in the past decades could when focused on social aspects lead to similar enhancements in data accessibility and maturity. Especially the SLCA development seems promising in order to achieve this goal.

There are a few reasons often mentioned against the introduction of social criteria in manufacturing simulation, namely, for example the false angle – emphasizing that simulation of manufacturing systems should focus on classical aspects and let social criteria be managed by human resource management and corporate social responsibility practices. To that we

argue that simulation, understood as a strategic method, is meant to give deciders a stronger foundation for their decision making process. In the past these decision were solely based on the outcome-oriented perspective, a change of this would be good for the involved human beings. Even though we agree with (Gasparator et al. 2007) conclusion, considering methodological pluralism (very simplified: more is not necessarily better), the key idea of the approach in this paper is the attempt of the integration and ability to put different perspectives in correlation. It is clear that the social aspects have yet to mature in their scientific provability, yet potentials can clearly already be indicated. This is what the tool already delivers as result, potentials compared to limit values (i.e. elevated by x%, without qualifying beyond stating that it is a positive or negative tendency and putting it into context).

Furthermore it is often argued that every human is different and hence a measurement would be pointless. The fact that every human is different is valid, however the main aspects of human health and psychic are not as different as a variety of studies suggest (see Westgaard and Winkel 2011). Of course it is complicated to derive exact numbers, but that is where the free definition of influences comes into play, by allowing for the modelling of workers, as well as the impact on different levels. So while the presented approach is far from scientifically established, its purpose is rather to promote the re-integration of social values in existing manufacturing processes and further develop on holistic perceptions of human actions.

REFERENCES

Andersson, J. 2014. Environmental Impact Assessment using Production Flow Simulation. Sweden

Andersson, J., Skoogh, A., Johansson, B. 2012. "Evaluation of Methods used for Life-Cycle Assessments in discrete event simulation." In Proceedings of the 2012 Winter Simulation Conference, Edited by Edited by C. Laroque, J. Himmelspach, R. Pasupathy, O. Rose, and A.M. Uhrmacher. IEEEBanks, J., Carson, J., Nelson, B. L., Nicol, D. 2005.Discrete-event system simulation. 4th edition, Upper Saddle River. New Jersey, USA

Benoît, C., Vickery-Niederman, G. 2010. "Social Sustainability Assessment Literature Review." White Paper. The Sustainability Consortium, Arizona State University and University of Arkansas, USA

Brousseau, E., Eldukhri, E. 2011. "Recent advances on key technologies for innovative manufacturing." In *Journal of Intelligent Manufacturing*, Vol. 22, Issue 5 (2011), pp. 675-691. Springer, LLC

Department of Labour New Zealand. 2007. "Managing shift work to minimise workplace fatigue - A Guide for Employers." Crown. Wellington, New Zealand

Gasparatos, A., El-Haram, M., Horner, M. 2007. "A critical review of reductionist approaches for assessing the progress towards sustainability." In: Environmental Impact Assessment Review, Vol. 28, Issue 4-5 (2007), pp. 286-311. Elsevier Inc. Dundee, UK

GRI (Global Reporting Initiative) 2013. "G4 Sustainability Reporting Guidelines Implementation Manual". GRI Report, The Netherlands

Heilala, J., Vatanen, S., Tonteri, H., Montonen, J., Lind, S., Johansson, B., Stahre, J. 2008. "Simulation-based Sustainable Manufacturing System Design." In Proceedings of the WSC 2008." IEEE. USA

Jahr, P., Schiemann, L., Wohlgemuth V. 2009. Development of simulation components for material flow simulation of production systems based on the plugin architecture framework EMPINIA. In: Wittmann, J.; Flechsig, M. (Eds.): *Simulation in Umwelt- und Geowissenschaften*. Shaker Verlag, Aachen, p. 57-69

Jain, S., Sigurðardóttir, S., Lindskog, E., Andersson, J., Skoogh, A., Johansson, B. 2013. "Multi-Resolution Modelling for Supply Chain Sustainability Analysis." In: Proceedings of the 2013 Winter Simulation Conference.", pp. 1996-2007. IEEE. Washington, DC, USA

Jørgensen, A. 2010. Developing the Social Life Cycle Assessment: Adressing Issues of Validity and Usability. Thesis (PhD). Lyngby, Denmark

Jørgensen, A., Le Bocq, A., Narzarkina, L., Hauschild, M. 2007. „Methodologies for Social Life Cycle Assessment." In International Journal of Life Cycle Assessment, Vol. 13, Issue 2 (2007), pp. 96-103.

Joschko, P., Page, B., Wohlgemuth, V., 2009. "Combination of Job Oriented Simulation with Ecological Material Flow Analysis as integrated Analysis Tool for Business Production Processes", *Proceedings of the 2009 Winter Simulation Conference*

Kellens, K., Dewulf, W., Overcash, M., Hauschild, M. Z., Duflou, J. R. 2011. "Methodology for systematic analysis and improvement of manufacturing unit process life-cycle inventory (UPLCI)" In: International Journal of Life Cycle Assessment, Vol. 17, Issue 1 (2011), pp. 69-78.

Krehahn, P., Ziep, T., Wohlgemuth, V. 2012. Mobile Computing as a Data Source for the Material Flow Management (MFM), *Proceedings of the EnvironInfo 2012*, Germany

Lind, S., Johansson, B., Stahre, J., Berlin, C., Fasth, A., Heilala, J., Helin, K., Kiviranta, S., Krassi, B., Montonen, J., Tonteri, H., Vantanen, S., Viitaniemi, J. 2009. "SIMTER - A Joint Simulation Tool for Production Development." In *VTT Working Paper*, No. 125. Espoo, Finland

Luczak, H., Cernavin, O., Scheuch, K., Sonntag, K. 2002. "Trends of Research and Practice in Occupational Risk Prevention as Seen in Germany." In: Industrial Health, Vol. 40, Issue 2, pp. 74-100

Makhbul, Z. M., Abdullah, N. L., Senik, Z. C. 2013. “Ergonomics and Stress at Workplace: Engineering Contributions to Social Sciences.” In: Jurnal Pengurusan, Vol. 37, Issue 1 (2013), pp. 125-131

OECD (Organization for Economic Cooperation and Development) 2008. "Measuring material flows and resource productivity." OECD Report. Paris, France

Reinhard, J., Zah, R., Wohlgemuth, V., Jahr, P. 2013. “Applying Life Cycle Assessment within Discrete Event Simulation: Practical Application of the MILAN/EcoFactory Material Flow Simulator.” In Proceedings of the 27nd Int. Conference Environmental Informatics.“ Hamburg, Germany

Seliger, G. 2012. *Sustainable Manufacturing*. 1st edition. Springer Verlag. Berlin, Germany

Schneider, R. 2008. “Measuring Social Dimensons of Sustainable Production.” In: Measuring Sustainable Production, Chapter 4, OECD Publishing. Paris, France

Spangenberg, J. H., Fuad-Luke, A., Blincoe, K. 2010. ”Design for Sustainability (DfS): the interface of sustainable production and consumption.” In: Journal of Cleaner Production, Vol. 18, Issue 15 (2010), pp. 1485-1493. Elsevier Ltd.. Cologne/Hornbæk, Germany/Denmark

Thiede, S. 2012. Energy Efficiency in Manufacturing Systems. 1st edition, Springer-Verlag. Germany

UN, (United Nations) 2007. *Indicators of Sustainable Development: Guidelines and Methodologies*. 3rd edition, United Nations. New York, USA

Westgaard, R. H., Winkel, J. 2011. “Occupational musculoskeletal and mental health: Significance of rationalization and opportunities to create sustainable production systems - A systematic review.” In: Applied Ergonomics, Vol. 42, Issue 2 (2011), pp. 261-296. Elsevier Ltd and The Ergonomics Society

Widok, A. H., Wohlgemuth, V., Page, B. 2011. “Combining Event Discrete Simulation with Sustainability Criteria.” In *Proceedings of the 2011 Winter Simulation Conference*. IEEE. Phoenix, USA

Widok, A. H., Schiemann, L., Jahr, P., Wohlgemuth, V. 2012. “Achieving Sustainability through the Combination of LCA and DES integrated in a Simulation Software for Production Processes.” In: Proceedings of the 2012 Winter Simulation Conference. IEEE. Berlin, Germany

Wohlgemuth, V., Bruns, L., Page, B. 2001. „Simulation als Ansatz zur ökologischen und ökonomischen Planungsunterstützung im Kontext betrieblicher Umweltinformationssysteme (BUIS).“ In: L. M. Hilty; P. Gilgen (Eds.): 15th International Symposium Informatics for Environmental Protection.

Wohlgemuth, V. 2005. Komponentenbasierte Unterstützung von Methoden der Modellbildung und Simulation im Einsatzkontext des betrieblichen. University of Hamburg: Thesis (PhD). Shaker. Germany

Wohlgemuth, V., Page, B., Kreutzer, W. 2006. “Combining discrete event simulation and material flow analysis in a component-based approach to industrial environmental protection.” *Environmental Modelling & Software*, pp. 1607-1617.

Wohlgemuth, V., Schnackenbeck, T., Panic, D., Barling, R.-L. 2008. Development of an Open Source Software Framework as a Basis for Implementing Plugin-Based Environmental Management Information Systems (EMIS). *Proceedings of the 22nd Int. Conference on Environmental Protection*, Sep. 2008

Yahaya, A., Yahaya, N., Bon, A. T., Ismail, S., Ing, T. C. 2011. “Stress level and its influencing factors among employees in a plastic manufacturing and the implication towards work performance.” In: Elixir Psychology, Vol. 41 (2011), pp. 5923-5941. Elixir

Zaeh, M. F., Prasch, M. 2007. “Systematic workplace and assembly redesign for aging workforces.” In: Production Engineering, Vol. 1, Issue 1 (2007), pp. 57-64. WGP. Munich, Germany

Zülch, G. 2013. „Ergonomische Abbildung des Menschen in der Digitalen Fabrik – Die neue VDI-Richtlinie 4499-4.“ In: Simulation in Produktion und Logistik 2013, edited by Dangelmaier W., Laroque C. and Klaas A., Paderborn, Germany

AUTHORS BIOGRAPHY

ANDI H. WIDOK studied Industrial Environmental Computer Science at the HTW Berlin, University of Applied Sciences. He holds a (M.Sc.) degree in Industrial Environmental Computer Science and works as a research assistant at the HTW Berlin, as well as the University of Hamburg. In 2011 he became a PhD student of the University of Hamburg. His research interests are mainly sustainability theory, its applications in computer simulations and sustainable software development for organizations. His email is <a.widok@htw-berlin.de>.

VOLKER WOHLGEMUTH studied Computer Science at the Universities of Hamburg and Canterbury, Christchurch, New Zealand. He received his PhD in 2005. He has been working as a professor for Industrial Environmental Informatics at the HTW Berlin, University of Applied Sciences since 2005. His research fields are material flow management, modeling and simulation and Environmental Management Information Systems (EMIS). His email is <volker.wohlgemuth@htw-berlin.de>.

TAKING HUMAN BEHAVIOR INTO ACCOUNT IN ENERGY CONSUMPTION SIMULATION

Eric Ferreri[(a)], Jean-Marc Salotti[(a)], Pierre-Alexandre Favier[(a)]

[(a)]IMS laboratory,CNRS, IPB, BORDEAUX UNIVERSITY

[(a)]eric.ferreri@ensc.fr, [(b)]jean-marc.salotti@ensc.fr, [(c)]pierre-alexandre.favier@ensc.fr

ABSTRACT

In recent years, continuously growing energy requirements have become an issue. This is particularly true concerning electrical energy as resources to produce it are limited. Numerous studies have shown that human behaviour plays a key role in the global consumption. Thus modelling human activity is part of the sustainable developpement challenge. To achieve good simulating and predicting performances in the field of electric consumption, various statistical and behavioural methods that take human factors into account have been implemented. Both families of methods have their respective strengths and weaknesses. We propose a review of these methods.

Signal processing techniques have been widely used to solve this problem. New methods based on behavioural models are promising. A recent work proposed by the authors is based on a psychological model that highlights the nature of decision-taking processes related to electrical consumption.

Keywords: sustainable development, energy consumption, inverse system.

1. INTRODUCTION

World energy use is quickly growing and has already raised concerns over supply difficulties, lack of energy resources and heavy environmental impacts such as green-house effect. Current predictions show that this trend will probably continue several decades. In recent years energy efficiency measures have made the energy end-user increasingly important and influential on the whole sustainable developpement challenge. One example is distributed electricity generation in low-voltage grids, where the impact of widespread on-site generation on network voltages is influenced by the matching with domestic electricity demand Thomson, M., & Infield, D. G. (2007). Modeling of domestic electricity demand for a large number of individual households is a complex task. In a realistic simulation, the shape of the demand curve must be reproduced taking account of variations between households and spread of demand levels for different end-uses over time. Markov-chains models can simulate adequately power consumption(Widén, J., & Wäckelgård, E.2010). However, the inhabitant's behavior, which is an important factor, is poorly considered in such stochastic modeling. Figures of predicted consumption may be strongly impacted by human factors. The multi-agent framework allows to takes account of inhabitants behavior. By explicitly defining a behavior model, a link between perception and action may be defined and used to predict energy consumption on the basis of the perceived surrounding. However, personal preferences –and important underlying factors of behavior- are still hard to take into account. In section 2 we propose an overview of the behavioral impact on energy consumption. Numerous simulators exist to predict energy consumptions. The main issues are discussed in section 3. There are two main approaches: the statistical approach is presented in section 4 and the behavioral one, which has been followed by the authors, is developed in section 5.

2. IMPACT OF HUMAN BEHAVIOR ON ENERGY CONSUMPTION

To illustrate how human factors have a strong influence on energy consumption, in figure 1, we show the mean daily consumption of two habitations. In spite of their same number of inhabitants, similar electrical equipment, same location and same type of habitation, the consumption profile is very different (Remodece database 2008).

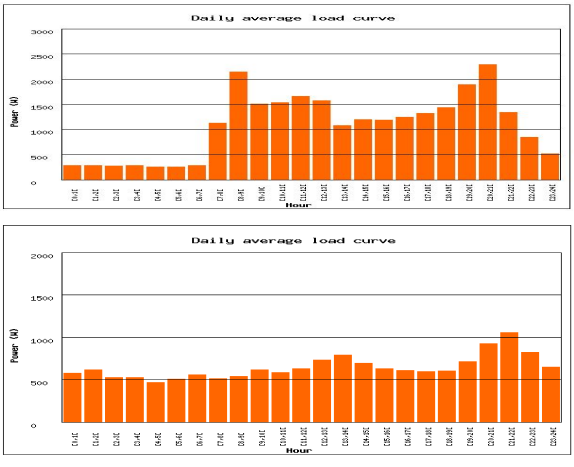

Figure 1: two different energy consumption profiles.

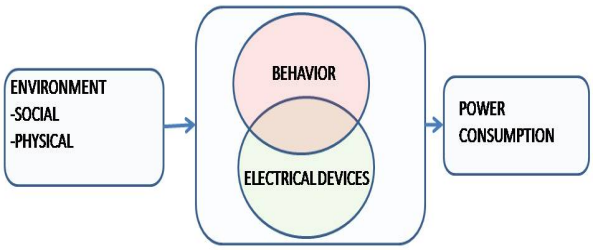

Figure 2: general model that links environment, behavior and power consumption.

Energy consumption in buildings depends on many parameters that can be split into three categories (see Figure 2):
- Environment: this category includes the local climate, the local context (close to a forest, a high building, a river, etc.) and the orientation of the house. It also includes the social context. At the conception level, the social context includes architectural constraints that are usually imposed by municipal administration and national rules. At the user level, the social context includes the profile of the inhabitants (family with children, old persons, students, socio-professional category, etc.).
- Physical devices: this category includes all electrical devices of the house and eventually other heat production devices.
- Behavior: this category includes all human behaviors. A behavior is usually defined by three parts: A perception process (perception of cold for instance), a decision process, and an action process (Merleau-Ponty 1976), (Fiske, Susan T & Neuberg, Steven L. 1990). Behaviors have an important impact on consumption. Humans have an impact on the conception of the house, taking into account ecological issues, costs issues, but also comfort, well-being and uses. At the realization level, there are human factors linked to the professionalism of the building teams, time constraints and costs, which may lead to errors and structural defects. At the user level, behaviors also have an important impact. Here are some examples:

- There are gender differences in the comfort temperature, which has a direct impact on thermostat regulation. (Karjalainen, S. 2007)

- A cultural behavior exists for window opening, even in modern houses with automatic ventilation.

- Some people leave their television switched on day long, even when there are not watching it (Remodece database 2008).

3. ENERGY CONSUMPTION SIMULATION

Power consumption can be seen as the output of a system that takes environment e (physical as well as social), electrical equipment a, and inhabitants' behavior b as inputs, whereas electrical consumption C is the output. The forward model can be expressed as $f(e,a,b) = C$. Figure 2 represents this general model.

In order to simulate energy consumptions, we need a model for the environment, models of physical devices including the house and behavioral models.
Modeling human behaviors is a very difficult task. Software solutions such as Pleiades-Comfie or Sketchup reduce human factors to basic stereotyped behaviors.

Fundamentally modeling behaviors can be seen as solving an inverse problem. In order to do so, electrical consumption data have to be collected. C becomes a known parameter and the inhabitants' behavior b becomes the output. Hence partial inversion of the model $f(e,a,b) = C$ is necessary, and can be expressed as $g(e,a,C) = b$ this partial inversion is illustrated in figure 3.

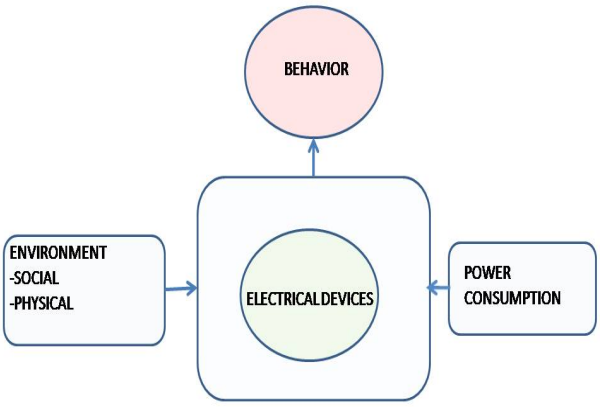

Figure 3: General model partially inverted to simulate behavior.

4. STATISTICAL APPROACH

In this case, the function $f(e,a,b) = C$ is a stochastic function that can be a linear combination of known probability distributions that describe the database in a parsimonious way. Markov-chain models are part of this framework (Widén, J., & Wäckelgård, E. 2010). Non linear probabilistic models are also used (Page, J., Robinson, D., Morel, N., Scartezzini, J.-L.2008) and succeed to reproduce non-repetitive behavioral patterns.

In both cases, methods to recover the g function earlier defined are well-known, and allow obtaining results that are close to actual measures if the database is well-suited. However, in this framework, behavior is entirely deduced from the database, and the parameters of the g function are a purely statistical description of the human factor. In this case, the results strongly rely on the relevance and exhaustivity of the database. Minor changes on the electrical equipment or on the habits of the studied population cannot be taken into account to adjust parameters of the g function.

5. BEHAVIORAL APPROACH

Methods presented earlier aimed to partially inverse the consumption function f. Since this function is not analytical and depends on complex hidden factors such as human behavior, this can be seen as an ill-posed

problem. In the statistical approach, authors face the problem by looking for a mathematical solution that is optimal in the least-squared error sense.

Behavioral methods are not based on a mathematical solution, but rather on a distributed solution that does not need to be expressed in a closed-form. There exist a plenty of methods to model the decision process that defines the behavior -BDI methods, competitive, collaborative, reactive, expert systems… - (Ferreri, Salotti, Favier 2014, Russell et al. 1995)
In order to do so, the multiagent framework has proven to be useful (Le, et al 2010).

In such a framework, each human is represented as a simplified system that aims to satisfy needs by optimally using resources at disposal. Specific scenarios can be programmed and simulated to empirically adjust the way the agents reach optimality from their point of view. This distributed non-analytical version of the least-square error allows a better understanding of the influence of human behavior.

6. CONCLUSION

Methods presented in this review try to take account of human behaviors in energy consumption simulations. Statistical methods allow obtaining quick results which are compatible with time-user databases. However, technologies are evolving, habits are changing, new norms are appearing, and motivations and beliefs concerning ecology and sustainable development are more and more taken into account. Hence the statistical approach based on past data is biased and the behavioral one might be more appropriated.

REFERENCES

Ferreri, Salotti, Favier, Simulation prédictive pour la gestion des consommationsElectriques dans un quartier, *IBPSA 2014* Russell, S. J., Norvig, P., Canny, J. F., Malik, J. M., & Edwards, D. D. (1995) Russell, S. J., Norvig, P., Canny, J. F., Malik, J. M., & Edwards, D. D. (1995).*Artificial intelligence: a modern approach* (Vol. 2). Englewood Cliffs: Prentice hall.

Fiske, Susan T. et Neuberg, Steven L. 1990. Fiske, Susan T. et Neuberg, Steven L. 1990. A continum of impression formation, from category―based to individuating processes: Influences of information and motivation on attention and interpretation. *Advances in experimental social psychology*, vol. 23, p. 1-74.

Karjalainen, S. (2007). Gender differences in thermal comfort and use of thermostats in everyday thermal environments. *Building and Environment*, *42*(4), 1594-1603.

Le, X. H. B., Kashif, A., Ploix, S., Dugdale, J., Di Mascolo, M., & Abras, S. 2010. Simulating inhabitant behaviour to manage energy at home. *International Building Performance Simulation Association Conference*, Moret-sur-Loing, France.

Merleau-Ponty 1976 ,Phénoménologie de la perception, Paris, Éditions Gallimard, collection «Tel»

Page, J., Robinson, D., Morel, N., Scartezzini, J.-L.(2008) A generalised stochastic model for the prediction of occupant presence, *Energy and Buildings*, 40(2) p83-98

Thomson, M., & Infield, D. G. (2007). Impact of widespread photovoltaics generation on distribution systems. Renewable Power Generation, IET, 1(1), 33-40.

Widén, J., & Wäckelgård, E. (2010). A high-resolution stochastic model of domestic activity patterns and electricity demand. Applied Energy, 87(6), 1880-1892.

Wilke, U., Scartezzini, J. L., et Haldi, F. 2013. Probabilistic Bottom-up Modelling of Occupancy and Activities to Predict Electricity Demand in Residential Buildings *Doctoral dissertation, EPFL*

Author's Index